



22

Invasive Hemodynamic Diagnosis of Cardiac Disease

MORTON J. KERN, ARNOLD H. SETO, AND JOERG HERRMANN

INTRODUCTION TO INVASIVE HEMODYNAMIC DIAGNOSIS OF CARDIAC DISEASE, 385

Indications for Cardiac Catheterization and Hemodynamic Assessment, 385
 Vascular Access, 386
 Left-Heart Catheterization, 390
 Right-Heart Catheterization, 391
 Technical Aspects and Artifacts of Pressure Measurements, 391
 Computations for Hemodynamic Measurements, 392
 Cardiac Output Measurements, 393

NORMAL RIGHT AND LEFT HEART WAVEFORMS AND VALVULAR HEMODYNAMICS INCLUDING HOCM (LVOT GRADIENTS), 394

The Cardiac Cycle and Generation of Pressure Waves, 394
 Normal Pressure Waveforms, 395
 Evaluation of Valvular Heart Disease, 398
 Calculation of Stenotic Valve Orifice Areas, 398
 Aortic Valve Stenosis, 399
 Low-Flow, Low-Gradient Aortic Stenosis, 400
 Hypertrophic Obstructive Cardiomyopathy, 400
 Mitral Valve Stenosis, 401
 Pulmonary and Tricuspid Valve Stenosis, 401
 Aortic Regurgitation, 401
 Mitral Regurgitation, 402
 Pulmonary and Tricuspid Valve Regurgitation, 402

SEPTAL DEFECTS AND LEFT-TO-RIGHT/ RIGHT-TO-LEFT SHUNTS, 403

Pericardial Disease and Restrictive Cardiomyopathy, 404
 Normal Pericardial Function and Pathophysiology of Constriction, 404
 Cardiac Tamponade, 405

PHYSIOLOGIC AND PHARMACOLOGIC MANEUVERS AND PV LOOPS, 405

Exercise Provocation, 406
 Dynamic Exercise, 406
 Static Exercise, 406
 Pacing Tachycardia, 406
 Pharmacologic Challenges, 407
 Pressure-Volume (PV) Relationships, 408

ACKNOWLEDGMENT, 409

REFERENCES, 409

INTRODUCTION TO INVASIVE HEMODYNAMIC DIAGNOSIS OF CARDIAC DISEASE

The cardiac catheterization laboratory serves multiple roles, which include not only angiography and vascular interventions but also, structural interventions. The latter are directed to percutaneously correct valve diseases, atrial and ventricular septal defects, and septal ablation for hypertrophic cardiomyopathy. Six to seven decades ago the cardiac catheterization laboratory was essential for the hemodynamic assessment and understanding of various disease entities and provided the diagnostic foundation for the application of surgical structural interventions as they arose in those days. At the end of the 1970s the pendulum started to shift with the advancing development of two-dimensional and Doppler echocardiography, which allowed for an alternative assessment of both cardiac anatomy and hemodynamics in patients with structural heart disease. Coupled with the excitement of being able to perform percutaneous coronary interventions (PCIs), the focus of many cardiac catheterization laboratories shifted to coronary artery disease, leading to dwindling interest and expertise in invasive hemodynamic assessment of cardiac diseases. This loss, however, had to be regained with the advent of transcatheter aortic valve replacement (TAVR) in the 21st century, especially as contemporary studies indicate that the correlation between non-invasively (echocardiography) and invasively (cardiac catheterization) measured aortic valve area and gradient is imperfect. This is critically important when decisions on valve procedures are made as well as when gauging the success of these interventions instantly in the catheterization laboratory. With the renaissance of hemodynamic assessment of cardiac diseases, cardiologists of today, especially those engaged in the catheterization laboratory, must have a proper understanding of the principles and nuances of invasive hemodynamic assessment as well as their limitations for proper interpretation and patient management decisions. This chapter will address these concepts and the technical aspects of the cardiac catheterization. As with most diagnostic tools in medicine, hemodynamics

cannot be used in a vacuum and must be coupled with the clinical presentation, physical examination, and adjunctive imaging modalities to arrive at accurate results.

Indications for Cardiac Catheterization and Hemodynamic Assessment

The scope of indications for cardiac catheterization are summarized in [eTable 22.1](#).¹ As outlined, the cardiac catheterization laboratory enables invasive testing for cardiac disease and includes the acquisition of tissue samples (biopsies), imaging of vasculatures and heart chambers (intravascular and intracardiac ultrasound, optical coherence tomography, angiograms, and ventriculograms), and hemodynamic assessments (fractional flow reserve, vascular resistance, cardiac output, pressure gradients, etc.). Clinical history, physical examination, and additional (noninvasive) diagnostic studies guide the invasive hemodynamic evaluation. The ACC/AHA valvular heart disease guidelines, for instance, make it clear (class III recommendation) that the invasive assessment is not the default first-step diagnostic modality in the evaluation of patients with structural heart diseases. Hemodynamics are to be used, however, in case of discrepancies in the results of noninvasive evaluations (in particular the echocardiogram but also additional imaging and stress studies) with the clinical presentation and examination.

Contraindications to cardiac catheterization include fever, anemia, coagulopathy, electrolyte imbalance (especially hypokalemia predisposing to arrhythmias), and other systemic illnesses or conditions needing stabilization ([eTable 22.2](#)). The clinical necessity of cardiac catheterization should also be carefully considered when the diagnostic information or therapeutic intervention will not meaningfully impact patient management and outcomes. Furthermore, the procedure is to be done only with full explanation of its benefits and risks and informed consent of the patient. Most catheterization laboratories will also mandate that “do not resuscitate/do not intubate” orders will be suspended during the procedure.



ETABLE 22.1 Indications for Cardiac Catheterization

INDICATIONS	PROCEDURES
1. Suspected or known coronary artery disease	LV, COR
a. New-onset angina	LV, COR
b. Unstable angina	LV, COR
c. Evaluation before a major surgical procedure	LV, COR
d. Silent ischemia	LV, COR
e. Positive exercise tolerance test	LV, COR
f. Atypical chest pain or coronary spasm	LV, COR, vasomotor stimuli
2. Myocardial infarction	LV, COR, PCI
a. Unstable angina postinfarction	LV, COR, PCI
b. Failed thrombolysis	LV, COR, PCI
c. Shock	LV, COR, RH, LV support
d. Mechanical complications (ventricular septal defect, rupture of wall or papillary muscle)	LV, COR, RH, pacemaker, LV support
3. Sudden cardiovascular death	LV, COR, R + L
4. Valvular heart disease	LV, COR, R + L, ± AO
5. Congenital heart disease (before anticipated corrective surgery or ASD/PFO closure)	LV, COR, R + L, ± AO
6. Aortic dissection	AO, COR
7. Pericardial constriction or tamponade	LV, COR, R + L
8. Cardiomyopathy	LV, COR, R + L, ± BX
9. Initial and follow-up assessment for heart transplant	LV, COR, R + L, BX

AO, Aortography; ASD, atrial septal defect; BX, endomyocardial biopsy; COR, coronary angiography; LV, left ventriculography; PCI, percutaneous coronary intervention; RH, right heart oxygen saturations and hemodynamics (e.g., placement of Swan-Ganz catheter); R + L, right and left heart hemodynamics; ±, optional.

From Sorraja P, et al. Kern's Cardiac Catheterization Handbook. 7th ed. Elsevier; 2020, p 4.

ETABLE 22.2 Complications of Cardiac Catheterization

Major
Cerebrovascular accident
Death
Myocardial infarction
Ventricular tachycardia, fibrillation, serious arrhythmia
Relative Contraindications
Aortic dissection
Cardiac perforation, tamponade
Congestive heart failure
Contrast reaction (anaphylaxis, nephrotoxicity)
Heart block, asystole
Hemorrhage (local, retroperitoneal, pelvic)
Infection
Protamine reaction
Supraventricular tachyarrhythmia, atrial fibrillation
Thrombosis, embolus, air embolus
Vascular injury, pseudoaneurysm
Vasovagal reaction

From Sorraja P, et al. Kern's Cardiac Catheterization Handbook. 7th ed. Elsevier; 2020, p 5.

Complications and Risks

For diagnostic catheterization, an analysis of the complications in more than 200,000 patients indicated the incidences of risks were death, ~0.2%; myocardial infarction, ~0.05%; stroke, ~0.07%; serious ventricular arrhythmia, ~0.5%; and major vascular complications (thrombosis, bleeding requiring transfusion, or pseudoaneurysm), ~1% (eTable 22.3). Compared with femoral or radial artery access, vascular complications occurred more often when the brachial artery approach was used and least when the radial approach was used.

Vascular Access

Arterial Access Percutaneous Radial Artery Technique

Radial artery access has become the default approach for many labs (Fig. 22.1).² Compared with femoral artery access, transradial procedures have a lower risk of bleeding and vascular complications, superior patient comfort, and improved efficiency in post-procedural care. Documentation of adequate dual blood supply to the hand by either the Allen or the Barbeau test is no longer required in most patients.

In preparation for radial access, the arm should be placed on an appropriate board, abducted at a 30- to 45-degree angle, and the wrist should be hyperextended over a gauze roll. Unless prompted by anatomy or demand (e.g., left internal mammary artery injection), the right radial artery is used. Its distal course can be mapped by palpation or ultrasound; the latter reduces the difficulty of access and can be used to screen for small radial arteries or anatomical challenges before radial sheath insertion.³ Only a small amount of 1% lidocaine (up to 1 mL) is injected at the skin entry site, which should be 1 to 2 cm cranial to the bony prominence of the distal radius. The radial artery is accessed by either a micropuncture needle (anterior wall technique) or a 20-gauge angiocatheter needle (posterior wall technique) at a 30- to 45-degree angle. With pulsatile blood return, a 0.018-inch guidewire is advanced into the artery, and there should be little or no resistance to wire advancement. If this were to be noted, access should be reexamined before proceeding. Otherwise, the needle is removed and the sheath is advanced over the wire into the artery. Once the sheath is in place, typically, 5000 units of unfractionated heparin are given as a bolus, or weight-adjusted (50 units per kg), to prevent postprocedural radial artery occlusion. Practices differ but one should consider smaller sizes for women (4 to 5F) yet larger sizes (6F, maximum 7F in men) if coronary intervention is likely. Overstretching of the artery is to be avoided as it leads to higher postprocedural occlusion rates. A longer sheath (up to 16 cm) has been considered to protect more against vasospasm at the level of the forearm. However, other studies suggest that it is the hydrophilic coating rather than the length of the sheath that reduces spasms. Arterial vasospasm is a complicating factor and prevented by adequate

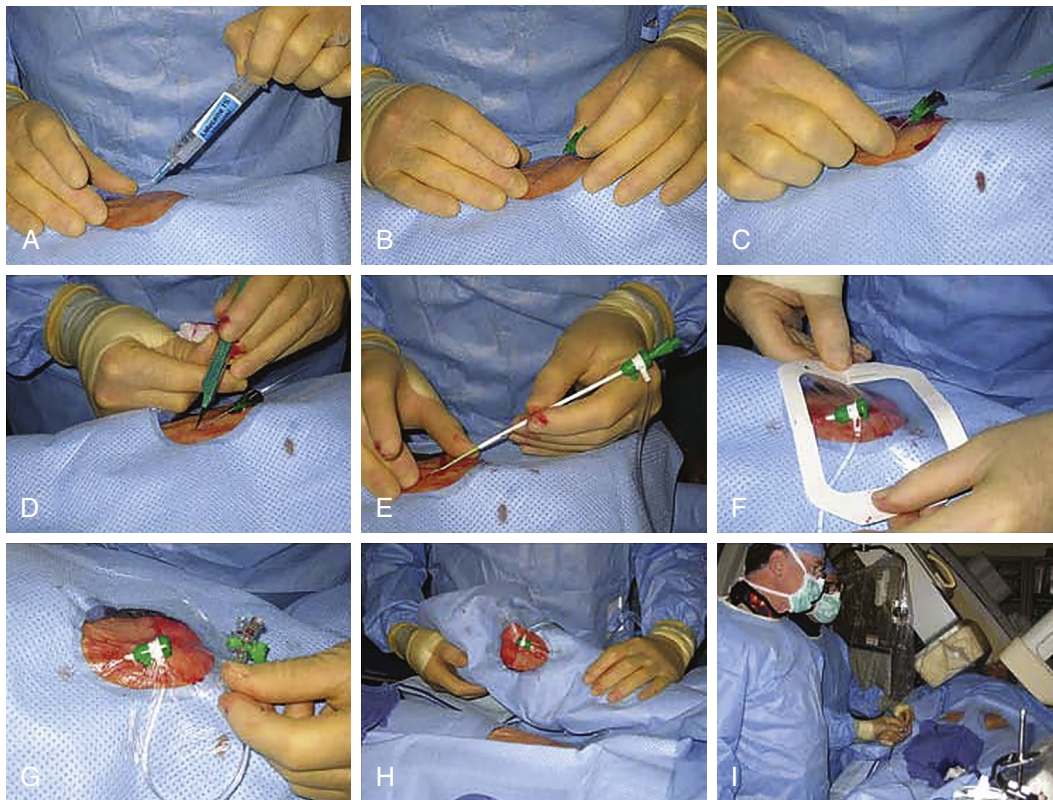


FIGURE 22.1 Radial artery access and sheath introduction. Once draped, the radial pulse is palpated. The point of puncture should be 1 to 2 cm cranial to the bony prominence of the distal radius. **A**, Administer a small amount of lidocaine into the skin. **B**, Use the needle (micropuncture needle shown here) at a 30- to 45-degree angulation. Slowly advance until blood pulsates out of needle. It will not be a strong pulsation because of the small bore of the needle. **C**, Fix needle position and carefully introduce a 0.018-inch guidewire with twirling motion. There should be little or no resistance to wire introduction. Remove needle. **D**, Make a small incision over the wire in preparation for sheath introduction (this step is optional). **E**, Advance the sheath over the wire into the artery. If sheath moves easily, advance to hub. If resistance is felt with sheath halfway in artery, remove wire and administer vasodilator cocktail. Reinsert wire and continue to advance the sheath. **F** and **G**, After the sheath is positioned and flushed, secure sheath with clear plastic dressing or suture (also optional). **H** and **I**, The arm can now be moved to the patient's side for catheter introduction. (From Sorraja P, et al. *Kern's Cardiac Catheterization Handbook*. 2020, p 104.)

sedation, avoidance of limb cooling, and administration of vasodilators. Most commonly, nitroglycerin (100 to 200 mcg) and verapamil (2.5 mg) are given. Other approaches are sublingual nitroglycerin, and/or intra-arterial (local) administration of diltiazem or nicardipine. With these preparations, coronary angiographic catheters are advanced over a 0.035-inch floppy or small J-tipped guidewire into the ascending aorta and then manipulated to engage the coronary artery ostia. Some operators note catheter instability or poor coronary ostial engagement from the radial approach. Larger (>7F) sheath sizes that may be required for complex PCI also present a challenge for radial access.

After the procedure is completed, arterial puncture hemostasis is most often obtained with air-bladder compression bands or other similar closure devices (Fig. 22.2). In addition to adequate initial anticoagulation, the use of "patent hemostasis" (occlusion to the point of bleeding control but not complete vessel occlusion) minimizes the risk of radial artery occlusion. Hematomas, while uncommon, can lead to pseudoaneurysms and very rarely compartment syndrome (eFig. 22.1). Other risks include radial artery vasospasm, dissections, transient hand dysfunction, and potentially a higher risk of future coronary artery bypass graft (CABG) radial graft dysfunction.

Percutaneous Femoral Artery Technique

Femoral artery access was the standard access over the last four decades.⁴ Femoral artery access uses the Seldinger needle puncture technique with the insertion of a valved sheath (6 to 8F or larger) and use of preshaped "Judkins" catheters. The optimal puncture location is the common femoral artery (CFA). Familiarity with the anatomy will

ETABLE 22.3 Incidence of Major Complications of Cardiac Catheterizations

PROCEDURE-RELATED COMPLICATIONS IN PATIENTS WITHOUT STEMI		
	PCI PATIENTS WITHOUT STEMI (N = 787,980)	DIAGNOSTIC CATHETERIZATION ONLY PATIENTS WITHOUT STEMI (N = 1,091,557)
Complications (%)		
Any adverse event	4.53	1.35
Cardiogenic shock	0.47	0.24
Heart failure	0.59	0.38
Pericardial tamponade	0.07	0.03
CVA/stroke	0.17	0.17
Total strokes that were hemorrhagic	15.6	9.16
New requirement for dialysis	0.19	0.14
In-hospital mortality		
Non-risk-adjusted	0.65	0.72
Non-risk-adjusted excluding CABG patients	0.62	0.60
CABG performed during admission	0.81	7.47
CABG status		
Salvage/emergency	0.01/0.17	0.01/0.27
Urgent/elective	0.47/0.16	5.27/1.92
CABG indication		
PCI failure without clinical deterioration	0.26	
PCI complication	0.14	
Bleeding Complications (%)		
Any bleeding event within 72 hours of procedure	1.40	0.49
Any other vascular complication requiring treatment	0.44	0.15
RBC/whole-blood transfusion	2.07	N/A

CABG, Coronary artery bypass graft; CVA, cerebrovascular accident; N/A, not applicable; PCI, percutaneous coronary intervention; RBC, red blood cell; STEMI, ST-segment elevation myocardial infarction.

From Dehmer GJ, et al. A contemporary view of diagnostic cardiac catheterization and percutaneous coronary intervention in the United States. A report from the CathPCI Registry of the National Cardiovascular Data Registry, 2010 through June 2011. *J Am Coll Cardiol* 2012;60:2017-2031.

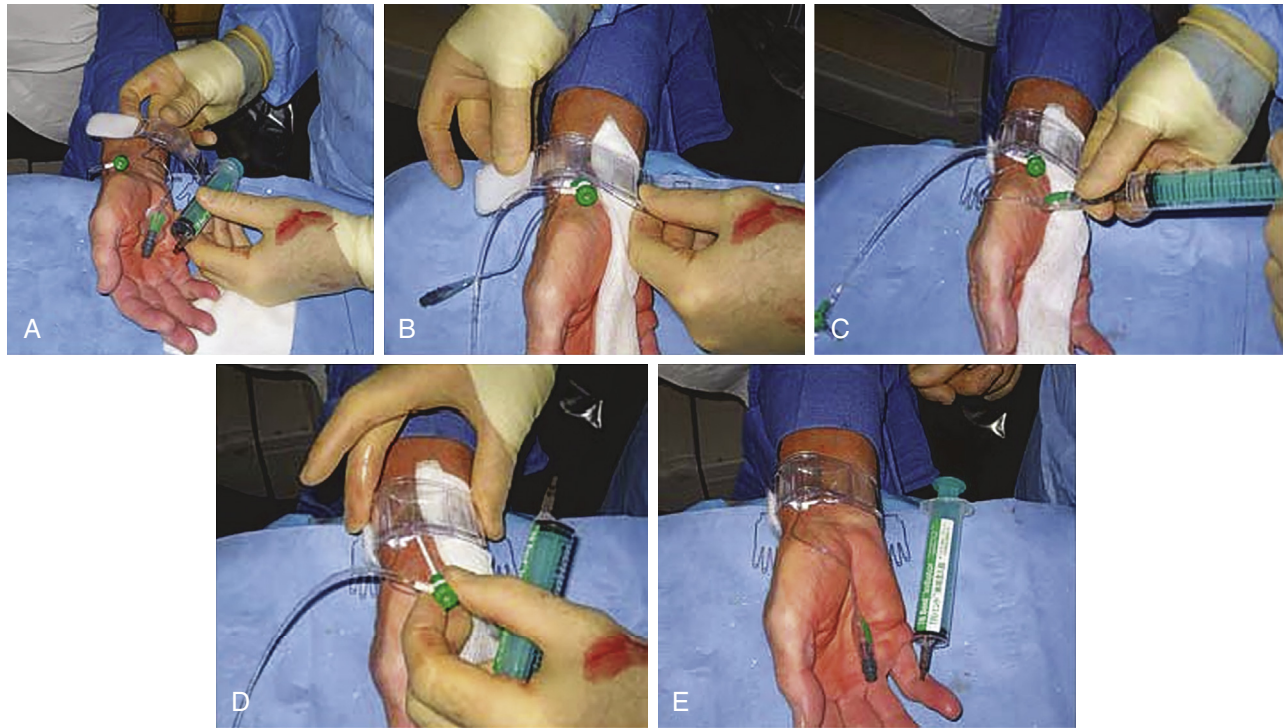


FIGURE 22.2 A, Radial sheath removal with Terumo band, which has an inflatable compression pad for hemostasis. B, Band is applied around the wrist with green dot over the arterial (not skin) puncture. A thin gauze wick is placed beneath the band to absorb blood when pressure is released to assess proper compression pressure in pad. C, Compression pad inflated. D, Sheath removed. E, Final result. (From Sorraja P, et al. *Kern's Cardiac Catheterization Handbook*. 7th ed. Elsevier; 2020, p 109.)

assist in identifying the point of needle entry, usually 1 to 3 cm below the inguinal ligament, in line with the palpable course of the CFA (Figs. 22.3 and 22.4). Superficial anatomic landmarks such as the inguinal crease can be misleading in obese as well as very thin individuals. Identifying the inferior edge of the femoral head by fluoroscopy using a hemostatic clamp is used to begin the puncture. Ultrasound imaging provides the best visualization and definition of the vascular location (Fig. 22.5) and has been shown to improve first-pass success rates and reduce vascular complications in general.⁵ Correct placement of the sheath in the CFA will reduce the chance of retroperitoneal hematoma (as occurs with puncture that are above the inferior epigastric artery) or pseudoaneurysm and arteriovenous fistula formation (as occurs with punctures below the profunda and superficial femoral artery bifurcation). Accidental cannulation of the superficial or profunda femoral artery may result in limb ischemia or inability to accommodate vascular closure devices.

Once localization of the vessel is completed, local anesthesia with 1% lidocaine is given and a small incision is performed followed by insertion of an 18- to 21-gauge needle into the CFA in a modified Seldinger technique (Fig. 22.6). Upon pulsatile blood return, a 0.038-inch guidewire is advanced and should pass freely through the vessel. Symptoms of pain or excessive resistance on wire advancement may indicate vascular trauma, such as dissections or perforations, and should be recognized immediately. The advantages of the Judkins technique are the relative ease, speed, and reliability, and yet vigilance is still required to ensure quality and safety.

After the procedure, femoral hemostasis can be achieved with a vascular closure device or with manual compression. Despite their perceived benefit, vascular closure devices are not superior to manual compression in general and may in fact be inferior in patients who have had multiple vascular access needle attempts. Vascular closure devices do play an important role in cases of large-bore (>10F) access which are now common in the era of TAVR with sheath sizes of 18F to 24F. Femoral sheaths should not be removed until the activated clotting time (ACT) is less than 160 to 180 seconds unless a vascular closure device is being used.

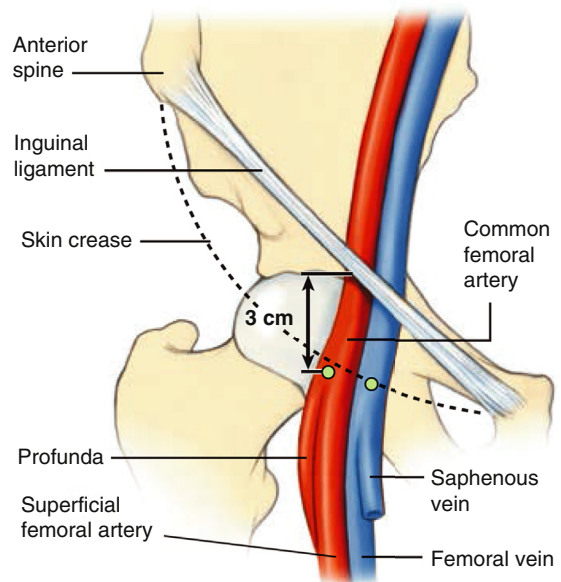
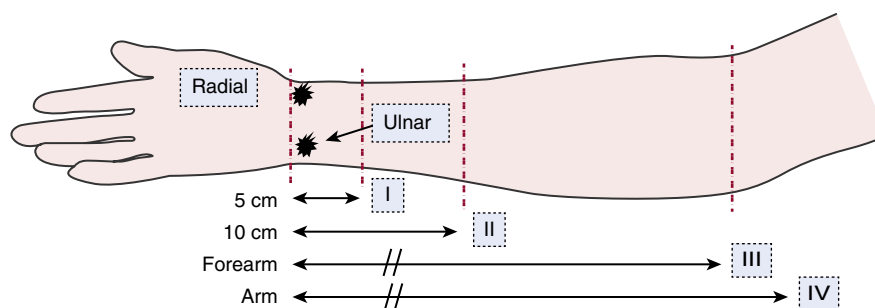


FIGURE 22.3 Regional anatomy relevant to percutaneous femoral arterial and venous catheterization. Diagram showing the right femoral artery and vein coursing underneath the inguinal ligament, which runs from the anterior superior iliac spine to the pubic tubercle. The arterial skin nick should be placed approximately 3 cm below the ligament and directly over the femoral arterial pulsation; the venous skin nick should be placed at the same level but approximately one fingerbreadth more medially. Although this level corresponds roughly to the skin crease in most patients, anatomic localization relative to the inguinal ligament provides a more constant landmark. (From Baim DS, Grossman W: *Percutaneous approach, including transseptal and apical puncture*. In Baim DS, Grossman W, editors. *Cardiac Catheterization, Angiography, and Intervention*. 7th ed. Philadelphia: Lea & Febiger; 2006, p 81.)

Patients with a history of peripheral arterial disease (PAD) require particular attention. Before the procedure, one should carefully review what types of interventions were performed in the past (e.g., balloon



Grade	I	II	III	IV	V
Incidence	≤5%	<3%	<2%	≤0.1%	<0.01%
Definition	Local hematoma, superficial	Hematoma with moderate muscular infiltration	Forearm hematoma and muscular infiltration, below the elbow	Hematoma and muscular infiltration extending above the elbow	Ischemic threat (compartment syndrome)
Treatment	Analgesia Additional bracelet Local ice	Analgesia Additional bracelet Local ice	Analgesia Additional bracelet Local ice Inflated BP cuff	Analgesia Additional bracelet, Local ice Inflated BP cuff	Consider surgery
Notes		Inform physician	Inform physician	Inform physician	STAT call to physician
Remarks	<ul style="list-style-type: none"> Control blood pressure (BP) (importance of pain management) Consider interruption of any anticoagulation and/or antiplatelet infusion Follow forearm and arm diameters to evaluate requirement for additional bracelet and/or BP cuff inflation Additional bracelet(s) can be placed alongside artery anatomy Ice cubes in a plastic bag or washcloth are placed on the hematoma Finger O₂ saturation can be monitored during inflated blood pressure cuff To inflate blood pressure cuff, select a pressure of 20 mmHg < systolic pressure and deflate every 15 minutes After bracelet removal, use "Velpeau bandage" around forearm/arm for a few hours to maintain mild positive pressure 				

EFigure 22.1 EASY trial hematoma grading scale with corresponding treatment strategies. (From Rao SV, et al. Clinical update: remaining challenges and opportunities for improvement in percutaneous transradial coronary procedures. *Eur Heart J* 2012;33:2521-2526.)

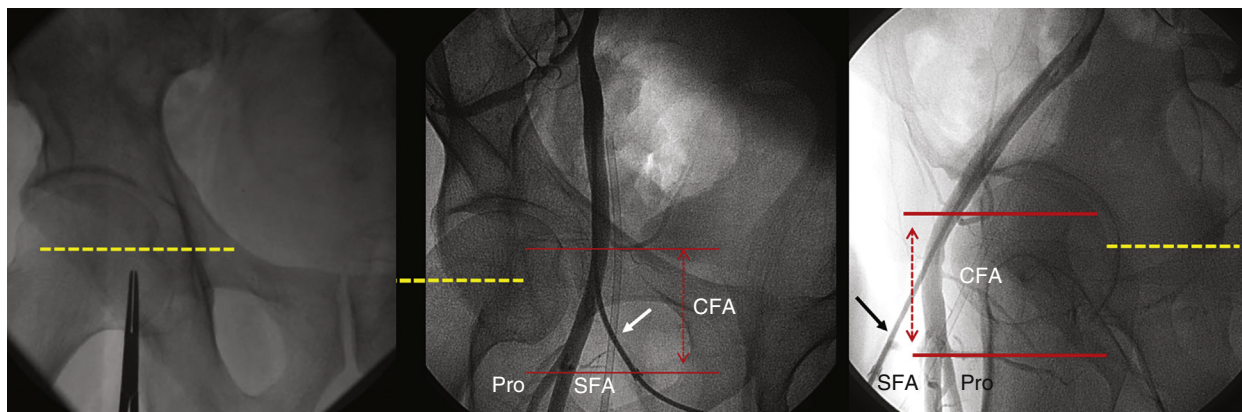


FIGURE 22.4 **Left**, Fluoroscopic localization of the skin nick (marked by the tip of the clamp). The middle of the femoral head is marked by the dashed yellow line. **Middle**, Angiogram of sheath in the femoral artery with a catheter (*arrow*) inserted in the common femoral artery. CFA is bounded by lower red line of the bifurcation of the superficial femoral artery (SFA) and profunda (Pro) branches and the upper red line of the inferior epigastric artery. **Right**, Lateral view of CFA (bounded by red lines) showing the relationship between the CFA and the bony femoral head, making manual compression effective.

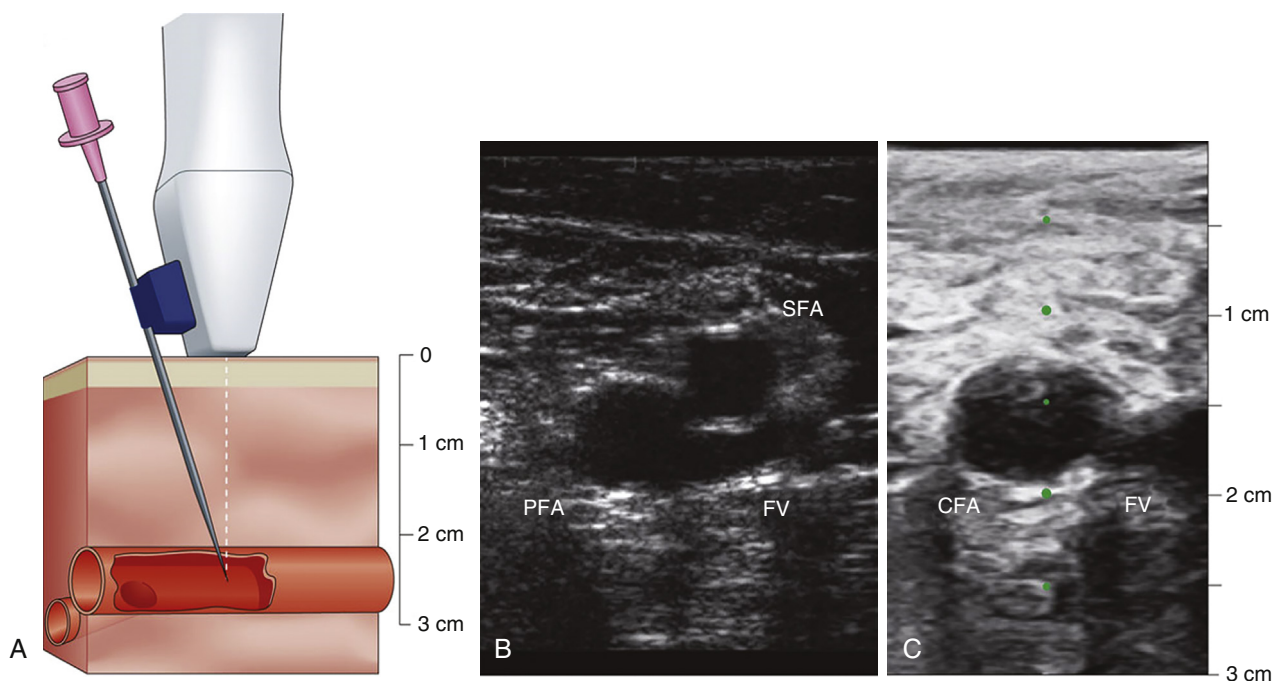


FIGURE 22.5 **Ultrasound-guided femoral artery access.** **A**, The attached needle guide fixes the needle’s angle of entry to intersect the vessel at the imaging plane 1.5 cm, 2.5 cm, or 3.5 cm below the skin, depending upon the guide chosen. The vessel bifurcation is kept inferior to the probe at the time of insertion. **B**, The right femoral artery bifurcation is imaged in the axial plane, identifying the separation of the profunda femoral artery (PFA) and superficial femoral artery (SFA). Compression is used to differentiate arteries from the femoral vein (FV). **C**, The probe is moved superiorly until the common femoral artery (CFA) is visualized. During needle advancement, the anterior wall of the vessel is kept under the central target line (*green dots*), which indicates the path of the needle. (From Seto A, et al. Real-time ultrasound guidance facilitates femoral arterial access and reduces vascular complications: FAUST (Femoral Artery Access with Ultrasound Trial). *JACC Cardiovasc Interv* 2010;3:751.)

angioplasty, patch endarterectomy, arterial conduits, and prosthetic grafts). The vascular anatomy should be defined for location and size such that large devices may be accommodated. Prosthetic peripheral vascular grafts are the most problematic vascular challenges, not because they cannot be cannulated but rather because of the lack of adequate closure and potential for thrombotic occlusion. For these reasons, these grafts are usually avoided. Complications arising from femoral access are outlined in [eTable 22.3](#).

Venous Access

Right-heart hemodynamic assessment is critical to accurately provide a set of differential diagnoses for the causes of dyspnea, the severity and types of pulmonary hypertension, and the determination of cardiac output, among others. Many patients may require simultaneous right- and left-heart pressure measurements. Venous access may use femoral, brachial, or internal jugular approaches.

Percutaneous Femoral Vein Access

Using the femoral arterial pulse as a landmark, the femoral vein sits approximately 1 cm medial to the femoral artery. If a combined arterial and venous access is needed, the entry skin area is infiltrated by lidocaine sufficient to cover both puncture sites. The venous puncture site is 0.5 to 1 cm medial and 0.5 to 1 cm caudal to the planned arterial entry site. Because venous pressure is low, a 10- or 20-mL syringe is attached to the Seldinger needle and gently aspirated during needle advancement. The operator inserts the needle through the skin at a 30- to 45-degree angle to the horizontal plane while palpating the femoral arterial pulse with light pressure so as to not occlude the vein. If arterial pulsations are felt at the tip of the needle, the needle is withdrawn and redirected at a slightly more medial angle. Ultrasound imaging guidance can improve successful cannulation and reduce accidental arterial puncture. Upon entry of the vein, venous (nonpulsatile) dark blood should flow easily into the syringe. If the vein has not been entered, the needle is withdrawn,

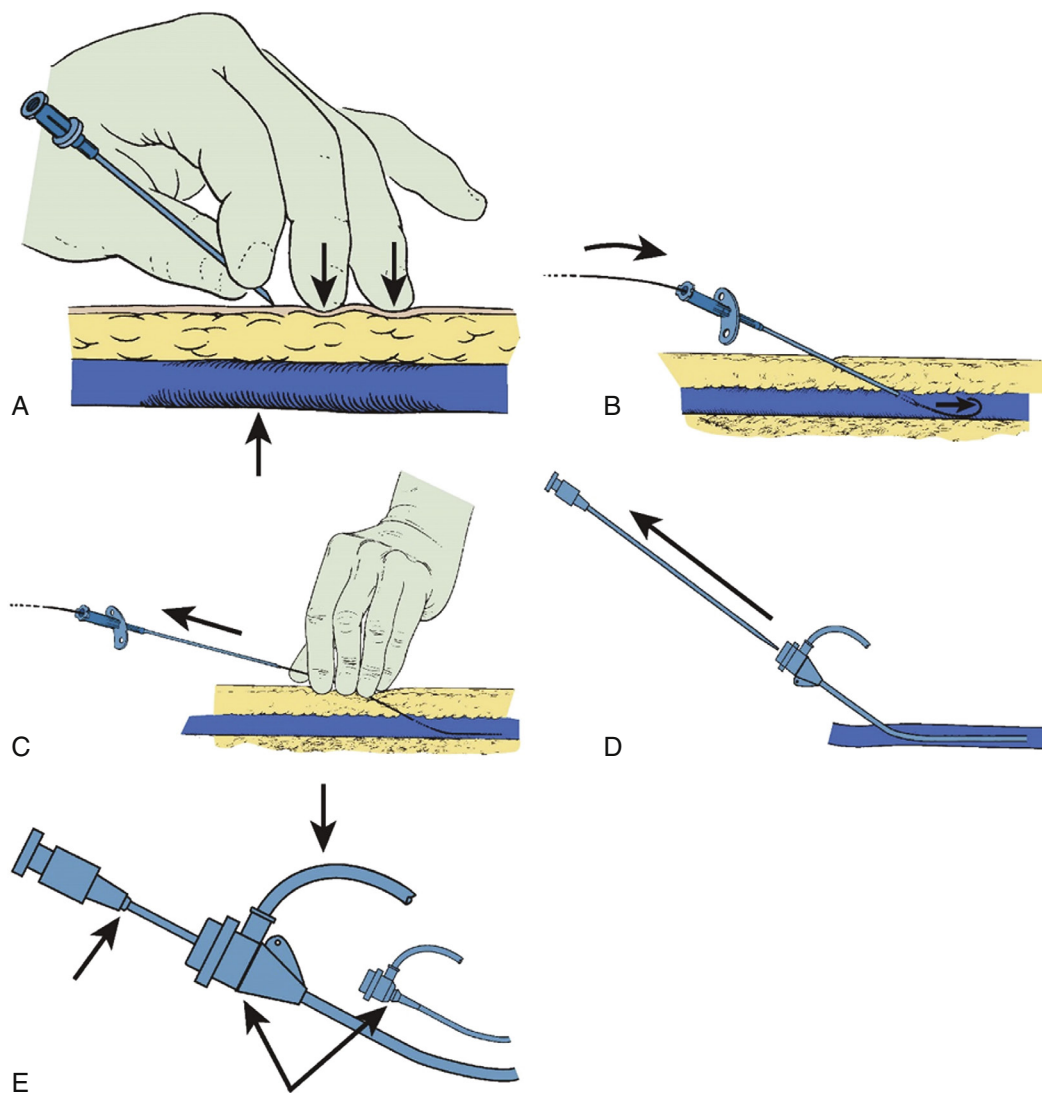


FIGURE 22.6 **A**, Femoral artery has been entered by a large-bore needle with backflow of blood. Note the operator's finger positions. As soon as the needle passes into the vessel through the anterior wall, brisk pulsatile flow occurs. This technique is called the "front wall stick." It prevents occult bleeding through the posterior wall. **B**, The flexible tip of the guidewire is passed through the needle into the vessel. **C**, Introducing a valve sheath into the artery. The needle is withdrawn, the artery is compressed, and the wire is pinched and fixed. **D**, The valve sheath is advanced over a guidewire, and the dilator and guidewire are removed. **E**, Arrows indicate position of sewing rings to attach valve to skin should prolonged insertion be required. (**A**, **B**, **C**, and **E** from Uretsky B, editor. *Cardiac Catheterization: Concepts, Techniques, and Applications*. Walden, Mass: Blackwell Science; 1997; **D** and **E** courtesy of Cordis Corporation, Miami, FL.)

flushed, and reintroduced in a slightly more lateral or medial direction. The remainder of the venous sheath placement is completed in the same fashion as described for the femoral arterial sheath insertion.

A vein that has been entered mistakenly during a femoral artery puncture attempt should be used only if the needle tip did not puncture both walls of the artery and go into the vein behind it. Placing a sheath through the artery into the vein may create an arteriovenous (AV) fistula or cause uncontrolled bleeding from a large hole in the posterior wall of the femoral artery.

After the procedure is completed, venous hemostasis can be achieved with light finger pressure applied over the vein as described for femoral artery sheath removal. Usually only 5 to 10 minutes of compression is needed to obtain adequate hemostasis.

Percutaneous Brachial Vein Access

In conjunction with radial artery catheterization, the brachial or antecubital vein may be considered for venous access for right-heart catheterization. Access to the antecubital vein can be obtained using a 20-gauge IV or ultrasound-guided needle puncture. Application of a tourniquet above the elbow will facilitate the identification of a suitable vein. A

medial antecubital vein is preferable over a lateral antecubital vein to avoid the acute angulation of the cephalic vein system as it joins with the axillary vein in the shoulder. Before sheath insertion, administration of 1% lidocaine over the puncture site will reduce discomfort. The arm vein sheath size is usually 5F sheath but can be as large as 7F with a suitably sized balloon-tipped pulmonary artery (PA) catheter. Advancing the PA catheter is often straightforward, but if venous tortuosity or valve obstruction is present, the operator can facilitate advancement with an angioplasty guidewire or use an injection of saline to straighten and stiffen the catheter and expand the vein. The balloon should not be expanded until the catheter is in the subclavian system.

Percutaneous Internal Jugular Vein Access

The internal jugular (IJ) vein, especially the right IJ, is the preferred venous access given the anatomic ease and for prolonged placement of sheath or PA catheter (Video 22.1). The IJ approach allows for greater patient comfort and lower infectious risk than a femoral approach, and is preferred over the subclavian approach because of reduced risk of pneumothorax. Use of a micropuncture kit with a 21-gauge needle and introducer will minimize inadvertent puncture of the carotid artery or

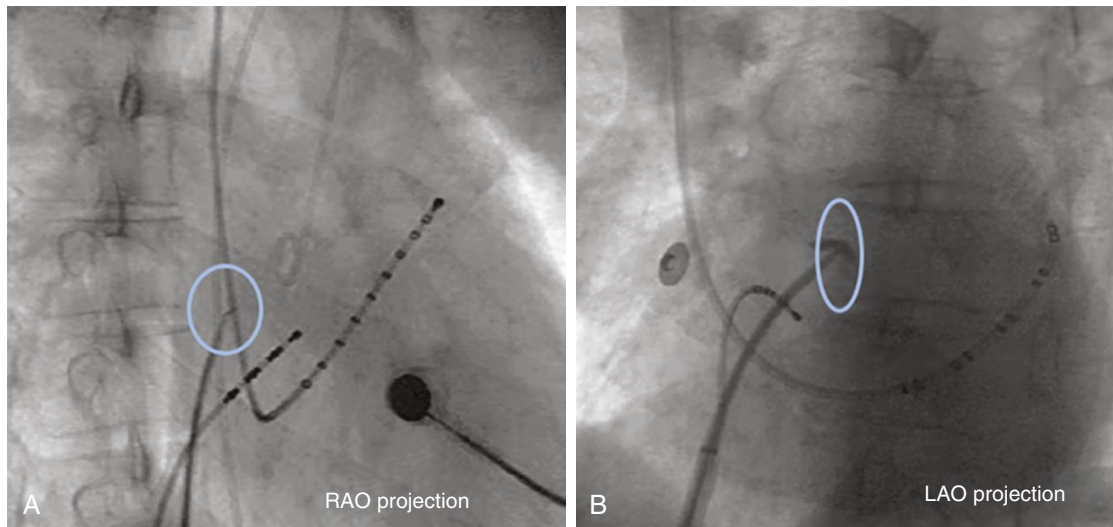


FIGURE 22.7 Septum crossing in fluoroscopy-guided transseptal puncture engaging the fossa ovalis in the right anterior oblique (RAO) (A) and left anterior oblique (LAO) (B) projections. Blue circle/oval indicate the fossa ovalis. Note the staining of the fossa ovalis in the LAO view. A pigtail is present in the RAO projection to mark the anterior location of the aorta.

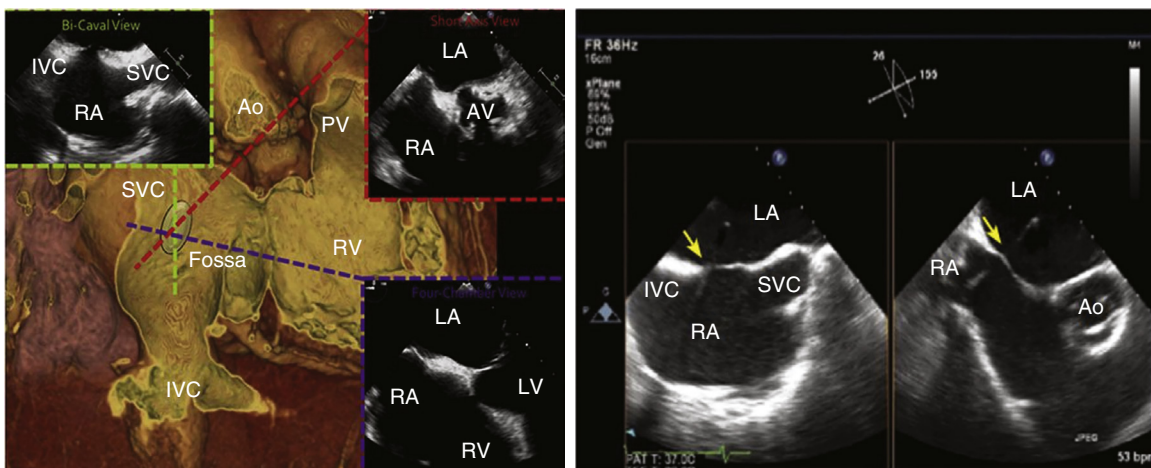


FIGURE 22.8 Biplane transesophageal echocardiography for transseptal puncture. AV, Aortic valve; PV, pulmonary vein; SVC, superior vena cava; other abbreviations as in Figure 22.2. (From Alkhouli M, et al. *JACC Cardiovasc Interv* 2016;9:2465-2480.)

lung. After entering the jugular vein, the micropuncture assembly can be exchanged for any larger sheath (e.g., 7F) for right-heart catheterization or right ventricular biopsy.

The internal jugular vein is located lateral to the carotid artery in the anatomic triangle of the two heads of the sternocleidomastoid muscle and the clavicle. For access, the patient is instructed to lie supine with the head turned 30 degrees to the contralateral side. Patients with low venous pressure may require leg elevation to increase venous filling volume. Routine use of ultrasound imaging facilitates localization of the IJ and can verify its patency. The use of ultrasound is recommended by national guidelines and reduces the overall risk of complications (carotid artery puncture, in particular) by 70%.⁶

Transseptal Catheterization

With increasing demands for certain structural heart disease evaluations and interventions (e.g., mitral valve disease) and some arrhythmia mapping procedures, transseptal catheterization has become an essential technique. In brief, the technique uses a right femoral venous access, through which a 0.032-inch guidewire and transseptal needle and catheter assembly is advanced into the right atrium and on into the superior vena cava (SVC). This catheter assembly is then brought back into the fossa ovalis using angiographic landmarks. Transesophageal or intracardiac echocardiography are also typically utilized, especially in difficult cases (e.g., large right atrium, postsurgical condition,

anatomic variant) (Figs. 22.7 and 22.8). Once confident in its correct position, the needle and catheter are advanced through the fossa ovalis and into the left atrium. Transseptal catheterization of the left atrium is described in detail elsewhere.⁷

Left-Heart Catheterization

Retrograde access to the left ventricle is commonly performed using a straight or angled pigtail-shaped catheter, initially advanced over a 0.035-inch J-tip guidewire and initially positioned at the level of the AV (Fig. 22.9). A common approach to crossing the AV is to position the pigtail catheter into the anterior sinus of Valsalva taking a “figure 6” configuration in the right anterior oblique (RAO) projection. The catheter is then pushed against the AV to form a U-shape. With deep inspiration, slight pullback and clockwise rotation, the tip loop usually falls across the valve into the left ventricle. Once inside the left ventricle, the catheter resumes a “figure 6” configuration with the loop directed toward the apex. Alternatively, the catheter can be positioned in front of the mitral valve, but not so deep as to interfere with its function or become entangled in the chordae. Repeated catheter repositioning may be required to eliminate ventricular ectopy.

With dilated aortic roots or horizontally oriented hearts, an angled pigtail catheter is preferable, whereas small aortic roots may require a right coronary Judkins for initial wiring and subsequent exchange for

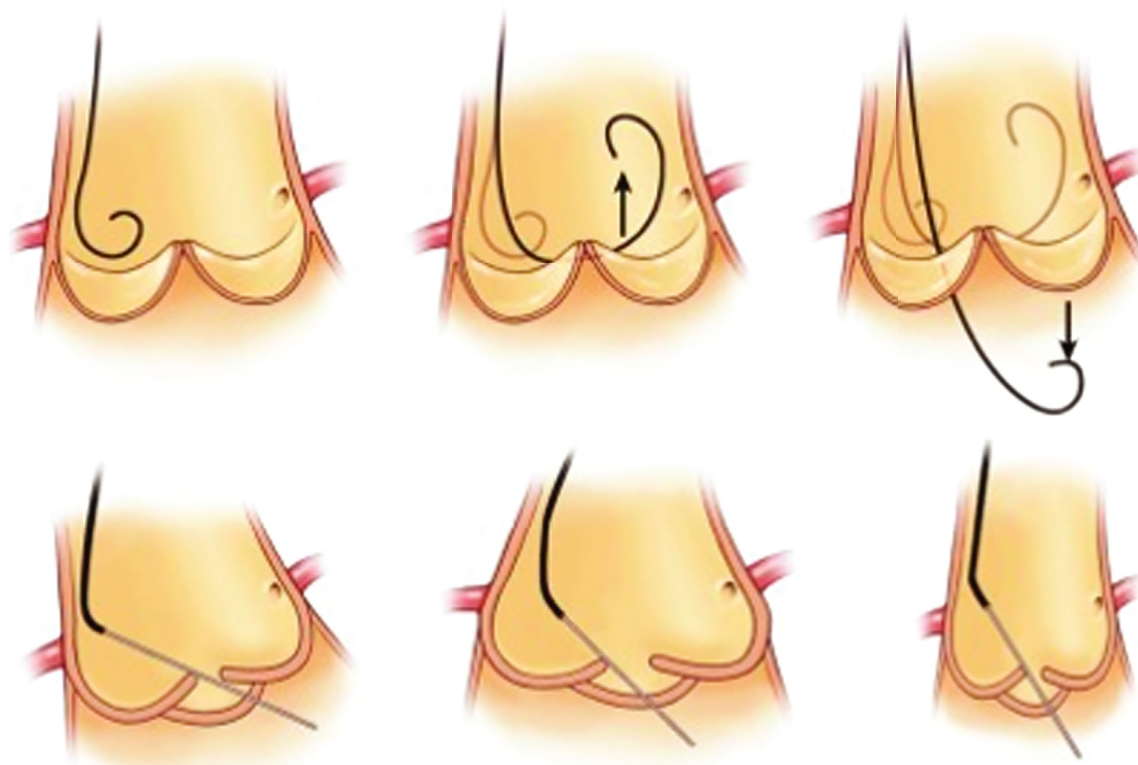


FIGURE 22.9 Technique for retrograde crossing of an aortic valve by a pigtail catheter. **Top row**, Technique for crossing a normal aortic valve. **Bottom row**: *Left*, Use of a straight guidewire and pigtail catheter in combination. Increasing the length of the protruding guidewire straightens the curve of the catheter and causes the wire to point more toward the right coronary ostium; reducing the length of the protruding wire restores the pigtail contour and deflects the tip of the guidewire toward the left coronary artery. When the correct length of wire and the correct rotational orientation of the catheter have been determined, repeated advancement and withdrawal of the catheter and guidewire together allow retrograde passage across the valve. *Middle*, In a dilated aortic root, an angled pigtail catheter is preferable. *Right*, In a small aortic root, a right coronary Judkins catheter may have advantages. In patients with bicuspid valves an Amplatz left catheter is often used because it directs the wire more superiorly. (From Baim DS, Grossman W. Percutaneous approach including transseptal and apical puncture. In Baim DS, Grossman W, editors. *Cardiac Catheterization, Angiography, and Intervention*. 6th ed. Philadelphia: Lea & Febiger; 2006, p 93.)

a pigtail catheter. In patients with bicuspid valves, a left Amplatz catheter directs the wire tip more superiorly and is also useful for placement of a guidewire into the left ventricle. A left Amplatz is also useful in patients with aortic stenosis, or a multipurpose catheter, depending on the angulation of the AV (more horizontal or more vertical). For sclerotic or stenotic AVs, straight rather than J-tipped guidewires facilitate probing of the AV orifice but also have greater potential for dislodging material from the AV or aorta with the risk of embolic ischemic events (including myocardial infarction and stroke).

For pressure measurements and contrast injections in the left ventricle, a pigtail catheter is preferred because of the high safety profile and inability to entrap the catheter tip in the LV musculature. Catheter tip entrapment leading to erroneous pressure signal readings is a problem for hypertrophic obstructive cardiomyopathy (HOCM) studies when end-hole catheters are used.

Aortic stenosis hemodynamics are best measured with simultaneous aortic and left ventricular (LV) pressures from a dual lumen catheter or use of a multipurpose catheter through which a 0.014-inch high-fidelity pressure sensor guidewire is advanced into the left ventricle while the catheter remains in the aorta. For gradients across the mitral valve, LV and pulmonary capillary wedge (PCW) or left atrial pressures are recorded simultaneously with two transducers. LV measurements include systolic, diastolic, and end-diastolic pressure; dP/dt can also be calculated. Details of obtaining and interpreting pressure measurements are discussed later in this chapter.

Right-Heart Catheterization

Right-heart catheterization is one of the central elements in the hemodynamic evaluation in the catheterization laboratory. The choice of venous access and catheter depends on the clinical presentation and patient-specific characteristics. The most commonly used right heart catheters

are pulmonary balloon-tipped flotation (e.g., Swan-Ganz) catheters with multiple lumens for pressure recording and a thermistor sensor for thermodilution-based cardiac output measurement (Fig. 22.10). Single-lumen balloon wedge catheters have similar rigidity, larger caliber, less catheter whip artifact, and thus higher fidelity for pressure measurement but lack the capacity to determine cardiac output by thermodilution.

A standard pulmonary balloon-tipped catheter is relatively easy to advance into the right atrium, the right ventricle, and on to the pulmonary artery and PCW position (Fig. 22.11). Although catheter location can be noted from pressure tracings alone, fluoroscopy is advisable, especially if any structural and functional difficulties (e.g., severe right atrial enlargement, severe TR, severe right ventricular [RV] dilation) are encountered or pacing/defibrillator leads are present. Even more so under the latter circumstances, fluoroscopy should be considered for a left IJ approach. Some maneuvering of the catheter may require guidewire assistance.

Technical Aspects and Artifacts of Pressure Measurements

Before addressing the normal and abnormal pressure waveforms used in the hemodynamic diagnosis of cardiac disease, a basic understanding of factors and artifacts affecting the accurate recording of pressure waveforms is required. A correct interpretation of the pressure waveforms requires confidence in the data. A *pressure wave* is the cyclic force generated by cardiac muscle contraction, and its amplitude and duration are influenced by various mechanical and physiologic parameters. The pressure waveform is influenced by the force of the contracting chamber. The waveform is also a function of chamber compliance, both intrinsic and extrinsic (i.e., the surrounding structures, including the contiguous chambers of the heart, pericardium, lungs, and vasculature). Physiologic variables of heart rate, respiratory cycle, and vascular resistance all influence the pressure waveform.

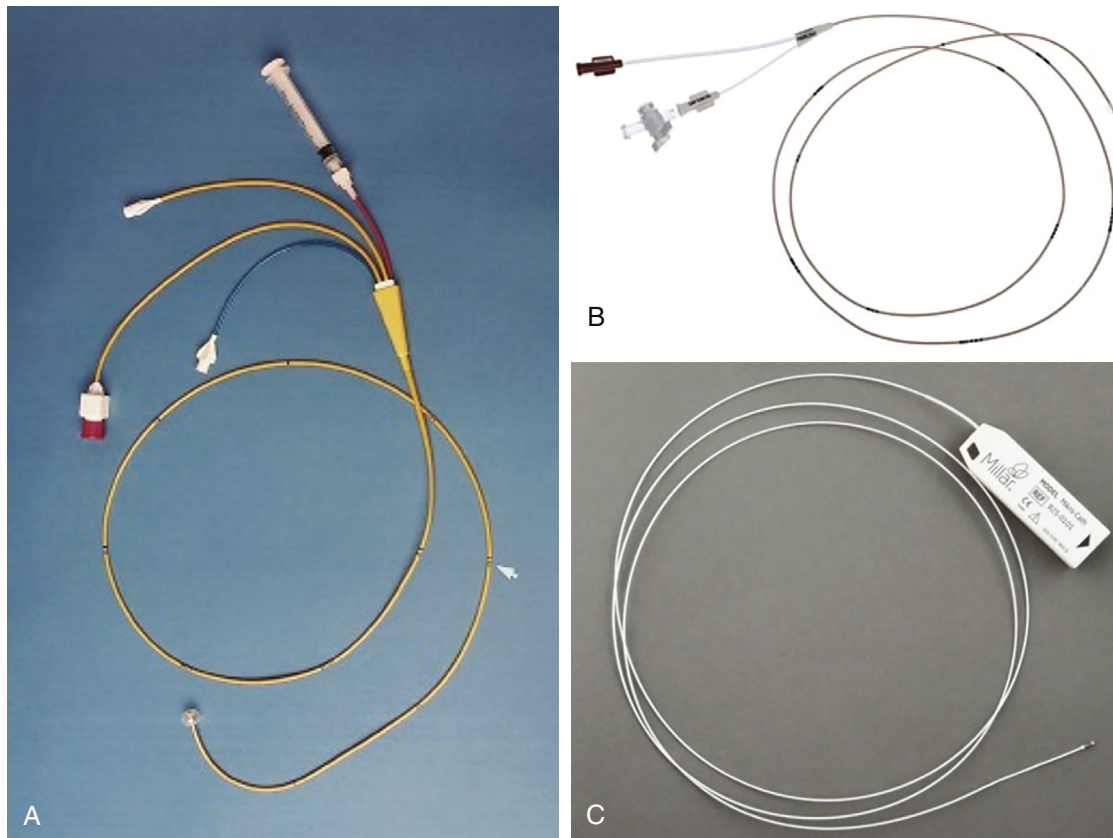


FIGURE 22.10 **A**, Typical Swan-Ganz catheter. The proximal ports, left to right, are the proximal injection hub, thermistor connector, distal lumen hub, and balloon inflation valve with syringe. The distal end of the catheter has a balloon and a distal end hole. The proximal injectate port exits 30 cm from the distal end of the lumen (arrow). The thermistor lies just proximal to the balloon. **B**, Example of a balloon wedge catheter, which has only one port besides the balloon inflation valve. **C**, Example of a diagnostic pressure catheter. (**A** from Davidson CJ, Bonow RO. Cardiac catheterization. In Mann DL, et al., editors: Braunwald's Heart Disease: A Textbook of Cardiovascular Medicine. 10th ed. Philadelphia: Elsevier; 2012, p 364; **B** from Arrow, Teleflex, Morrisville, NC; **C**, from Mikro-Cath, Millar, Houston, TX.)

Fluid-Filled Pressure Systems

Catheter-based pressure recording is accomplished by converting the force of the pressure wave from the catheter tip into an electrical signal by a transducer. A fluid-filled system (catheter plus tubing and connectors) transmits the pressure wave to the transducer in which the distortion of a diaphragm is converted into an electrical analog or digital signal to be visualized on the hemodynamic display monitor/recorder.

Various factors influence the pressure signal, which can impact signal accuracy. In such cases, the output amplitude would not be a true representation of the physiologic input amplitude. The most common technical artifacts of fluid-filled systems are underdamping (also known as excessive resonant artifact or ringing) (Fig. 22.12), overdamping (e.g., blunted waveforms), and improper calibrations or setting (i.e., zeroing) the transducer to atmospheric pressure. An output-to-input ratio less than 1 represents *damping* (dissipation of energy), as may be caused by friction. This cause of error can be reduced by using a short, wide-bore, noncompliant tubing system that is directly connected to the transducer. Damped signals are frequently associated with air bubbles, blood, or contrast in the tubing. Aspiration and catheter flushing with saline will produce more accurate measurements. The higher the density of the liquid (e.g., contrast media) within the catheter, the greater is the damping effect. Furthermore, any luminal compromise ("kink") of the catheter-tubing system is also a source of damping and needs to be considered with any unexpected or unexplained pressure drop (e.g., during extensive catheter torquing or manipulation). Another explanation for a damped signal may be catheter tip obstruction by small vessel orifices or by engagement against vessel walls or thrombus within a catheter. Other sources of error are related to catheter motion artifact or impacts on the catheter (internal) or tubing (external). An impact artifact (a brief, very high-frequency signal) can be noted when the catheter is struck by the walls or valves of the cardiac chambers.

Critical for all measurements is correct positioning (heart level) and calibration of the pressure transducer against atmospheric pressure, a

function known as *zeroing*. This is performed by placing the fluid-filled tubing to the transducer open to air at the level of the atria, which corresponds to the mid-axillary line. Because fluid-filled transducer signals may fluctuate over time, the signal may "drift" from its initial zero calibration. To address signal drift, all transducers should be zeroed immediately before any simultaneous recordings. Several key points to accurate pressure are summarized in eTable 22.4.

Micromanometer Catheters and Pressure Sensor Guidewires

Micromanometer pressure catheters and sensor guidewires allow for superior pressure recording because they have a miniaturized high-fidelity solid-state pressure transducer mounted at the tip, which eliminates the interposing fluid column and its damping effect as well as the 30- to 40-millisecond delay in wave transmission (see later). The pressure waveform is less distorted and the whip (motion) artifact is greatly reduced. High-fidelity catheters can assess the rate of rise in ventricular pressure (dP/dt), wall stress, rate of decay in ventricular pressure ($-dP/dt$), and time constant of relaxation (τ), and when coupled to impedance catheters can provide ventricular pressure-volume relationships. Catheters with two transducers separated by a short distance allow for accurate determination of gradients within chambers (e.g., intraventricular gradient in HCM) and across structures (e.g., stenotic AV). Some high-fidelity micromanometer systems allow for over-the-wire insertion and angiography.

Computations for Hemodynamic Measurements

When the pressure waveform data have been obtained, computations are made to quantify various cardiac and vascular functions. The most common computations and standard formulas are provided in Table 22.1. These computations provide metrics to determine cardiac work,

ETABLE 22.4 Key Points for Accurate Hemodynamics

1. Poorly collected or inaccurately obtained hemodynamic data can confuse or obscure the diagnosis and lead to improper therapy.
2. Properly collected data requires simultaneous electrocardiogram (ECG) tracings, accurate leveling or zeroing, an appropriate pressure scale (e.g., 0 to 200 mm Hg), and appropriate time scale.
3. The most common pressure wave artifact of a fluid-filled system is damping from blood or contrast in the catheter, which is easily resolved with a saline flush.
4. Exaggerated resonance or ringing of an underdamped pressure system can also occur and is resolved by using short stiff pressure tubing, properly debubbled lines, and calibrated recordings.
5. Correct interpretation of hemodynamic waveforms requires review of individual pressure waves and their timing to the ECG.
6. Distorted pressure waveforms on the hemodynamic tracing may be caused by an arrhythmia or conduction defect.

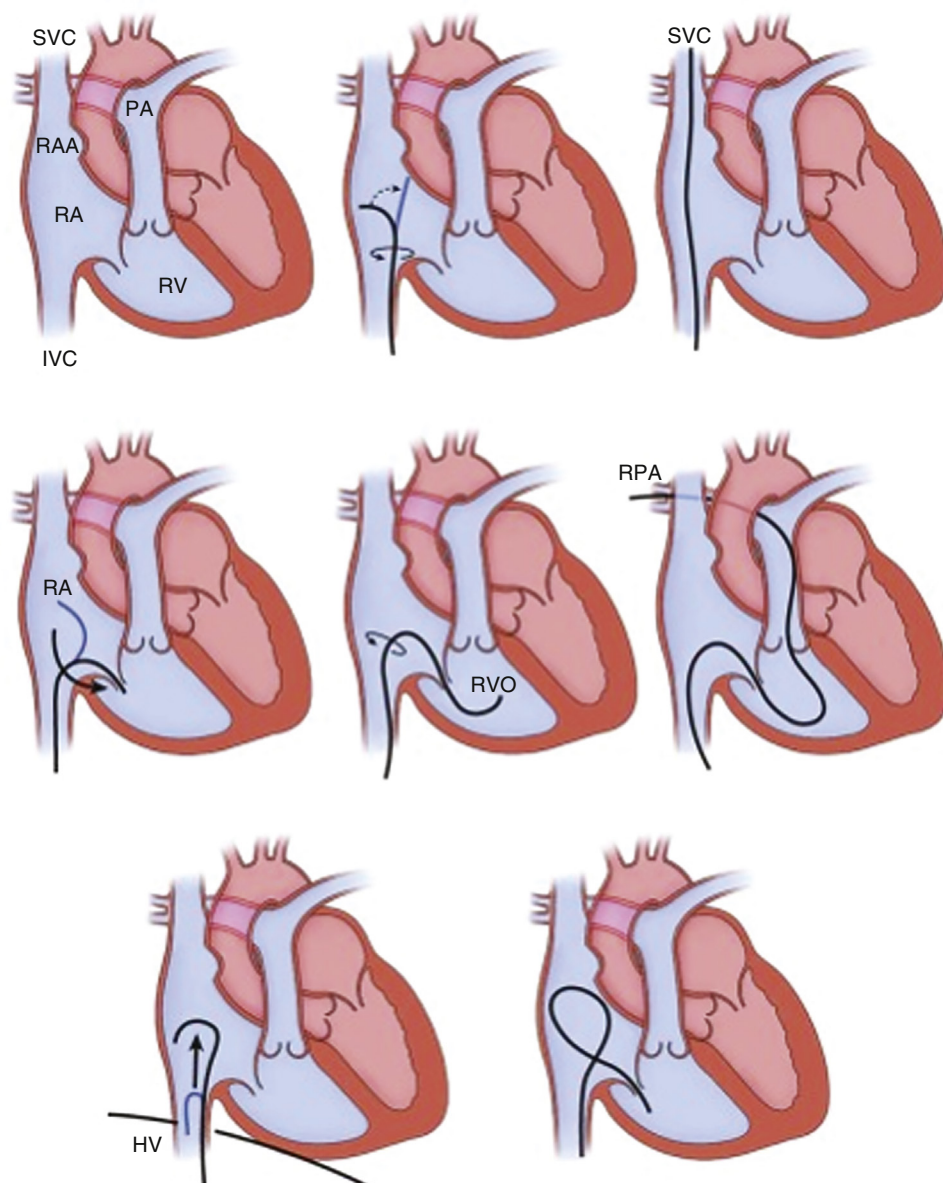


FIGURE 22.11 Right-heart catheterization via the femoral venous approach. **Top row**, The right-heart catheter is initially placed in the right atrium (RA) aiming at the lateral atrial wall. Counterclockwise rotation then directs the catheter posteriorly and allows advancement into the superior vena cava (SVC). Although it is not evident in the figure, clockwise catheter rotation into an anterior orientation would lead to advancement into the right atrial appendage (RAA) and thereby preclude SVC catheterization. **IVC**, Inferior vena cava; **PA**, pulmonary artery; **RA**, right atrium; **RV**, right ventricle. **Center row**, The catheter is withdrawn back into the RA and aimed laterally. Clockwise rotation causes the tip of the catheter to sweep anteromedially and cross the tricuspid valve. With the catheter tip in a horizontal orientation just beyond the spine, it is positioned below the RV outflow (RVO) tract. Additional clockwise rotation causes the catheter to point straight up and allows advancement into the main PA and from there into the right PA (RPA). **Bottom row**, Two maneuvers useful in catheterization of a dilated right heart. A larger loop with a downward-directed tip may be required to reach the tricuspid valve and can be formed by catching the tip of the catheter in the hepatic vein (HV) and advancing the catheter quickly into the RA. The reverse-loop technique (right) gives the tip of the catheter an upward direction, aimed toward the outflow tract. (From Baim DS, Grossman W. Percutaneous approach, including transeptal and apical puncture. In Baim DS, Grossman W, editors. Cardiac Catheterization, Angiography, and Intervention. 7th ed. Philadelphia: Lea & Febiger; 2006, p 86.)

flow resistance, valve areas, and shunts. Specific derivations and applications of these formulas can be found elsewhere.⁸

Cardiac Output Measurements

Catheterization-derived cardiac output measurements represent only estimates of the true cardiac output. The most common methods used in the catheterization laboratory are thermodilution and the Fick method.

Thermodilution Method

Thermodilution utilizes the indicator-dilution method for flow assessment with the indicator being temperature change after

injection of a saline bolus cooler than blood temperature. The faster the circulation or flow (i.e., cardiac output), the quicker the neutralization of the temperature change. A distal thermistor records the temperature change in the blood that is induced by injection of a set amount (10 cc) of room temperature (25°C) saline at the proximal injection port. The change in temperature over time is displayed as a curve function, and the cardiac output correlates inversely with the area under the curve. The cardiac output can be calculated provided that the temperature and volume of the injectate along with a computation constant from each pulmonary artery catheter are known (Fig. 22.13).

The advantage of this method is the relative ease of use and results. However, thermodilution is less accurate in patients with significant tricuspid or pulmonic regurgitation, intracardiac shunts, low cardiac output, or irregular rhythms.

Fick Method

As blood circulates, oxygen is extracted by the tissues at the capillary level. The degree of oxygen extraction is inversely proportional to the rate of oxygen delivery. The Fick method relies on this principle that blood flow (cardiac output) is inversely proportional to the extent of oxygen extraction, that is, the difference in the concentration of oxygen between arterial and venous blood and the rate of oxygen uptake in the lungs (Fig. 22.14). It further assumes that pulmonary blood flow (PBF) is equal to systemic blood flow (SBF) in the absence of an intracardiac shunt. In other words, the same number of red blood cells (RBCs) that enter the lung must leave the lung in the absence of an intracardiac shunt. Therefore, knowing the number of oxygen molecules attached to RBCs entering the lung, the number of oxygen molecules attached to RBCs leaving the lung, and the number of oxygen molecules added during travel through the lung, the rate of RBC flow through the lung can be determined. This can be expressed in the following terms:

$$CO = \frac{O_2 \text{ consumption } \left(\frac{\text{mL}}{\text{min}} \right)}{A - V_{O_2} \text{ difference } \left(\frac{\text{mL } O_2}{100 \text{ mL blood}} \right) \times 10}$$

where $A - V_{O_2}$ is the arterial-venous oxygen saturation difference. Oxygen consumption is best measured from a metabolic hood or cart. Because of limited metabolic cart availability, the oxygen consumption is more commonly estimated as 3 mL O_2 /kg or 125 mL/min/m² (generating an “assumed Fick” measurement). These estimated values may differ as much as 40% compared with the measured oxygen consumption. The arteriovenous oxygen difference is calculated from arterial–mixed venous (PA) O_2 content, where O_2 content = saturation \times 1.36 \times hemoglobin. For example, if the arterial



saturation is 95%, then the O_2 content = $0.95 \times 1.36 \times 13.0 \text{ g} = 16.7 \text{ mL}$, PA saturation is 65%, and O_2 consumption is 210 mL/min (i.e., $70 \text{ kg} \times 3 \text{ mL/kg}$) or a measured value. CO would be determined as follows:

$$\frac{210}{(0.95 - 0.65) \times 1.36 \times 13.0 \times 10} = \frac{210}{53} = 3.96 \text{ L/min}$$

In contrast to thermodilution, the Fick method retains accuracy in patients with low cardiac output and tricuspid regurgitation. However, the Fick method should not be used in patients with significant mitral regurgitation (MR) or AR and is not suitable under conditions of rapid changes in flow. Also, patients should not be on supplemental oxygen during the measurement period.

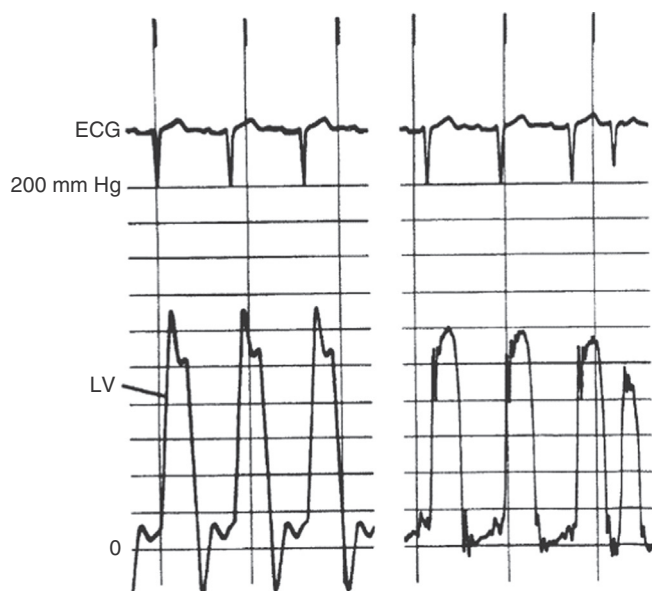


FIGURE 22.12 Left ventricular (LV) pressure with a 7F pigtail catheter using fluid-filled transducers. Left panel demonstrates “ringing” artifact with overshoot of the pressure signal during ejection and an exaggerated negative response during relaxation. On the right, a correctly damped LV pressure signal with minimal ringing during diastasis and no overshoot during systole. (From Kern MJ, et al. Hemodynamic Rounds. 4th ed. Elsevier; 2019.)

NORMAL RIGHT AND LEFT HEART WAVEFORMS AND VALVULAR HEMODYNAMICS INCLUDING HOCM (LVOT GRADIENTS)

The Cardiac Cycle and Generation of Pressure Waves

Dr. Carl J. Wiggers (1883–1963) was an eminent cardiovascular physiologist and the 21st president of the American Physiological Society. He is renowned for creating the classic diagram of cardiovascular physiology

TABLE 22.1 Common Hemodynamic Calculations

The cardiac index (CI, L/min/m²) is calculated as follows:

$$CI = \frac{CO \text{ (ml/beat)}}{BSA \text{ (m}^2\text{)}}, \text{ where BSA is body surface area.}$$

The stroke volume (SV, mL/beat) is calculated as follows:

$$SV = \frac{CO \text{ (ml/min)}}{HR \text{ (bpm)}}, \text{ where HR is heart rate.}$$

The stroke volume index (SI, mL/beat/m²) is calculated as follows:

$$SI = \frac{SV \text{ (ml/beat)}}{BSA \text{ (m}^2\text{)}}, \text{ where BSA is body surface area.}$$

The pulmonary vascular resistance (PVR, Wood units) is calculated as follows:

$$PVR = \frac{\text{mean pulmonary} - \text{mean LA pressure}}{\text{arterial pressure (or mean PCW)}} \times \frac{80}{CO}$$

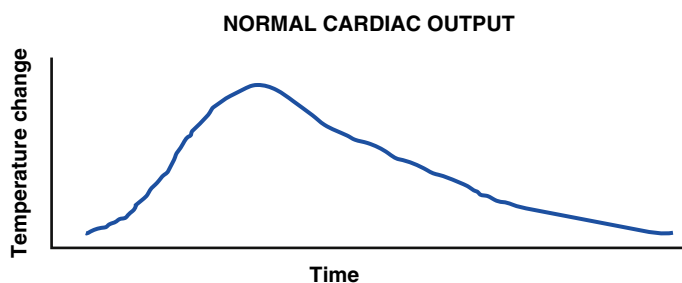
The total pulmonary resistance (TPR, Wood units) is calculated as follows:

$$TPR = \frac{\text{mean pulmonary arterial pressure}}{CO} \times 80$$

The systemic vascular resistance (SVR, Wood units) is calculated as follows:

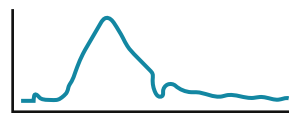
$$SVR = \frac{\text{mean systemic} - \text{mean right}}{\text{arterial pressure arterial pressure}} \times \frac{80}{CO}$$

Note: Resistance calculations follow the form of the Ohm law, $R = \Delta p/Q$, where R is resistance; Δp is mean pressure differential across the vascular bed; and Q is blood flow. Resistance units (mm Hg/L/min) are also called hybrid resistance units or Wood units. To convert Wood units to metric resistance (dynes \times s \times cm⁻⁵), multiply by 80.



$$Q = \frac{V \times (T_b - T_i) K_1 \times K_2}{T_b(t) dt}$$

Q = cardiac output
V = injected volume
T_b = blood temperature
T_i = injectate temperature
K₁ and K₂ = corrections for specific heat and density of the injectate and for blood and dead space volume
T_b(t) dt = change in blood temperature as a function of time



High cardiac output



Low cardiac output



Improper injection technique

FIGURE 22.13 Display of a normal cardiac output reading by the thermodilution method (top), which plots temperature change over time; the area under the curve is converted into flow L/min by the Stewart-Hamilton formula. Bottom, Configurations of thermodilution curves in high and low cardiac output states and with improper injection technique. (Modified from Davidson CJ, Bonow RO. Cardiac catheterization. In Mann DL, et al., editors. Braunwald’s Heart Disease: A Textbook of Cardiovascular Medicine. 10th ed. Philadelphia: Elsevier; 2012, p 364.)

that summarizes the cardiac cycle. By reviewing the electrical and mechanical activity of the heart as shown on the Wigger's diagram (Fig. 22.15), one can understand each of the pressure waves of the cardiac cycle.

The timing of mechanical events such as myocardial contraction and relaxation can be matched with an electrical stimulus as marked by the electrocardiogram (ECG). Each electrical event (e.g., P wave,

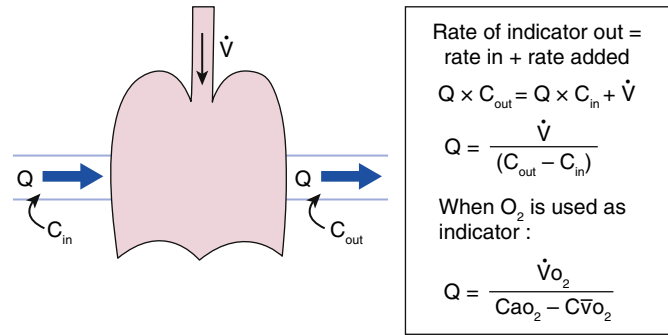


FIGURE 22.14 Schematic illustration showing measurement of flow by the Fick principle. Fluid containing a known concentration of an indicator enters a system at flow rate (C_{in}). As the fluid passes through the system, indicator is continuously added at rate, thereby raising the concentration in the outflow (C_{out}). In a steady state the rate of indicator leaving the system must equal the rate at which it enters plus the rate at which it is added. When oxygen is used as the indicator, cardiac output can be determined by measuring oxygen consumption, arterial oxygen content, and mixed venous oxygen content. (From Winniford MD, et al. Blood flow measurement. In Pepine CJ, et al., editors. Diagnostic and Therapeutic Cardiac Catheterization. 3rd ed. Baltimore: Williams & Wilkins; 1998, p 400.)

QRS, T wave) is followed normally by a corresponding mechanical function resulting in a specific pressure wave. The ECG P wave is responsible for atrial contraction. The QRS complex triggers ventricular activation beginning the generation of ventricular (LV or RV) pressure rise and ejection. The T wave is the signal for ventricular repolarization and muscular relaxation. This normal chronology of electrical-mechanical activity is disturbed by arrhythmias and conduction defects, while principally anatomic pathologies (valvular disease, cardiomyopathy, pericardial disease) will affect the characteristics of pressure waveforms but less often their sequence of activation.

Normal Pressure Waveforms

The cardiac cycle starts with the electrocardiographic P wave, which initiates atrial contraction. The pressure waves of atrial systole and diastole are denoted as the *a* wave (see Fig. 22.15) and *x* descent, respectively. The P wave is followed by the QRS, triggering depolarization of the ventricles. The LV pressure at the end of the *a* wave is called the end-diastolic pressure (also known as LVEDP). The LVEDP corresponds to the ECG R wave. About 15 to 30 msec after the QRS, the ventricles contract, the LV (and RV) pressure increases rapidly before blood is ejected. This phase is called the isovolumetric contraction period. When the LV pressure rises above the aortic pressure, the AV opens. Systolic ejection with matching increases in LV and aortic pressures continues until repolarization, signaled by the T wave, ends contraction and starts LV muscular relaxation with a corresponding fall in the LV and aortic pressures. When the LV pressure falls below the aortic pressure, the AV closes, forming the dicrotic notch on the aortic

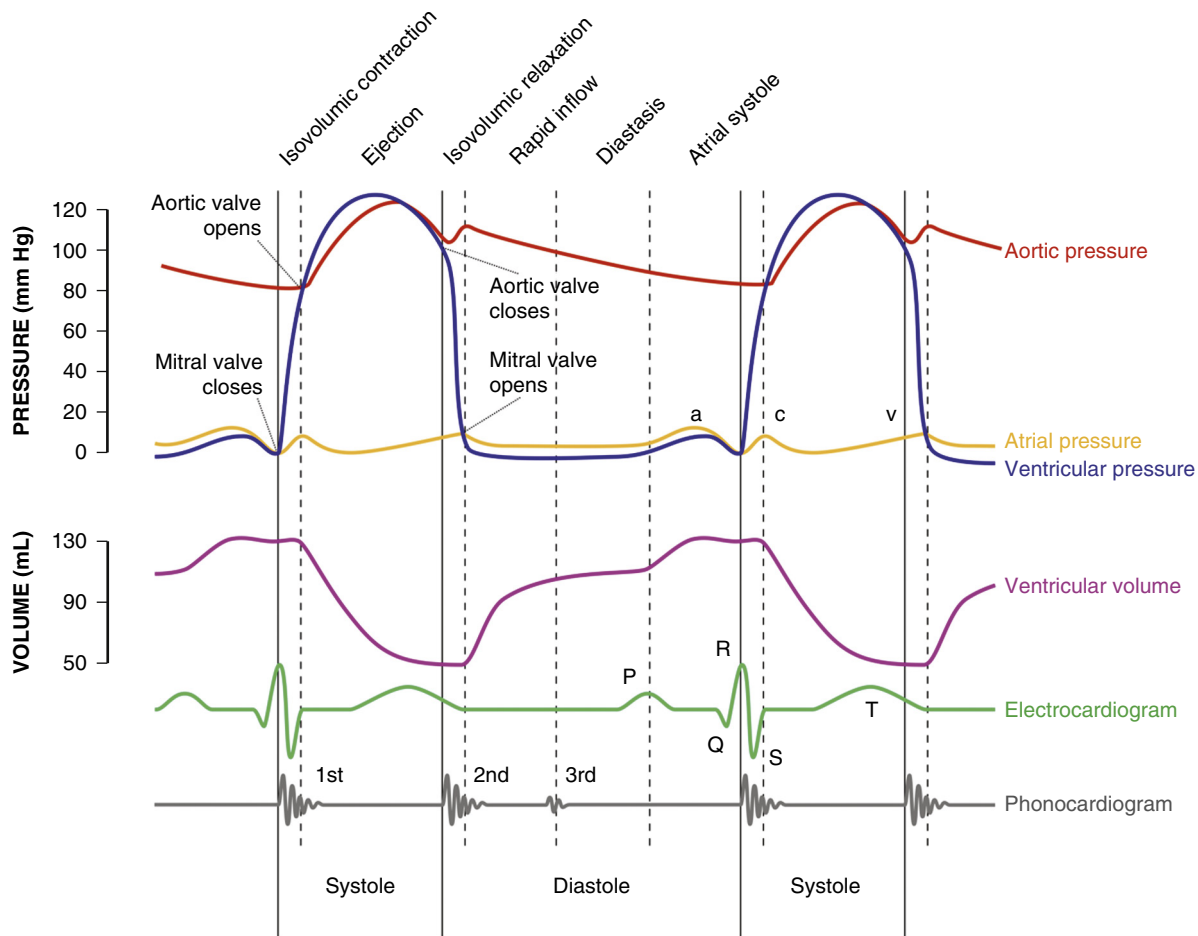


FIGURE 22.15 Wigger's diagram. Pressure curves of the left atrium and left ventricle are superimposed with the corresponding portions of the electrocardiogram at bottom. In the atrial pressure plot: wave *a* corresponds to atrial contraction, wave *c* corresponds to an increase in pressure from the mitral valve bulging into the atrium after closure, and wave *v* corresponds to passive atrial filling. In the electrocardiogram: wave *P* corresponds to atrial depolarization, waves *QRS* correspond to ventricular depolarization, and wave *T* corresponds to ventricular repolarization. In the phonocardiogram: The sound labeled first contributes to the S1 heart sound and is the reverberation of blood from the sudden closure of the mitral valve (left A-V valve) and the sound labeled "second" contributes to the S2 heart sound and is the reverberation of blood from the sudden closure of the aortic valve. (From https://commons.wikimedia.org/wiki/File:Wiggers_Diagram_2.svg.)

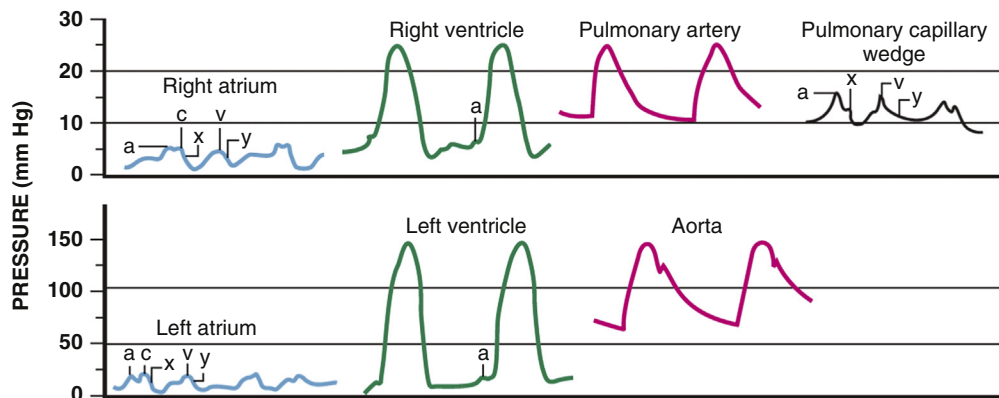


FIGURE 22.16 Normal pressure waveforms. From Normal right- and left-heart pressures recorded from fluid-filled catheter systems in a human. (In Zipes. Braunwald's Heart Disease: A Textbook of Cardiovascular Medicine. 7th ed.)

TABLE 22.2 Normal Pressure and Vascular Resistance Values

PRESSURE	MEAN (mm Hg)	RANGE (mm Hg)
Right Atrium		
a wave	6	2-7
v wave	5	2-7
Mean	3	1-5
Right Ventricle		
Peak systolic	25	15-30
End-diastolic	4	1-7
Pulmonary Artery		
Peak systolic	25	15-30
End-diastolic	9	4-12
Mean	15	9-19
Pulmonary Capillary Wedge		
Mean	9	4-12
Left Atrium		
a wave	10	4-16
v wave	12	6-21
Mean	8	2-12
Left Ventricle		
Peak systolic	130	90-140
End-diastolic	8	5-12
Central Aorta		
Peak systolic	130	90-140
End-diastolic	70	60-90
Mean	85	70-105
VASCULAR RESISTANCE	MEAN (DYNE-SEC • CM ⁻⁵)	RANGE (DYNE-SEC • CM ⁻⁵)
Systemic vascular resistance	1100	700-1600
Total pulmonary resistance	200	100-300
Pulmonary vascular resistance	70	20-130

waveform. The ventricular pressure continues to fall without a change in volume, a phase called isovolumic relaxation. When the LV pressure falls below the left atrial (LA) pressure, the mitral valve opens and the LA empties into the LV. The slope of the fall is LV pressure during the isovolumic period and is one of several indicators of normal or abnormal diastolic function.

Normal cardiac pressure waveforms are shown on [Figure 22.16](#) and reference values are defined for all hemodynamic parameters

in [Table 22.2](#). Intrathoracic pressure and respiration influence these values, particularly for the right-sided chambers. Inhalation leads to a drop in intrathoracic and right atrial pressure, and exhalation has the opposite effect. The reverse is true for patients on mechanical ventilation. Pressure measurements should be obtained at end-expiration for consistency and averaged over several respiratory cycles.

Atrial Pressures

Focusing on atrial physiology, the atrial waveform has three positive deflections or waves (*a*, *c*, and *v*) and two negative deflections or descents (*x* and *y*) ([Fig. 22.17](#)). The

a wave follows the P wave on the ECG and reflects atrial contraction, and atrial contractility and downstream resistance determine its height. Following the *a*, the *x* descent represents atrial relaxation and downward pulling of the tricuspid annulus as the right ventricle contracts. The *x* descent is interrupted by a second peak, the *c* wave, due to the atrioventricular (tricuspid or mitral) valve bulging into the atria during isovolumic ventricular contraction (early systole). Over the remainder of ventricular systole, atrial pressure slowly rises with atrial filling reaching its maximum at the end of ventricular isovolumetric relaxation, producing a peaked ventricular filling wave, the *v* wave. As ventricular pressure continues to drop below atrial pressure and the atrioventricular valve opens and ventricular filling begins, atrial pressure drops, called the *y* descent.

The pressure waveforms are strongly influenced by the specific pressure-volume relationship (also known as compliance) of the chamber in which the pressure is measured. The *a* wave is usually smaller than the *v* wave in the right atrium while the reverse tends to be true for the left atrium because the right atrium can easily decompress through the SVC and inferior vena cava (IVC), whereas the left atrium is constrained posteriorly by the pulmonary veins. While valvular regurgitation is often cited as one cause for large *v* waves, a highly compliant atrium may accommodate a large amount of volume from acute valvular regurgitation and produce only small *v* waves. Conversely, stiff, poorly compliant chambers can produce exaggerated pressure waves with normal filling volumes.

Pulmonary Capillary Wedge Pressure

The pulmonary capillary wedge pressure (PCWP) derived its name from advancing an end-hole catheter to the most distal part of the pulmonary artery and wedging it in place to register the pressure reflected through the pulmonary veins from the left atrium. A balloon-tipped (Swan-Ganz) catheter floated through the right heart to the pulmonary artery made this technique safer and more efficient. The PCWP is an indirect measure of the LA pressure transmitted through the pulmonary vein and pulmonary capillaries.

There are two common methods to confirm an accurate PCWP that closely agrees with LA pressure. The operator should confirm that PCWP wave is not a damped PA pressure by identifying clear *a* and *v* waveforms timed against the ECG or LV pressure. Fidelity is higher with the use of an end-hole catheter that is connected to the pressure transducer with stiff, short pressure tubing thoroughly flushed and bubble free. The operator should note the time delay (i.e., phase shift) of the PCW *v* wave to match the LV down stroke. The PCW position can also be confirmed by obtaining an oxygen saturation > 95% reflecting oxygenated pulmonary venous blood.

The PCWP waveform represents a slightly damped and delayed reflection of the left atrial pressure waveform, and *c* waves may not be seen ([Fig. 22.18](#)). With the normally low resistance of the pulmonary circulation, pulmonary artery diastolic pressure matches mean PCWP. This is not the case under circumstances of elevated pulmonary vascular resistance (hypoxemia, pulmonary embolism,

chronic pulmonary hypertension). Also, PCWP may not reflect left atrial pressure as accurately as needed for mitral valve assessment. In general, "over wedging" of the balloon catheter causes an excessively dampened signal leading to falsely low values, whereas "under wedging" with a signal contaminated in part by higher PA pressure leads to falsely high pressure readings. These two scenarios can

be recognized by the pressure waveform lacking its desired atrial waveform configuration: noticeably flat with over wedging and appearing as a dampened pulmonary artery pressure (PAP) tracing with under wedging (eFig. 22.2). For optimal left atrial pressure measurements, a transeptal puncture and direct chamber access should be used.

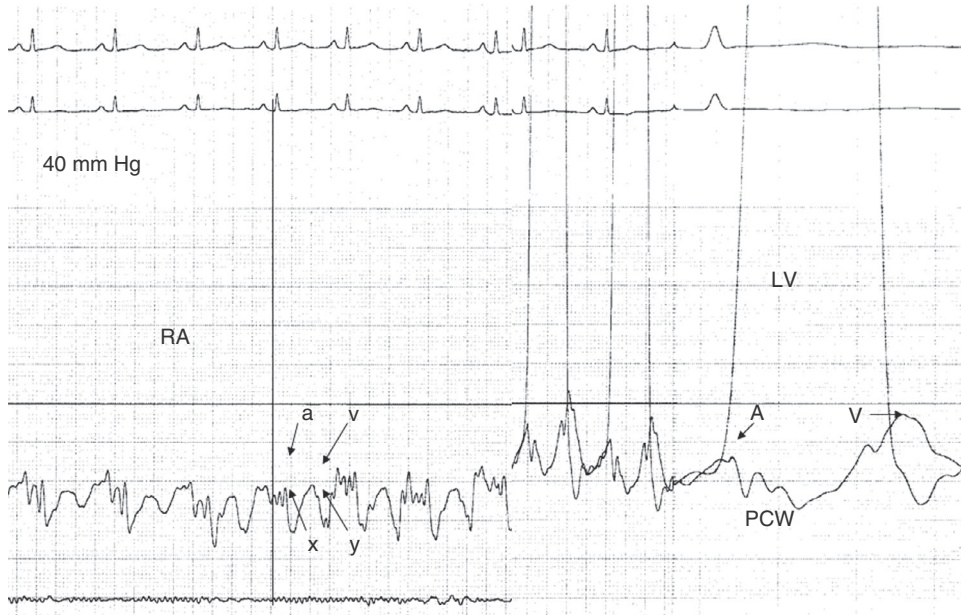


FIGURE 22.17 **Left**, Normal right atrial (RA) pressure with *a* and *v* waves and their associated *x* and *y* descents. The timing of any individual wave can be established from the ECG (vertical line from the R wave); in this case denotes atrial contraction. **Right**, Left ventricular (LV) and pulmonary capillary wedge (PCW) waveforms. The LA is usually higher than the RA and left-sided *v* waves are usually larger than right-sided *v* wave due to atrial chamber compliance and pressure.

Aortic and Pulmonary Artery Pressure Waveforms

During systole, ventricular ejection transmits pressure to the great vessels (aorta and pulmonary artery) through the semilunar aortic and pulmonary valves. Normally, the upstroke of aortic pressure matches that of the LV pressure. As diastole begins, peak aortic and ventricular pressures decline together until LV pressure falls below aortic pressure at which time the AV closes producing an abrupt cessation of the pressure signal, the dicrotic notch. Aortic pressure slowly dissipates as blood is distributed into the peripheral vascular circulation. An identical but lower amplitude set of waveforms is observed for the right ventricle and pulmonary artery. The shape and magnitude of the aortic pressure is also the result of systemic wave reflections and summation. eFigure 22.3 illustrates the contribution of a forward and a backward-traveling (reflected) wave contributing to pressure changes in the central aorta in a healthy subject and in a patient with hypertension. In the normal subject,

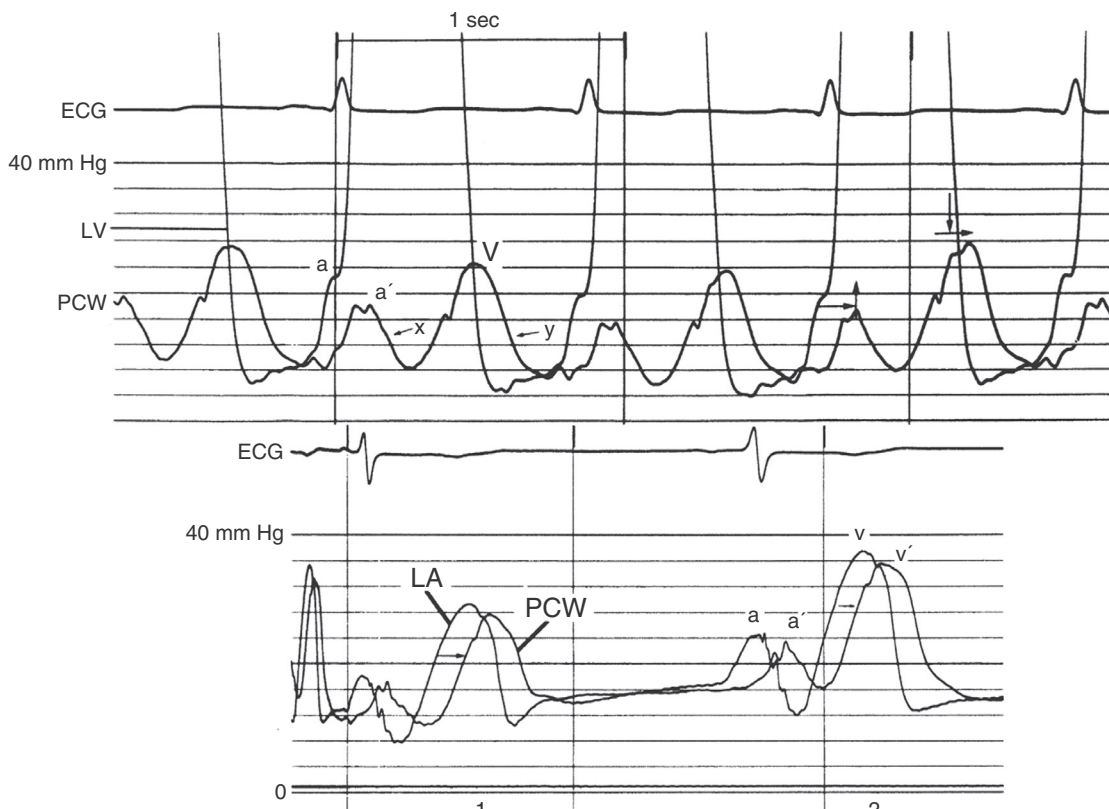


FIGURE 22.18 **Top**, Simultaneous left ventricular and pulmonary capillary wedge pressures (PCWPs) measured with fluid-filled catheters. Note the delay in pressure waves in the PCW compared with the LV, particularly the *a* and *a'* waves. The *v* wave from the PCW is also delayed on or after the LV downstroke. **Bottom**, Simultaneous LA and PCW tracings showing time delay in the PCW relative to the LA pressure waves.

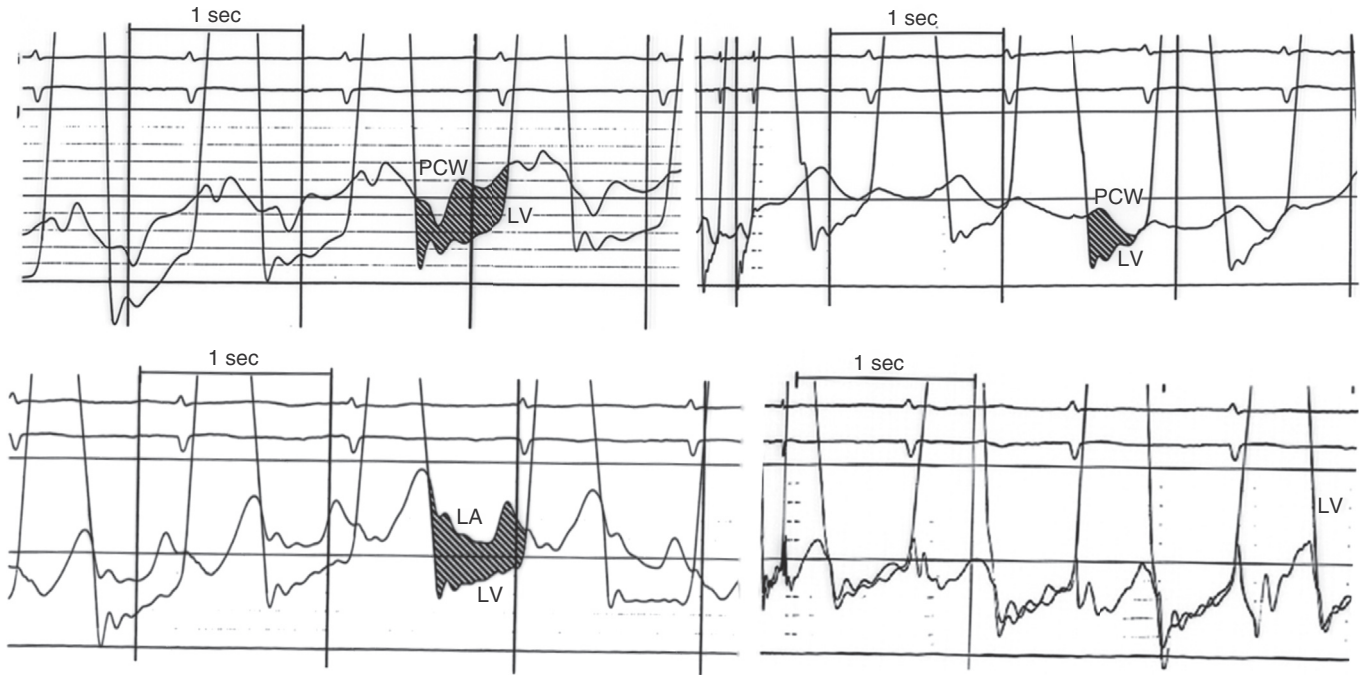


FIGURE 22.2 Pulmonary artery wedge pressure (PAWP) readings are most obtained by balloon-tipped flotation catheter. Because these catheters are soft with small lumens, PAWP waveforms may be damped (*top left*) or have excessive motion artifact leading to erroneous values suggesting a transmittal gradient (*top right*) may be present when it is not after confirming with a transeptal LA pressure catheters (e.g., Brockenbrough or Mullins-type sheath) (*bottom left and right*). Waveform fidelity with stiff with large lumen LA catheters is superior. However, in most clinical settings, PCWP is sufficient to assess LA and LV filling pressures. In patients with mitral valvular disease or mitral valve prostheses, transeptal LA catheterization is preferred over PCWP measurements. (From Kern MJ, et al., editors. Hemodynamic Rounds: Interpretation of Cardiac Pathophysiology from Pressure Waveform Analysis. 4th ed. New York: Wiley-Liss; 2018, p 285.)



FIGURE 22.19 Normal LV and aortic pressures. **Left**, Micromanometer dual transducer pressure catheter with near ideal waveforms of aortic and left ventricular pressure. *Red arrow* denotes anacrotic shoulder and small normal impulse LV outflow tract gradient. **Right**, Pressures measured with fluid-filled transducer systems using 5F pigtail catheter through a 6F femoral artery sheath side arm. Note the resonant artifact (fling or ringing, *blue arrow*).

the backward-traveling wave arrives at end-systole and contributes to the closing of the AV and to increasing diastolic perfusion pressure. In the hypertensive subject (eFig. 22.3, right side), the backward-traveling wave reaches the proximal aorta in early systole and contributes to the late systolic peak in pressure. The magnitude of the reflected wave (and the late systolic pressure) has a well-validated and independent prognostic significance.⁹

Ventricular Pressure Waveforms

The LV pressure reflects the ejection force of blood into the higher resistance circuit of the systemic circulation while the RV ejects into the lower resistance pulmonary circuit. Although similar in morphology, the right and LV pressure differ in magnitude, timing of activation, and force of contraction. Under normal conditions, the magnitude of the LV waveform is significantly higher than that of the RV waveform. The duration of LV systole, isovolumic contraction, and relaxation are longer, and the ejection period is shorter than that for the right ventricle. In the early rapid-filling phase of diastole, ventricular pressures initially drop quickly below atrial pressures (often producing suction, i.e., a LA-LV gradient promoting rapid ventricular filling). Across diastole, as the LV fills, ventricular pressure rises, reaching a plateau (diastasis) ending in a more rapid upward deflection due to atrial contraction (the ventricular *a* wave). The end diastolic pressure after the *a* is taken at the onset of isovolumic contraction usually corresponding to the R wave on the simultaneous ECG (Fig. 22.19).

Normally, the LVEDP is only marginally higher than the PCWP but in certain states, such as hypertrophy or other causes of low ventricular compliance, it can be significantly higher. Although this post-*a* LVEDP value represents the true preload exerted on the ventricle, the PCWP correlates better with a pre-*a* LVEDP, which reflects the mean LV filling pressure.

Evaluation of Valvular Heart Disease

Cardiac catheterization and hemodynamic evaluation plays an important part in the diagnosis of patients with valvular pathology,

particularly if there is discordance in the estimated degree of severity by physical examination and noninvasive tests such as echocardiography. The need for hemodynamic evaluation depends on the accuracy of the echocardiographic data, invasive assessment being most valuable in borderline or low-flow clinical states.

Calculation of Stenotic Valve Orifice Areas

The orifice area of a valve can be calculated from hydraulic principles. The volume of flow (*F*) across an orifice equals the area of the orifice (*A*) times the velocity of flow (*V*): $F = A \times V$, and accordingly, the orifice area can be calculated as $A = F/V$. *F* equals the cardiac output, and *V* can be calculated from the transvalvular gradient based on a special case of the Bernoulli principle called Torricelli's law:

$$V = \sqrt{2gh}$$

where *g* is the effect of gravity and *h* the pressure gradient (derived from the height of a water column).

Gorlin and Gorlin refined this equation in 1951, which has become known as the "Gorlin formula" for the calculation of valve areas¹⁰:

$$A = F / (C_c \times C_v \sqrt{2gh})$$

C_c is the coefficient of orifice contraction, which accounts for the fact that fluids tend to move through the center of an orifice, generating a physiologic orifice that is smaller than the anatomic orifice. C_v is the velocity coefficient, which allows for the pressure gradient not being fully converted to flow because some of the velocity is lost to friction. Neither of these two coefficients has ever been determined. Instead, an empiric value has been used to align the calculated area with the actual area on autopsy or surgery in 11 patients with mitral valve disease. The maximal discrepancy between the actual mitral valve area and calculated values was just 0.2 cm² for a constant *C* of 0.85. Importantly, such direct comparison data have never been obtained for any of the other three valves, and not even empiric constants were developed for these. Rather, a constant of 1.0 has been assumed for any valve

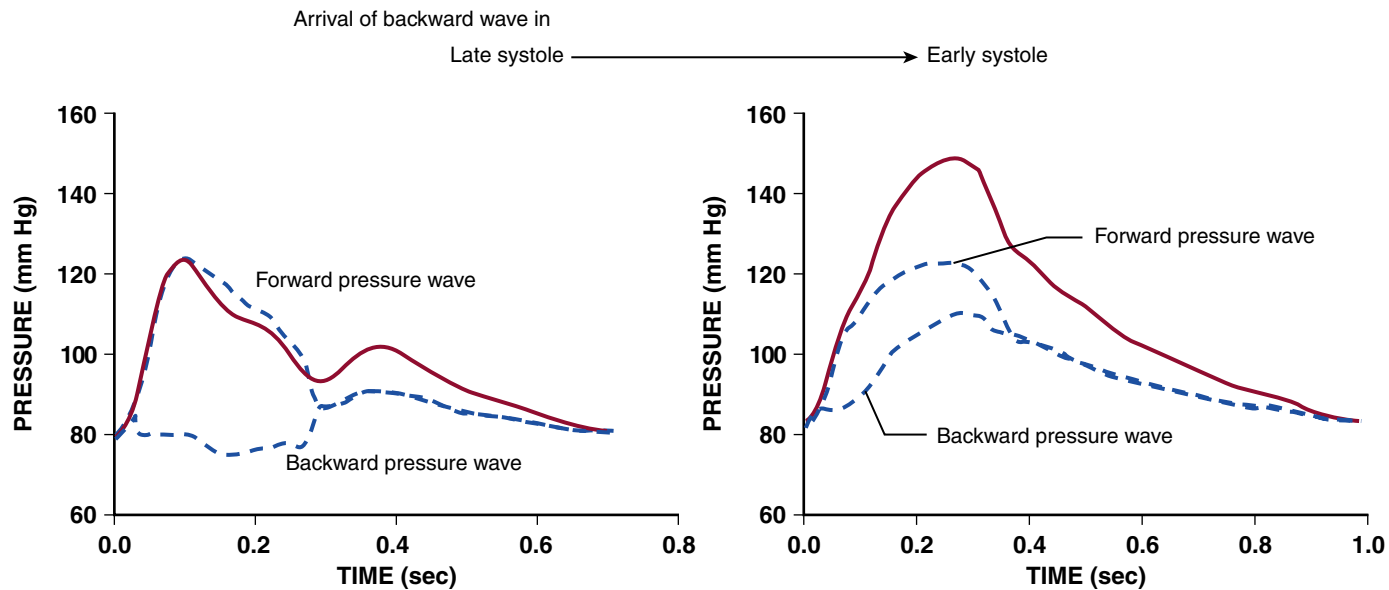


FIGURE 22.3 A forward and a backward-traveling (reflected) wave contribute to pressure changes in the central aorta. In the young and healthy subject on the left, the backward-traveling wave arrives at end-systole, contributing to closing the aortic valve and to increasing diastolic perfusion pressure. In the hypertensive subject on the right, the backward-traveling wave reaches the proximal aorta in early systole and contributes to the late systolic peak in pressure. The magnitude of the reflected wave (and the late systolic pressure) has a well-validated and independent prognostic significance. (From Nagueh SF. *J Am Soc Echocardiogr* 2016;29:277-314.)

other than the mitral valve, which points out that the derived areas are best estimates only.

To derive a more accurate AV area, because flow across the AV occurs only during systole, the cardiac output is divided by the actual systolic ejection period (SEP), the period from opening to closure of the AV, times the heart rate (HR). In agreement with the Gorlin formula and factoring in a combined constant of 44.3 for C_c and C_v , the AV area (AVA) can be calculated as follows:

$$\text{AVA (cm}^2\text{)} = \frac{[\text{Cardiac output (mL/min)} \div (\text{SEP} \times \text{HR})]}{\div [44.3 \times \sqrt{\text{Mean gradient}}]}$$

The normal AVA is 2.6 to 3.5 cm² in adults. Valve areas <1.0 cm² represent severe aortic stenosis.

The calculation is similar for the mitral valve area (MVA). Because mitral flow occurs only during diastole, cardiac output is corrected for the diastolic filling period (DFP), the period of opening to closure of the mitral valve, yielding the following formula:

$$\text{MVA (cm}^2\text{)} = \frac{[\text{Cardiac output (mL/min)} \div (\text{DFP} \times \text{HR})]}{\div [37.7 \sqrt{\text{Mean gradient}}]}$$

The normal MVA is 4 to 6 cm², and severe mitral stenosis is present with valve areas smaller than 1.0 cm².

A simplified formula has been proposed by Hakki and colleagues.¹¹ The effects of SEP and DFP are relatively constant at normal heart rates, which leads to the following equation:

$$\text{AVA (cm}^2\text{)} = \frac{\text{Cardiac output (L/min)}}{\div \sqrt{\text{Peak LV} - \text{peak Ao or Mean gradient}}}$$

Of note, mean aortic transvalvular gradient and peak-to-peak gradient yield similar correlation with the Gorlin formula and thus can be used in this formula. For the MVA, only the mean gradient was validated:

$$\text{MVA (cm}^2\text{)} = \frac{\text{Cardiac output (L/min)}}{\div \sqrt{\text{Mean gradient}}}$$

The valve area estimated by using the Hakki formula can differ by almost 20% from the valve area using the Gorlin formula in patients with bradycardia or tachycardia. As readily evident from the formulas, the accuracy of the measurements of pressure gradient and cardiac output is critical for obtaining the correct valve values, which are a major determinant for management decisions.

There are several sources of errors in the valve area calculations. Because the square root of the mean gradient is used, miscalculation of the cardiac output leads to more erroneous valve areas than miscalculation of the gradient. The imprecision in calculating the cardiac output is greatest in patients with a low cardiac output, in whom the pressure gradient is often inappropriately low and the severity of stenosis relies even more on accurate valve area determinations. In these patients, as well as in those with tricuspid regurgitation (TR), the Fick method should be used. Both the thermodilution and the Fick method overestimates stenosis severity in patients with mixed valvular disease (stenosis and regurgitation) of the same valve. If both AR and MR are present, accurate assessment of either the aortic or the MVA is not possible.

Inherent to the Gorlin formula area calculation is the dependence on transvalvular flow. Although greater flow could lead to greater opening pressure and thus greater valve area, correlation studies with planimetry by transesophageal echocardiography (TEE) argue against this occurring. Accordingly, even under increasing flow conditions, the AVA by planimetry remains unchanged, whereas it increases with use of the Gorlin formula, suggesting that at high flow states the Gorlin equation may overestimate true valve area.

Aortic Valve Stenosis

Aortic stenosis is one the most common valvular stenosis encountered in practice. For optimal hemodynamic assessment of the AV, simultaneous aortic and LV pressures are required. A single pressure pullback recording from the left ventricle into the aorta should only be used as a screening technique given the risk that premature contractions

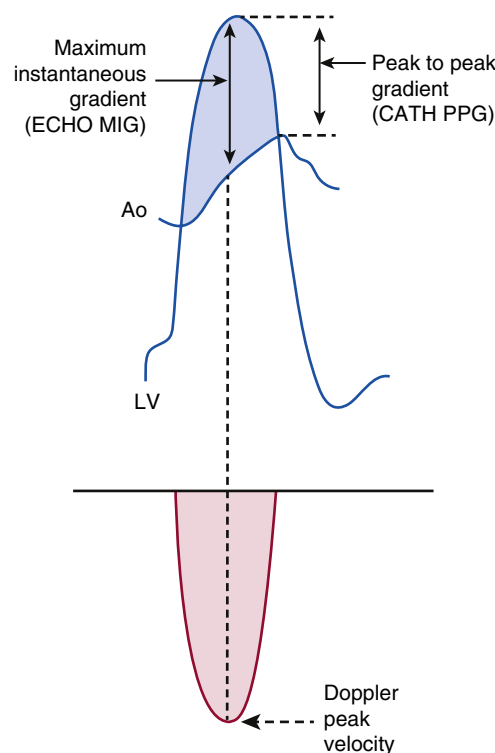


FIGURE 22.20 **Top**, Simultaneous left ventricular (LV) and central aortic (Ao) pressures in a patient with aortic stenosis. The optimal way to measure the gradient in a patient with aortic stenosis is to use these simultaneous pressures. The peak-to-peak gradient is the difference between the peak left ventricular and peak aortic pressures, which is a nonphysiological measurement because the peak pressures occur at different points in time. The mean pressure gradient (the integrated gradient between the left ventricular and aortic pressure throughout the entire systolic ejection period) should be used to determine the severity of the aortic stenosis. **Bottom**, ECHO vs. CATH gradients: ECHO maximum instantaneous gradient (MIG), CATH peak-to-peak gradient (PPG), CATH mean gradient (ΔP mean) (dotted area), and ECHO Δp mean (shaded area). ECHO MIG is the gradient between the peak LV pressure and the aortic pressure at the same point in time. CATH PPG is the gradient between the peak LV pressure and the peak aortic pressure at two different points in time. ECHO MIG is inherently higher than PPG. However, ECHO and CATH ΔP mean are closer in value in the absence of significant pressure recovery. (From Abbas AE, Pibarot P. Hemodynamic characterization of aortic stenosis states. *Catheter Cardiovasc Interv* 2019;93:1002-1023.)

or respiration changes the relative values. In the past, femoral artery (FA) pressure measured from the sheath side arm was compared with LV pressure that was obtained from a smaller size catheter placed through the sheath to the LV. FA pressure approximates but mostly overestimates central aortic pressure due to resonance and peripheral amplification of pressure. Using a dual-lumen catheter or micromanometers eliminates any difference in pressure transmission time or effect of peripheral amplification. Figure 22.19 shows the LV-aortic pressure measured from a high-fidelity catheter with micromanometer pressure transducers above and below the AV compared with a fluid-filled LV catheter with the fluid-filled FA sheath pressure. Techniques to measure LV-aortic pressure gradients are shown in eTable 22.5, with demonstrations in eFigure 22.3.

The mean integrated gradient between the left ventricle and aortic pressure waves over the systolic ejection period is the best measure of the stenosis severity (eFig. 22.4). The AV area is calculated as detailed above, and as alluded to, the Hakki formula should only be used as an estimate of AV area as it does not correlate with Doppler maximal velocity (a true measure of peak instantaneous gradient)¹¹ (Fig. 22.20).

Abbas and Pibarot¹² reviewed the detailed pathophysiology of the stenosed AV (eFig. 22.5). The ejection of blood from the LV is forced through the fixed reduced aortic orifice area (i.e., the anatomic orifice area [AOA]). Energy is lost due to valvular resistance, resulting in a pressure drop and acceleration of flow. After crossing the AV, (i.e., the effective orifice area [EOA]), part of the kinetic energy is reconverted back to potential energy, and the pressure increases (also called the “pressure recovery”). Doppler echocardiography

ETABLE 22.5 Catheter Techniques to Measure LV-Aortic Pressure Gradients

1. Single catheter LV-aorta pullback
2. LV and femoral sheath
3. LV and long aortic sheath
4. Bilateral femoral access
5. Double-lumen pigtail catheter
6. Transseptal LV access with ascending aortic pressure
7. Pressure guidewire with ascending aortic pressure
8. Multitransducer micromanometer catheters

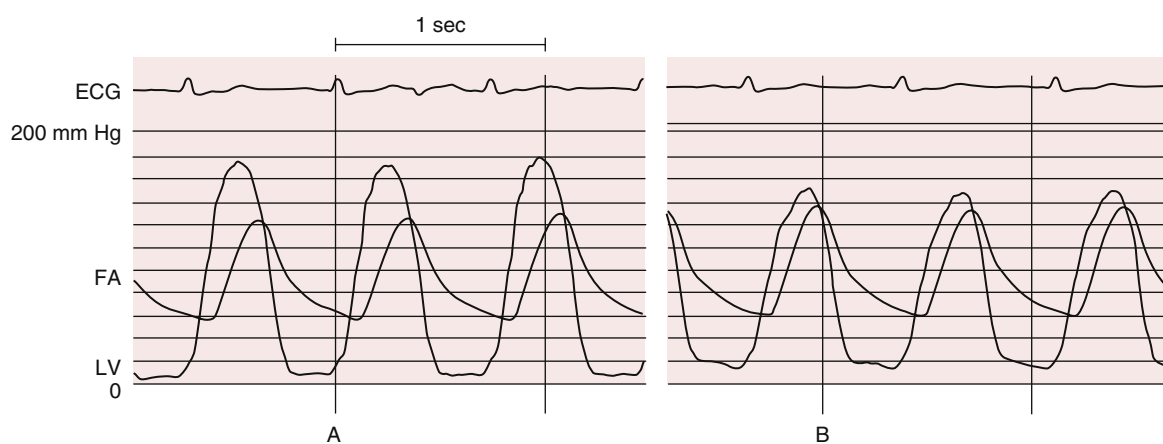


FIGURE 22.4 Aortic stenosis gradient measured with LV catheter through a femoral artery sheath providing systemic pressure. While this technique is no longer recommended, it illustrates the delay in aortic pressure transmission (*left side*) limiting the validity of peak-peak pressure measurement, a nonphysiologic comparison. Additionally, there is artifact of pressure loss when side holes from the LV catheter move into the aorta, creating an abnormal early diastolic waveform and loss of true aortic-LV pressure gradient (*right side*). The optimal way to measure the gradient in a patient with aortic stenosis is to use simultaneous left ventricular (LV) and central aortic (Ao) pressure, often with a dual lumen pigtail catheter and to calculate the mean pressure gradient (the integrated gradient between LV and Ao pressure throughout the entire systolic ejection period). (From Kern MJ, et al., editor. Hemodynamic Rounds: Interpretation of Cardiac Pathophysiology from Pressure Waveform Analysis. 4th ed. New York: Wiley-Liss; 2018, p 89.)

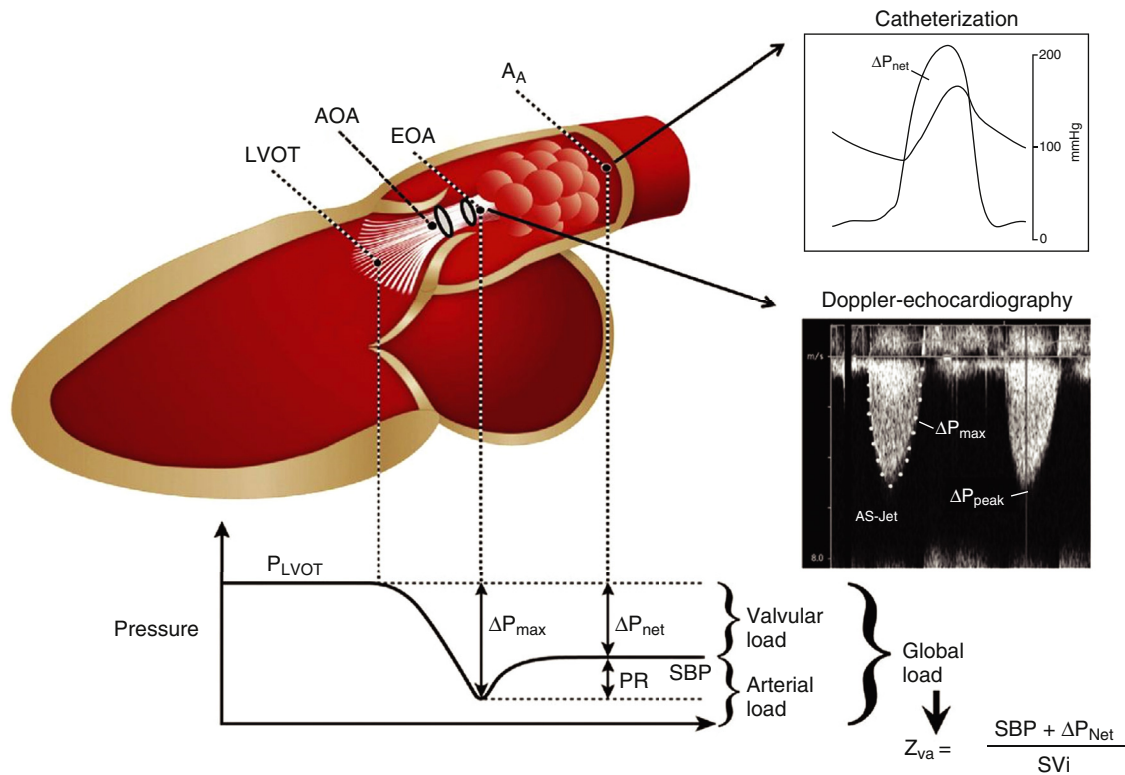


FIGURE 22.5 Blood flow and pressure across LVOT, aortic valve, and ascending aorta during systole. When the blood flow contracts to pass through a stenotic orifice (i.e., the anatomic orifice area [AOA]), a portion of the potential energy of the blood, namely, pressure, is converted into kinetic energy, namely, velocity, thus resulting in a pressure drop and acceleration of flow. Downstream of the vena contracta (i.e., the effective orifice area [EOA]), a large part of the kinetic energy is irreversibly dissipated as heat because of flow turbulences. The remaining portion of the kinetic energy that is reconverted back to potential energy is called the pressure recovery (PR). The global hemodynamic load imposed on the left ventricle results from the summation of the valvular load and the arterial load. This global load can be estimated by calculating the valvuloarterial impedance. In patients with medium- or large-sized ascending aorta, the impedance can be calculated with the standard Doppler mean gradient in place of the net mean gradient. A_{Ar} , Cross-sectional area of the aorta at the level of the sinotubular junction; ΔP_{max} , maximum transvalvular pressure gradient recorded at the level of vena contracta (i.e., mean gradient measured by Doppler); ΔP_{net} , net transvalvular pressure gradient recorded after pressure recovery (i.e., mean gradient measured by catheterization); LVOT, left ventricular outflow tract; P_{LVOT} , pressure in the LVOT; SBP, systolic blood pressure; SV_i , stroke volume index; V_{peak} , peak aortic jet velocity; Z_{va} , valvuloarterial impedance. (From Pibarot P, Dumesnil JG. J Am Coll Cardiol 2012 Jul 17;60(3):169-180.)



FIGURE 22.21 Hemodynamic left ventricular (blue) and aortic (red) pressure tracings in patient with hypertrophic cardiomyopathy. The LV catheter is pulled back from distal LV (left side) to subaortic position (right side). Note the reduction in LV-Ao pressure gradient while still recording LV pressure. In addition, one can appreciate the configuration of the aortic pressure matching the LV upstroke with a typical “spike-and-dome” appearance.

measures the peak instantaneous gradient across the entire outflow tract and aorta and is thus able to capture this phenomenon of pressure recovery. Because catheter-based measurement of aortic pressure is typically acquired several centimeters distal in the aorta after pressure recovery has already occurred, it is less affected by pressure recovery.

Low-Flow, Low-Gradient Aortic Stenosis

In patients with low-flow, low-gradient (LF/LG) severe aortic stenosis (AS) (i.e., valve area <1 cm² but mean gradient <40 mm Hg), pharmacologic maneuvers can help to establish the true anatomic severity of the stenosis for decisions regarding valve replacement. In patients with low-gradient severe AS with a preserved ejection fraction (paradoxical LF/LG AS), cardiac output is limited by relaxation abnormalities, low stroke volume, and impaired ventriculovascular coupling rather than systolic function. For such paradoxical LF/LG severe AS, lowering of the peripheral resistance with nitroprusside should lead to an increase in the AV gradient without a change in the valve area (eFig. 22.6).¹³

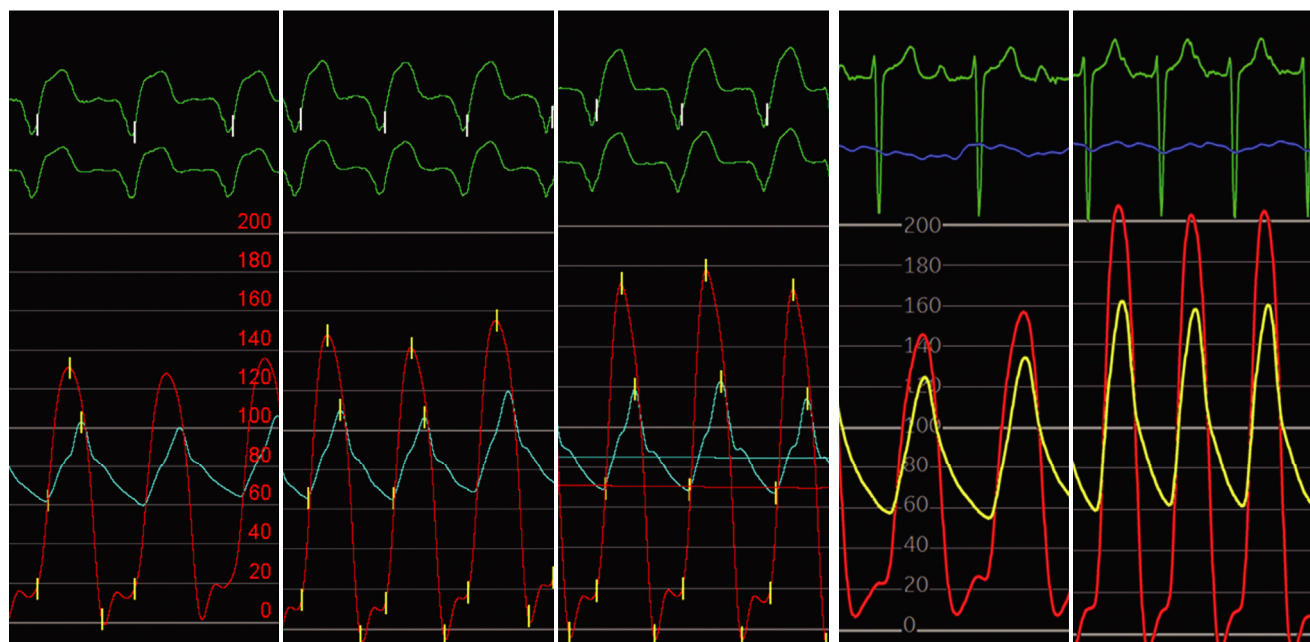
In patients with LG/LF AS with a reduced ejection fraction, a dobutamine challenge will increase cardiac output and permit reassessment of the valve gradient and area in the setting of an improved cardiac performance (eFig. 22.6B). In patients with mild or minimal AS, in response to low-dose dobutamine, the valve area should increase by >0.2 cm² with minimal or no change in the transvalvular gradient. In patients with true anatomic stenosis, the valve gradient should increase with a higher cardiac output while the AV area will remain small (eFig. 22.6A). Dobutamine also provides prognostic information, as patients without an adequate contractile reserve (e.g., stroke volume increase $<20\%$) have poor outcomes irrespective of valve intervention.

Hypertrophic Obstructive Cardiomyopathy

An LV outflow gradient can be present not only at the AV but also at the subvalvular level within the ventricle. Whereas valvular AS is structural in nature and the gradient is usually constant in daily life, the LVOT-aortic gradient caused by HOCM is dynamic and sensitive to ventricular loading conditions and changes in contractility.^{14,15} A low LVOT gradient at rest should be challenged with dynamic and provocative maneuvers (e.g., variation with respiration, post-PVC accentuation, isometric exercise) to identify the true obstructive nature of the disease and suitability for septal myectomy or percutaneous alcohol septal ablation.

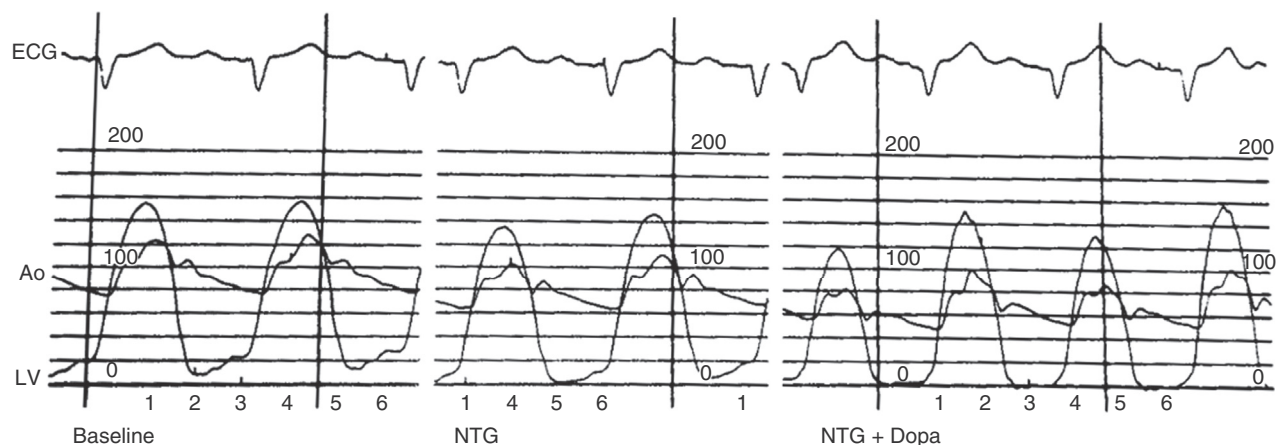
Confirmation of the subvalvular location of the intracavitary gradient is obtained by pressure pullback from the LV apex to a position just beneath the AV (eFig. 22.6B). The location of the intraventricular gradient is defined by the resolution point of the aortic-LV gradient while still registering LV pressure. A standard pigtail catheter has shaft side holes and is not suitable for gradient location assessment because some or all of the holes may be positioned above the intracavitary obstruction producing an erroneously small LVOT gradient. Alternative methods for the invasive assessment of intracavitary gradients include the use of a dual-lumen catheter, a double-sensor micromanometer catheter, or an end-hole catheter in the LV outflow tract and a second catheter in the left ventricle placed by transeptal puncture.

Compared with fixed AV obstruction, in dynamic subaortic outflow tract obstruction the aortic and LV waveforms display distinctly different characteristics (Fig. 22.21). Patients with valvular AS have a slow and delayed upstroke (*parvus et tardus*) in the aortic waveform. In contrast, HOCM patients have a rapid rise of the aortic pressure corresponding to the LV pressure at the onset of AV opening. The rapid rise is followed by a blunted and rounded wave in late systole, leading to a “spike-and-dome contour”, which is characteristic of a dynamic LV outflow obstruction. While both AS and HOCM have increased post-PVC



A

B



C

FIGURE 22.6 **A**, Dobutamine pharmacologic challenge for low-flow, low-gradient aortic stenosis to differentiate true aortic stenosis from pseudo-AS. In a patient with reduced ejection fraction (EF), increase in contractility with dobutamine stimulation leads to an increase in the gradient. In this patient with LF/LG AS was pacemaker dependent. Dobutamine at 10 mcg/kg increased base (*left panel*) from 28 to 35 mm Hg (*middle panel*) and after 20 mcg/kg/min and increasing pacemaker rate to 95 bpm (*right panel*), the gradient rose to 50 mm Hg with increasing cardiac output. The valve area remained unchanged at 0.7 cm², consistent with a severe fixed valvular stenosis. **B**, In patients with pseudo stenosis, the valve area would increase with increasing cardiac output. Base line (*left panel*) shows aortic pressure 136/60 with LV pressure of 164/24 and peak-peak gradient of 28 mm Hg with thermodilution cardiac output of 3.9 L/m, aortic valve area was 0.7 cm². During infusion of dobutamine 20 mcg/kg (*right panel*), aortic pressure increased to 158/60, LV pressure 205/15, and peak-peak gradient to 50 mm Hg with cardiac output increasing to 6.3 L/m with aortic valve area of 0.9 cm² suggesting partial pseudo stenosis. However, if Fick cardiac output is used, the calculation of cardiac output is lower, 5.1 L/m yielding an unchanged valve area. In low flow states use thermodilution cardiac output with caution. **C**, Pharmacologic challenge of AS with NTG, Dopa demonstrates the impact of afterload reduction with nitroglycerin on aortic stenosis hemodynamics. Before the challenge, baseline hemodynamic data (*left panel*) demonstrated an aortic valve gradient of 30 mm Hg, cardiac output of 4.9 L/m with calculated valve area of 0.9 cm². LVEF was 32%. Sublingual NTG (*middle panel*) reduced systemic pressure without significant impact on gradient. During low-dose dobutamine infusion (5 mcg/kg/min) cardiac increased to 6.5 L/m, with gradient of 45 to 55 mm Hg (and induction of pulsus alternans reflecting poor LV function) resulted in fixed valve area of 0.9 cm². (From Kern MJ, et al., editors. Hemodynamic Rounds: Interpretation of Cardiac Pathophysiology from Pressure Waveform Analysis. 4th ed. New York: Wiley-Liss; 2018, p 61.)

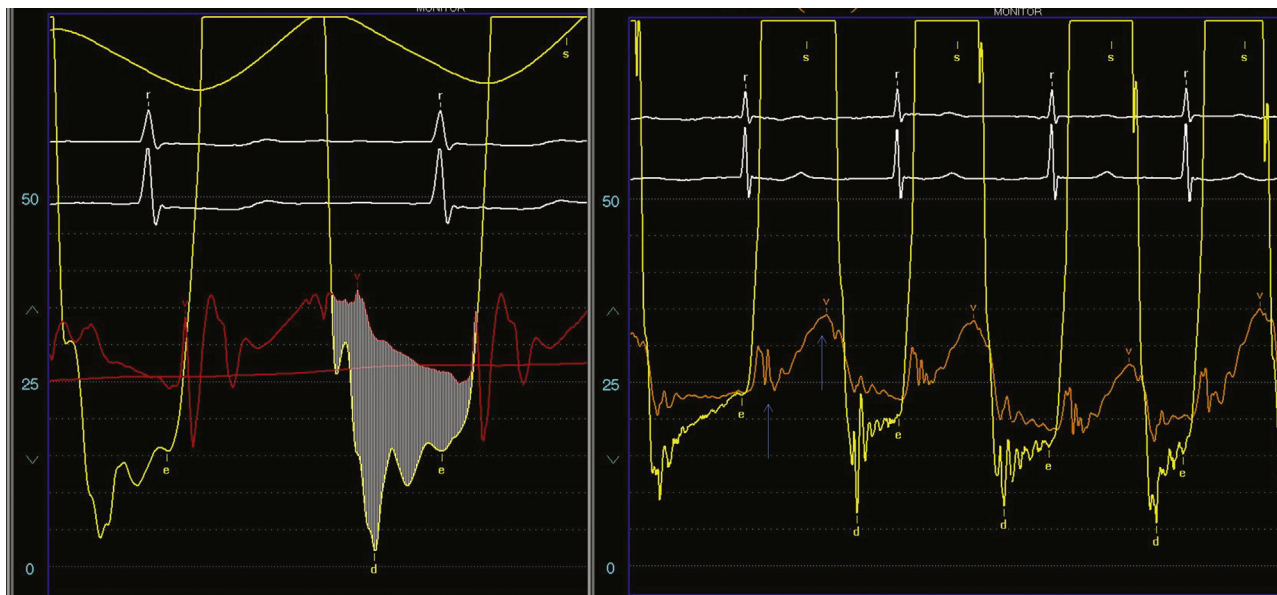


FIGURE 22.22 Hemodynamic tracings in a patient with mitral stenosis. *Left*, LV and PCWP tracings show a large mitral valve gradient of approximately 20 mm Hg (pressure scale is 0 to 50 mm Hg). *Right*, LV and directly measured LA pressures (via transeptal approach) show higher fidelity pressure waveforms and marked reduction in the mitral pressure gradient (6 mm Hg). On the LA pressure, the c notch and v wave are distinct compared with the waveforms on the PCWP.

LVOT gradients, HOCM tracings show a smaller post-PVC aortic pulse pressure (eFig. 22.7). The diminished aortic pulse pressure following a PVC is the pathognomonic hemodynamic pattern of HOCM, named the Braunwald-Brockenbrough-Morrow sign.

Other provocative maneuvers used in the hemodynamic evaluation of HOCM include alteration of loading conditions with Valsalva maneuver, inhalation of amyl nitrate, or increasing contractility by a dobutamine or isoproterenol infusion (eFig. 22.8). Each of these has the potential to exacerbate the LVOT gradient and reveal the underlying physiology, just as physical examination maneuvers can increase (Valsalva, standing up) or reduce (squatting, leg raise) the murmur of HOCM.

Symptomatic patients, refractory to medical therapy with appropriate morphologic abnormalities of HOCM, may benefit from myectomy or percutaneous alcohol septal ablation. The specific details of the alcohol septal ablation are described elsewhere.¹⁶

Mitral Valve Stenosis

The hemodynamic assessment of the stenotic mitral valve is performed initially with combined left and right heart hemodynamics examining the LV-PCWP (LA) pressure gradient at rest. In patients with borderline normal/abnormal findings, measurements should be made during exercise (e.g., arm lifting with weights or bicycle ergometer). Important to recall is the fact that the PCWP often overestimates LA pressure in patients with mitral stenosis or prosthetic mitral valves due to delayed and poor-quality pressure transmission.

For patients with elevated PCWP and suspected mitral valve abnormalities, direct measurement of the LA pressure by transeptal puncture is the most accurate method for decisions regarding mitral valvuloplasty or replacement. Figure 22.22 shows a PCWP (red) and a LA pressure (orange) demonstrating different timing of V waves and higher mean for PCWP which falsely increased the mitral valve gradient measurement. However, if the PCW/LV pressure tracings show no significant gradients, transeptal catheterization is often unnecessary. A simplified formula for the estimation of the mean mitral valve gradient (MVG = mean left atrial pressure – LVEDP/2) has been proposed.¹⁷ MVA can be calculated as outlined above.

The classic hemodynamic sign of mitral stenosis on left atrial pressure tracing is a markedly elevated *a* wave. Further, due to the stenosis of the mitral valve, the pressure only gradually decreases after opening and the *y* descent is gradual. The LV pressure waveform may show a lower end-diastolic pressure due to the impaired filling and a reduced atrial kick (i.e., *a* wave amplitude).

Pulmonary and Tricuspid Valve Stenosis

The same principles and techniques outlined above apply to right-sided valvular heart diseases. For the pulmonic valve, the transvalvular gradient is not infrequently obtained on catheter pullback from the pulmonary artery into the right ventricle, although ideally it should be measured simultaneously using multi-lumen catheters or two separate catheters. Invasive hemodynamic measurements are performed when the severity of pulmonary stenosis is unclear, when an infundibular stenosis is suspected, and when balloon valvotomy is considered.

With tricuspid stenosis, the obstruction of blood flow from the right atrium into the right ventricle, the volume of blood in the right atrium and the mean right atrial pressure are increased in diastole, generating a diastolic pressure gradient between these two chambers. This translates into a markedly elevated *a* wave. Opening of the stenotic tricuspid valve leads to a slow decrease in right atrial pressure and gradual *y* descent. Right ventricular pressure tracings show a reduced end-diastolic *a* wave amplitude secondary to the reduced atrial filling.

Aortic Regurgitation

Aortic regurgitation (AR) occurs when there is inadequate closure or malcoaptation of the AV leaflets, allowing blood to enter the LV cavity from the aorta during diastole. Common causes of aortic regurgitation include aortic root dilation, bicuspid AV, and endocarditis. An aortogram can be used to visualize and semi-quantitatively measure the degree of aortic regurgitation by the extent the regurgitation of contrast volume injected into the aortic root is opacifying the left ventricle.

It is important to be cognizant that the results are influenced by catheter position, volume of contrast, and chamber size and contractility, not just regurgitant volume alone. Nevertheless, the semi-quantitative classification scheme by Sellers and colleagues remains the reporting standard:

- 1+ Minimal regurgitant jet seen.
Clears rapidly from the proximal chamber with each beat.
- 2+ Moderate opacification of the proximal chamber and clearing with subsequent beats.
- 3+ Intense opacification of the proximal chamber that becomes equal to that of the distal chamber.
- 4+ Intense opacification of the proximal chamber that becomes denser than that of the distal chamber. Opacification often persists over the entire series of images obtained.

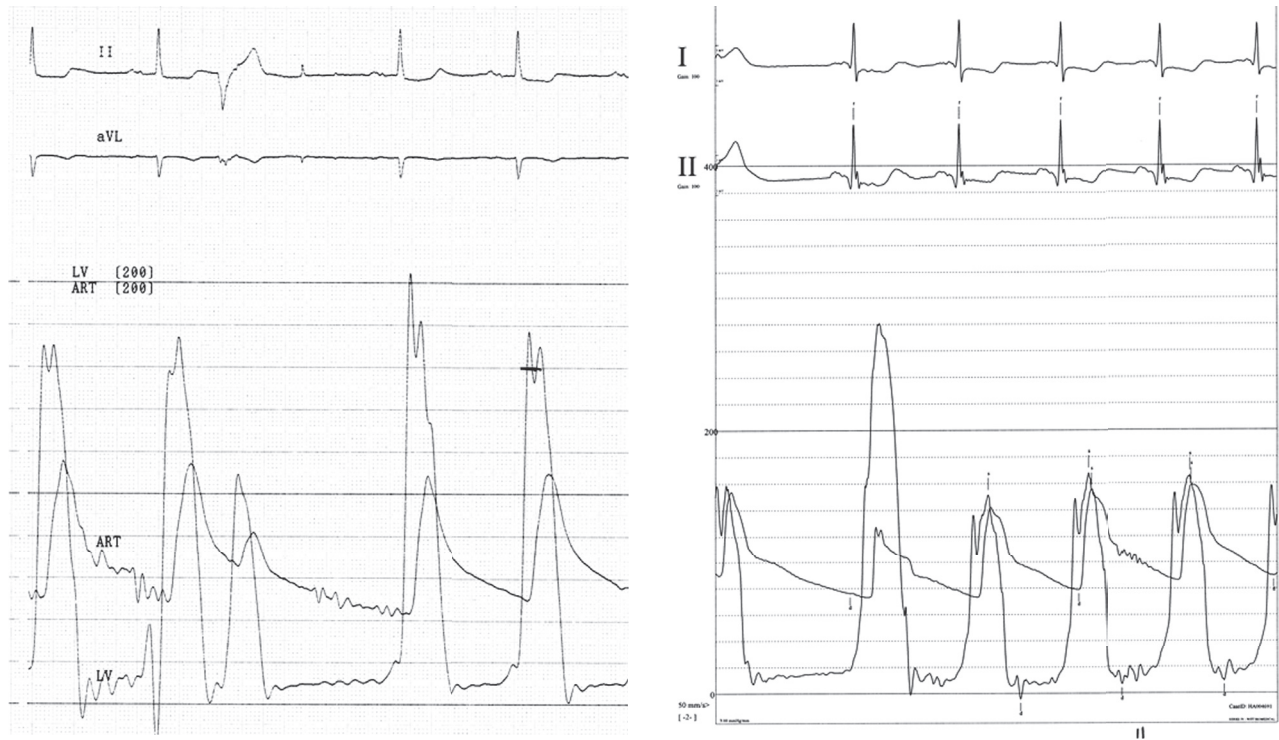


FIGURE 22.7 Hemodynamic tracings differentiating aortic stenosis and hypertrophic obstructive cardiomyopathy. Aortic stenosis (*left panel*) is an example of a fixed LVOT obstruction (either valvular stenosis or fixed subvalvular stenosis), typically leading to a parvus and tardus upstroke of the aortic pressure. The post-PVC LV-Ao tracings show an increased gradient, delayed aortic pressure upstroke, and normal or widened pulse pressure. In contrast, in patients with HOCM (*right panel*) hemodynamics are characterized by an increased gradient, rapid aortic pressure upstroke, and reduced pulse pressure and marked change in the configuration of the aortic pressure with a sharp spike and delay pressure (dome) of impaired ejection from the ventricle. (From Kern MJ, et al., editors. Hemodynamic Rounds: Interpretation of Cardiac Pathophysiology from Pressure Waveform Analysis. 4th ed. New York: Wiley-Liss; 2018, p 167.)

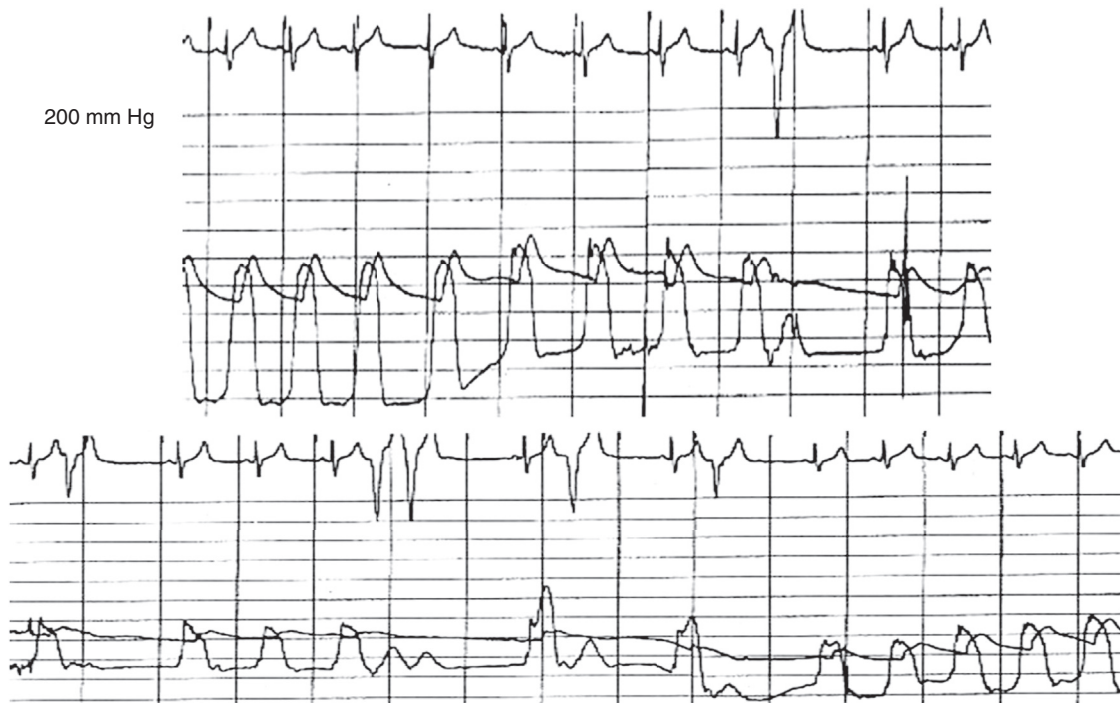


FIGURE 22.8 Valsalva maneuver induces dynamic changes in the LVOT gradient in a patient with HOCM. Top panel shows beginning of Valsalva maneuver with elevation of all pressures, particularly the LVEDP, as intrathoracic pressure increases. During Valsalva, venous return is reduced, preload is reduced, and LV filling is reduced, producing more LVOT obstruction. In the lower panel, the Valsalva hemodynamics are accentuated by PVCs generating significant LVOT gradients. (From Kern MJ, et al., editors. Hemodynamic Rounds: Interpretation of Cardiac Pathophysiology from Pressure Waveform Analysis. 4th ed. New York: Wiley-Liss; 2018, p 45.)

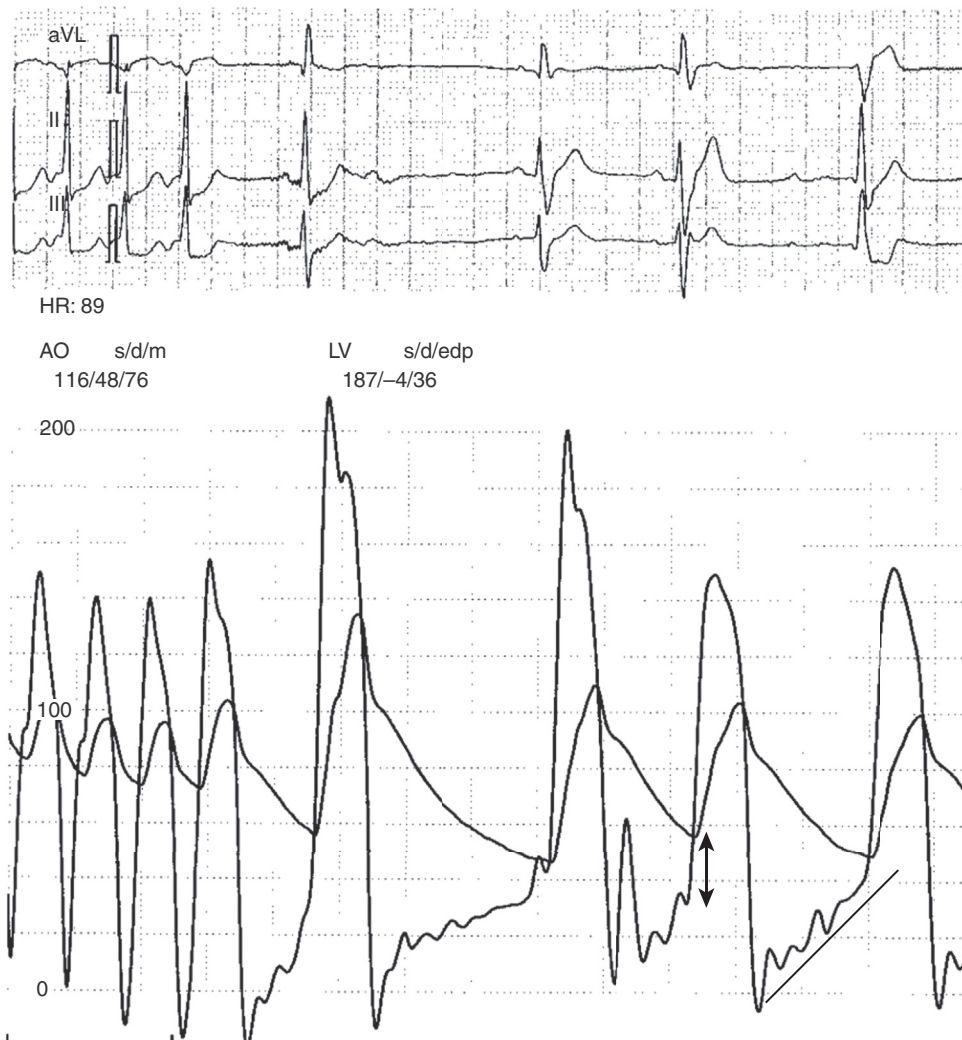


FIGURE 22.23 Hemodynamics of combined mixed AS and AI with LV-Ao systolic gradient and rapidly increasing diastolic LV filling pressure (*diagonal line*), wide pulse pressure, and close approximation of aortic diastolic pressure with LV EDP (*double arrowhead*).

By cardiac catheterization the regurgitant volume can be calculated as the fraction of the stroke volume that does not contribute to net cardiac output, that is,

$$\text{Regurgitant stroke volume} = \text{angiographic stroke volume} - \text{forward stroke volume.}$$

The regurgitant stroke volume can also be used to produce a regurgitant fraction, that is

$$\text{Regurgitant fraction (RF)} = \frac{\text{regurgitant stroke volume}}{\text{angiographic stroke volume}}$$

The angiographic stroke volume is calculated by the cardiac output measurement on the left ventriculogram, the forward stroke volume by Fick or thermodilution cardiac output measurement; either value is then divided by the heart rate. Prerequisites for this calculation are similar heart rates for both output measurements, stable hemodynamic states between measurements, and the presence of only a single regurgitant valve. Considering these limitations, volumetric approaches by echocardiography and MRI provide easier and more precise quantitative measurements.

The three typical hemodynamic findings of AR are widened aortic pulse pressure, rapid upstroke of LV diastolic filling pressure, and near equilibration of end-diastolic aortic and LV pressure. [Figure 22.23](#) shows a patient with mixed AS and regurgitation. Note the wide pulse pressure and rapid LV diastolic filling slope up to the LV EDP. [eFigure 22.9](#) shows the hemodynamic waveforms of a patient with isolated

severe AR. Occasionally, measurements made with a stiff exchange wire across a severely calcific stenotic valve may prop the leaflet open and produce an artifactual hemodynamic picture of severe AR.

Mitral Regurgitation

Mitral regurgitation (MR) is typically the result of the mitral apparatus failing to maintain the coaptation of the mitral leaflets during systole. The mitral apparatus consists of four components: the annulus, the anterior and posterior leaflets, the chordae tendineae, and the papillary muscles. Failure of any of these structures can result in leaflet malcoaptation with valvular regurgitation. Semi-quantitative assessment of MR with left ventriculography remains a useful screening tool during coronary angiography.

In particular, pulmonary artery pressure (PAP) and PCWP at rest and with exercise are important parameters for clinical assessment of MR. With severe MR, a prominent *v* wave is characteristic and the hemodynamic consequence is postcapillary pulmonary hypertension, especially under conditions of increased workload. It is a class I ACC/AHA guideline recommendation to perform a hemodynamic evaluation of either aortic or mitral regurgitant lesions when PAPs are disproportionate to the severity of regurgitation on noninvasive testing or when clinical and noninvasive findings are inconsistent.

Acute MR produced by stretching or tearing of leaflets is characterized by a large *v* wave ([Fig. 22.24](#)). However, as with all hemodynamic waveforms, atrial and ventricular compliance determine the waveform and thus a

large *v* wave, may be present due to low compliance of the LA rather than MR ([Fig. 22.25](#)). A new large *v* wave after mitral balloon valvuloplasty, however, is usually a valid demonstration of acute MR. [Freihage et al.¹⁸](#) reported that the ratio of the area under the *v* wave to the LV systolic area, that is V_a/LV_a , correlates best with the degree of MR.

Pulmonary and Tricuspid Valve Regurgitation

Invasive hemodynamic assessment of patients with pulmonary regurgitation serves primarily the purpose of determining pulmonary arterial pressures and pulmonary vascular resistance, especially as part of comprehensive assessment when other structural cardiac abnormalities are present and/or pulmonary valve intervention is considered. The hemodynamic characteristics of severe pulmonary regurgitation include low pulmonary artery end-diastolic pressure, wide pulmonary pulse pressure, and increased RV end-diastolic pressure. With severe degrees of regurgitation, PAP tracings may take on the appearance of an RV pressure tracing (“ventricularization”).

In patients with tricuspid regurgitation (TR), measurement of pulmonary pressures and pulmonary vascular resistance will assist in determining secondary causes of regurgitation, for example pre- or postcapillary pulmonary hypertension and septal defects. The characteristic hemodynamic finding is an elevated *v* wave generated by the open communication between the two chambers and the volume ejection from the right ventricle into the right atrium with the onset of systole. The magnitude of the *v* wave pressure elevation is determined



FIGURE 22.9 Hemodynamic tracing showing elevated left ventricular (LV) end-diastolic pressure (*arrow*), widened aortic pulse pressure (*arrowheads*), and near equalization of LV and aortic end-diastolic pressures. (From Ren X, Banki NM. *Circulation* 2012;126:e28-e29.)

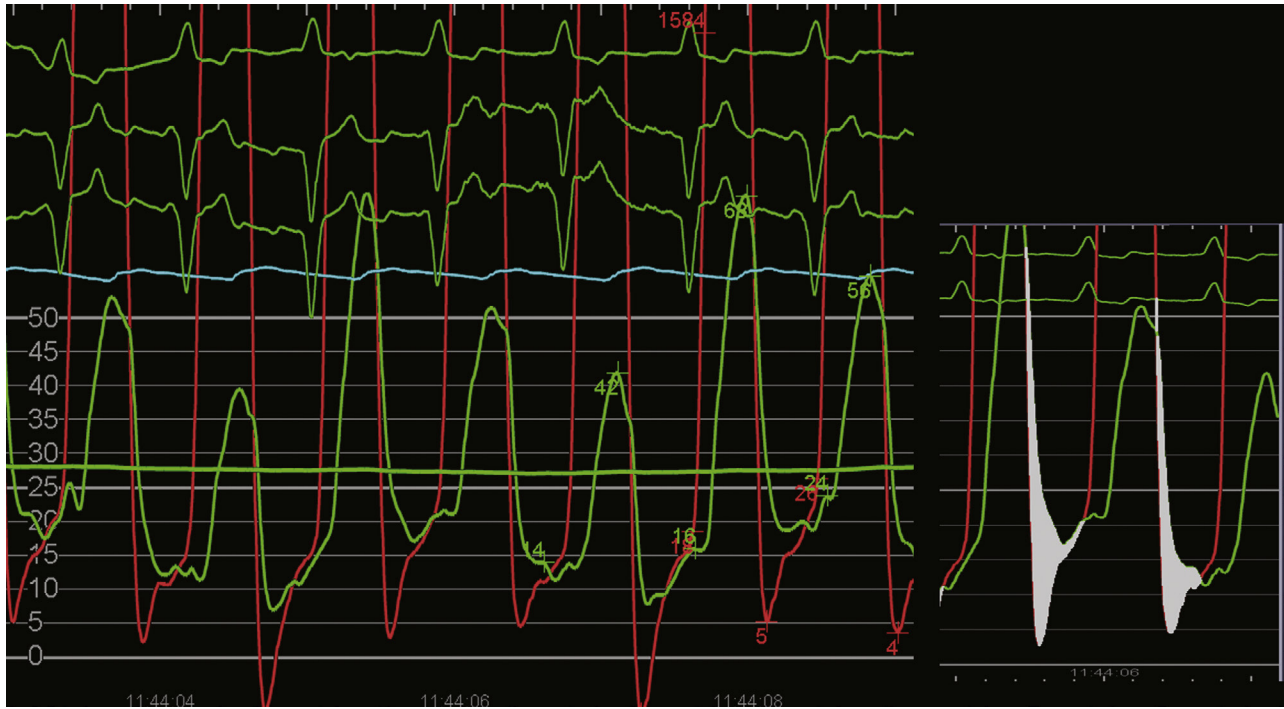


FIGURE 22.24 Simultaneous LV (red) and LA (green) pressure in a patient with severe mitral regurgitation and giant v waves. Right, Mild mitral valve gradient (white shaded area) with large v waves. Scale is 0 to 50 mm Hg.

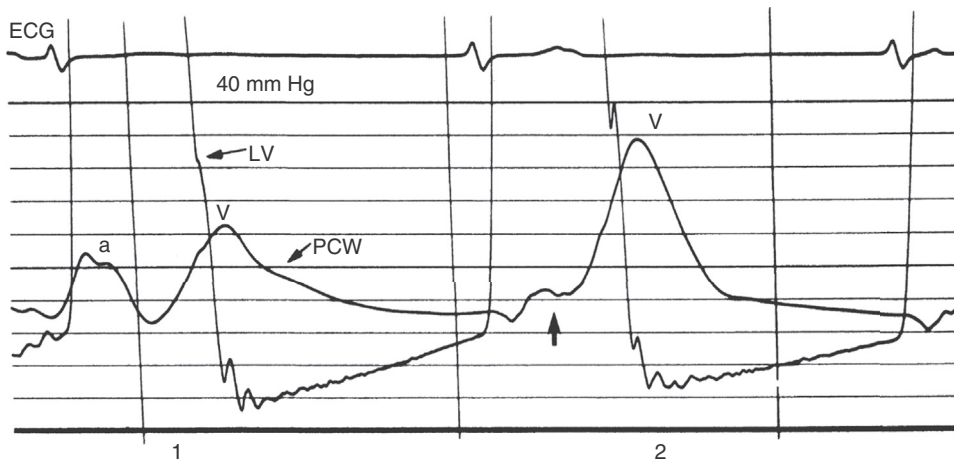


FIGURE 22.25 Left ventricular (LV) and pulmonary capillary wedge pressure in patient with mitral stenosis without evidence of mitral regurgitation. Beat 1 demonstrates large a with prominent v wave, an 12 mm Hg mitral gradient. Beat 2 shows a junction beat with a retrograde P wave (arrow) producing a significantly large v wave and larger gradient in the absence of regurgitation due to low compliance of the diseased left atrium.

not only by the regurgitant volume but also by the compliance of the right atrial chamber. Accordingly, v wave amplitude and mean right atrial pressure may be very minimally elevated in relation to the chronicity of TR. Furthermore, right atrial distension due to chronic volume expansion with evolving reduction in contractility also leads to a reduction in the a wave.

SEPTAL DEFECTS AND LEFT-TO-RIGHT/RIGHT-TO-LEFT SHUNTS

As with valvular heart disease, echocardiography takes the leading role in the initial diagnosis of atrial or ventricular defects and pulmonary arteriovenous malformations. Hemodynamic assessment is used in the determination and quantification of the extent and consequences of shunts. Hemodynamics provide information on the status of PAP, resistance, and their reversibility in case of elevation.

The systemic and pulmonary circulations operate in series, and thus normally their output is the same. Any abnormal communication between them then generates a short circuit or shunt. This can be from the systemic circulation to the pulmonary circulation (left-to-right shunt), from the pulmonary circulation to the systemic circulation (right-to-left shunt), or in both directions (bidirectional shunt). Most shunt assessments in the cardiac catheterization laboratory are made by determination of the oxygen content in the blood at different levels of the circuit given the normally very well defined and distinct oxygenation values in the systemic and pulmonary circulation.

As a general rule, pulmonary artery oxygen saturations exceeding 80% should raise the suspicion for a left-to-right shunt. On the contrary, systemic, arterial oxygen saturations <93% that persist after several deep breaths to counteract alveolar hypoventilation (as seen with over sedation or pulmonary venous congestion) should raise suspicion for a right-to-left shunt.

In addition to pulmonary artery oxygen sampling, a screening oxygen saturation should also be obtained from the SVC routinely with right-heart catheterization to possibly detect even small left-to-right shunts. If the difference in oxygen saturation between these two samples is $\geq 8\%$, a left-to-right shunt may be present, and the oximetry run should be extended to also include samples from the IVC, right atrium, and right ventricle. In fact, if an inter-atrial shunt is suspected, samples should be obtained at the level of the low, mid, and high right atrium, and for an inter-ventricular shunt from the RV inflow tract, apex, and outflow tract. An absolute increase in oxygen saturation by 5% or more defines a significant step-up and the location of the shunt.

A small left-to-right shunt might be missed if the right atrium is used for screening purposes because of incomplete mixing of blood in the right atrium from the SVC, IVC, and coronary sinus. When taking blood



samples in the right atrium, the catheter should always be directed away from the coronary sinus, which has one of the lowest oxygen saturations in the human body. Further to note oxygen saturation in the IVC is higher than in the SVC as oxygen extraction of the internal organs and lower extremity muscles is lower in a fasting and resting state than that of the brain. The best method for determination of the mixed venous saturation is by Flamm's formula, which is based on IVC and SVC samples (see later).

A full saturation run entails samples from the high and low IVC; high and low SVC; high, middle, and low right atrium; RV inflow, midcavity, and outflow tract; main pulmonary artery; left or right pulmonary artery; pulmonary vein and left atrium, if possible; left ventricle; and distal aorta. Right-to-left shunt assessments require samples from the pulmonary veins, left atrium, left ventricle, and aorta. A decrease (step-down) in oxygen saturation is expected in such cases.

To quantify the extent of a shunt, PBF and SBF need to be calculated, which is, in essence, oxygen consumption divided by the difference in oxygen content across the pulmonary or systemic bed. The effective blood flow (EBF) is the fraction of mixed venous return received by the lungs without contamination by shunt flow. Under normal conditions, PBF, SBF, and EBF are equal.

These equations are as follows:

$$\text{PBF} = \text{VO}_2 \div [(\text{PvO}_2 - \text{PaO}_2) \times \text{Hb} \times 1.36 \times 10]$$

$$\text{SBF} = \text{VO}_2 \div [(\text{SaO}_2 - \text{MvO}_2) \times \text{Hb} \times 1.36 \times 10]$$

$$\text{EBF} = \text{VO}_2 \div [(\text{PvO}_2 - \text{MvO}_2) \times \text{Hb} \times 1.36 \times 10]$$

VO_2 (oxygen content) is determined as outlined in the section on Fick cardiac output. PvO_2 , PaO_2 , SaO_2 , MvO_2 are oxygen saturation of pulmonary venous, pulmonary arterial, systemic arterial, and mixed venous blood, respectively.

MvO_2 is calculated by Flamm's formula:

$$[\text{MvO}_2 = (3 \times \text{SVC O}_2 + 1 \times \text{IVC O}_2) / 4]$$

Systemic arterial oxygen saturation may be substituted for pulmonary venous sampling, if at least 95%. Otherwise, in the absence of a right-to-left shunt, systemic arterial oxygen content is used. If a right-to-left shunt is present, pulmonary venous oxygen content is calculated as 98% of the oxygen capacity.

The size of an isolated left-to-right shunt is

$$\text{L} \rightarrow \text{R shunt} = \text{PBF} - \text{SBF}$$

If an additional right-to-left shunt is present (bidirectional shunt), the approximate size of the left-to-right shunt is

$$\text{L} \rightarrow \text{R shunt} = \text{PBF} - \text{EBF}$$

and the approximate size of the right-to-left shunt is

$$\text{R} \rightarrow \text{L shunt} = \text{SBF} - \text{EBF}$$

Clinically, the ratio of PBF to SBF (or Qp/Qs) is often used to express shunt significance. A ratio <1.5 indicates a small left-to-right shunt, a ratio of 1.5 to 2.0 a moderate-sized shunt, and a ratio of >2.0 a large left-to-right shunt. A flow ratio <1.0 indicates a net right-to-left shunt.

If oxygen consumption is not measured, the PBF/SBF ratio may be calculated as follows:

$$\text{PBF/SBF ratio} = (\text{SaO}_2 - \text{MvO}_2) \div (\text{PvO}_2 - \text{PaO}_2)$$

where SaO_2 , MvO_2 , PvO_2 , and PaO_2 are systemic arterial, mixed venous, pulmonary venous, and pulmonary arterial blood oxygen saturation, respectively.

Pericardial Disease and Restrictive Cardiomyopathy

Impairment of ventricular filling or diastolic dysfunction can be caused by a number of intrinsic and extrinsic pathologies. Intrinsic causes of diastolic dysfunction include hypertrophic cardiomyopathies, infiltrative diseases such as amyloid, sarcoid, or hemochromatosis, scarring

after radiation or chemotherapy, and other restrictive myopathic conditions. Extrinsic impairment of diastolic filling is most commonly due to pericardial constraint from pericarditis, cancer with metastases to the pericardial space, or pericardial effusion with tamponade physiology from a number of causes. Rarely, very large pleural effusions can limit cardiac filling and masquerade as pericardial constriction, though more frequently pleural effusions are the result rather than the cause of the abnormal physiology.

Normal Pericardial Function and Pathophysiology of Constriction

While not critical to maintenance of normal cardiovascular function, the pericardium has important subsidiary functions including stabilization of intrathoracic cardiac motion, balancing right and LV cardiac output through diastolic and systolic interactions, limiting acute cardiac dilation, minimizing friction between cardiac chambers and surrounding thoracic structures, and providing an anatomic barrier to infection from the lung and other contiguous structures. The diseased pericardium becomes stiffer, thicker, and less compliant (from progressive inflammation). Ultimately the pericardium can become adherent to the myocardium and limit cardiac filling through its constrictive effect on the global cardiac volume.

Differentiating between constrictive and restrictive causes for impaired cardiac filling may occur through the patient history, as the causes of intrinsic myocardial restriction are often distinct from constrictive pericardial diseases. From a hemodynamic standpoint, both constrictive and restrictive diseases produce elevation and equalization of right and LV diastolic pressures. Both demonstrate abrupt cessation of early ventricular filling (Fig. 22.26), classically described as a "dip and plateau" waveform of the ventricular pressures.

Unique to restrictive cardiomyopathy is the decreased ventricular chamber compliance due to increased myocardial stiffness. The steep compliance curve results in an abnormal increase in impedance throughout the entire diastolic period and a reduced atrial filling component at end-diastole (often associated with biatrial enlargement). In contrast, in constrictive pericarditis, the ventricular chamber compliance is normal in early diastole, allowing for normal or rapid early filling. In mid-diastole, ventricular filling is abruptly decelerated as the intracardiac volume approaches the fixed limit of the constricting pericardium. The limitation in global cardiac volume results in an increase in ventricular interdependence or ventricular coupling; that is, the right and left ventricles are unable to fill independently of each other. The intraventricular septum shifts over the course of the respiratory cycle such that the filling of one ventricle impairs the filling of the other ventricle. These dynamic respiratory changes of ventricular interdependence allow for accurate discrimination of constrictive pericarditis from restrictive cardiomyopathy (eFig. 22.10).

In addition, the constricting pericardium dissociates the intrathoracic from the intracardiac pressures such that intrathoracic pressure is not fully transmitted through the diseased pericardium to the intracardiac structures. Normally, decreased intrathoracic and intracardiac pressures increases systemic venous return as the SVC and IVC are mostly extrathoracic and flow can proceed to the lower-pressure right heart structures. This causes right-sided cardiac output and murmurs to increase during inspiration (Carvalho sign). LV filling is mostly unchanged with respiration as the pulmonary veins are intrathoracic and any changes to thoracic pressure are transmitted to the LA/LV, though a small decrease in LV filling occurs with increased pulmonary pooling of blood volume with inspiration.

In contrast, in the setting of constriction, inspiration leads to decreased pulmonary venous pressure (as these are intrathoracic and extrapericardial) without a decrease in intracardiac pressures, resulting in significantly reduced left-sided preload and stroke volume during inspiration. At the same time, right-sided filling is augmented by increased IVC flow and paradoxically increasing jugular venous pressure with inspiration, termed Kussmaul's sign. Kussmaul's sign is only occasionally seen in patients with cardiac tamponade wherein the increase in negative intrathoracic pressure is generally still transmitted

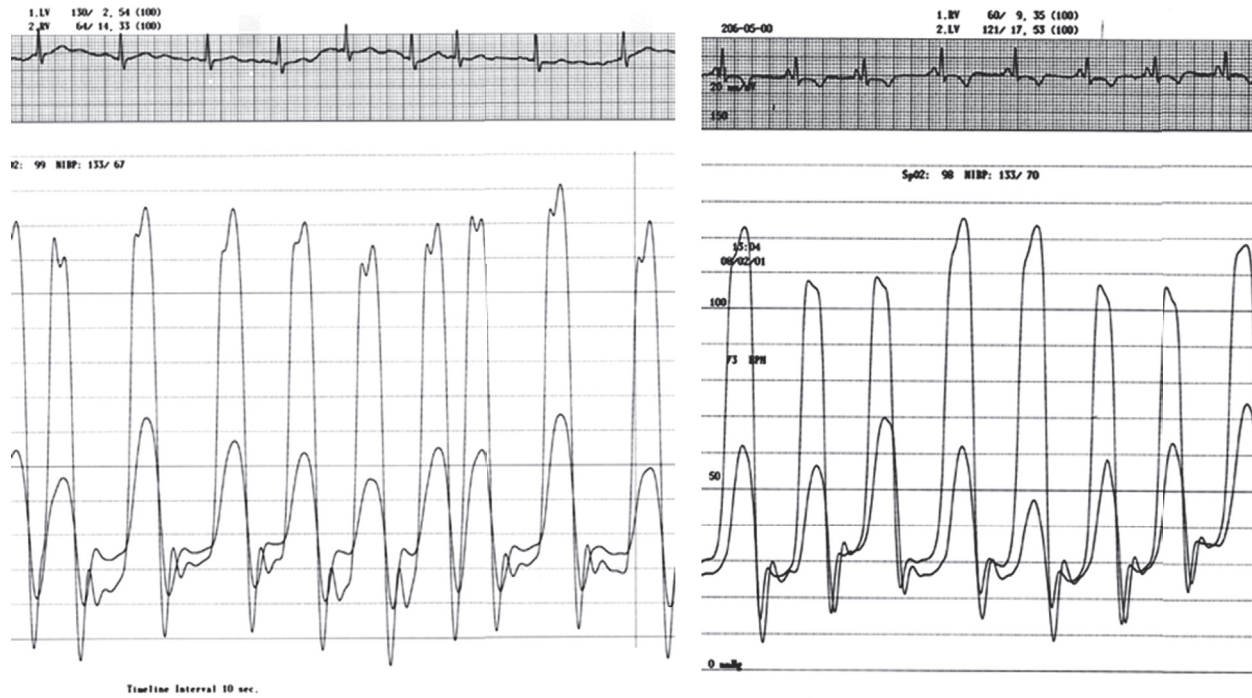


FIGURE 22.10 Hemodynamics of constrictive and restrictive physiology are characterized by differences in ventricular pressure interaction during dynamic respiratory activity. The pathophysiology of both conditions are characterized by elevated and equalized intracardiac filling pressures with rapid early filling and the cessation of further filling (“dip and plateau pattern”). In constrictive physiology (*right panel*), inspiration increases RV filling, shifting the intraventricular septum into the LV at the expense of LV volume. The opposite occurs during expiration. Thus, the LV and RV pressure changes over the respiratory cycle are discordant. In contrast, restrictive physiology (*left panel*) differs in that both chambers can fill during respiration and there is no septal shift. LV and RV systolic pressures move concordantly during respiration. (From Kern MJ, et al., editors. Hemodynamic Rounds: Interpretation of Cardiac Pathophysiology from Pressure Waveform analysis. 4th ed. New York: Wiley-Liss; 2018, p 226.)



FIGURE 22.26 LV and RV hemodynamic pressure pattern of constrictive/restrictive physiology demonstrating an abrupt cessation of early diastolic filling with a “dip and plateau” configuration. While common, this pattern is not diagnostic of constrictive pericarditis (scale 0 to 40 mm Hg).

to the right side of the heart in the absence of a constrictive component to the physiology (effusive-constrictive, see later).

The traditional hemodynamic criteria for the diagnosis of constrictive pericarditis include (1) end-diastolic pressure equalization (LV end-diastolic pressure minus RV end-diastolic pressure >5 mm Hg), (2) PAP <55 mm Hg, (3) RV end-diastolic pressure divided by RV systolic pressure $>1/3$, (4) dip and plateau diastolic pressure morphology as reflected by the height of the LV rapid filling wave (>7 mm Hg), (5) and Kussmaul’s sign (lack of an inspiratory fall in mean right atrial pressure) (Table 22.3). Unfortunately, these criteria are neither highly specific nor sensitive to differentiate constrictive from restrictive physiology.

Dynamic ventricular interdependence (correspondence of LV:RV systolic pressures) exhibited during respiration, on the other hand, is the most sensitive and specific hemodynamic finding differentiating constrictive pericarditis from restrictive physiology. Hurrell et al.¹⁹ examined dynamic respiratory changes in LV and RV pressures in 36 patients: 15 with surgically proven constrictive pericarditis and 21 with congestive heart failure. The dissociation of the intrathoracic and intracardiac pressures was assessed at end inspiration and end expiration. The exaggerated respiratory variation was significantly greater in those with constrictive pericarditis than restrictive diseases. During peak inspiration, there was discordance between RV and LV function with an increase in RV systolic pressure and simultaneous decrease in LV systolic pressure. In contrast, patients with congestive heart failure (and other restrictive cardiomyopathies) usually demonstrate concordant changes in right and LV systolic pressures during peak respiration. Dynamic respiratory variation in this study was 100% sensitive and 95% specific for the diagnosis of constrictive pericarditis (eFig. 22.11).

Recently, the ratio of the RV to the LV systolic pressure–time area in inspiration versus expiration, the *systolic area index*, was noted to

be positive in constriction but not in restriction (1.4 ± 0.2 versus 0.92 ± 0.019 ; $P < 0.0001$). A systolic area index ≥ 1.1 has a sensitivity of 97% and predicted accuracy of 100% for identifying constriction.²⁰ In real time, ventricular interdependence (indicative of constriction) is often assessed in the catheterization laboratory by observing discordance in the movement of peak RV and LV systolic pressures over the respiratory cycle.

Cardiac Tamponade

Cardiac tamponade is a clinical syndrome associated with extrinsic compression of the heart by elevated pericardial pressures, usually due to accumulation of pericardial fluid, bleeding, or masses. Increased intrapericardial pressure results in an inability to fill the heart, leading to reduced stroke volumes, cardiac output, arterial pressure, and ultimately death. The classic signs in cardiac tamponade (Beck’s triad) include hypotension, jugular venous distension, and muffled heart sounds. Elevated pericardial pressures have characteristic hemodynamic and echocardiographic findings even before full clinical signs manifest. The magnitude of pericardial pressure increase depends on the rate of fluid accumulation and the compliance of the pericardium.

One of the classically associated clinical signs is pulsus paradoxus, the exaggerated decline (>10 mm Hg) in systemic arterial pressure during inspiration. Although characteristic of cardiac tamponade, it can also be seen with restrictive and constrictive physiology, but to a lesser degree. When fluid accumulates in the pericardial space, intrapericardial pressure increases, leading to compression of the RA and RV, increasing their diastolic pressures. Right-heart filling becomes more heavily reliant on decreased intrathoracic pressures during inspiration to fill, exaggerating the left-sided cardiac output and arterial blood pressure change over each respiratory cycle. The interventricular septum shifts to the left during inspiration and encroaches on the left ventricle, leading to a further reduction in stroke volume of the left ventricle and enhancing the pulsus paradoxus.

Cardiac tamponade produces elevation and near equalization of diastolic chamber pressures matching intrapericardial pressures. As described above, there is also inspiratory increase in right-sided volumes and reduction in left-sided volumes that are responsible for pulsus paradoxus (Fig. 22.27A). Incomplete resolution of elevated right atrial pressure and RV filling after pericardiocentesis can indicate the presence of both constrictive and tamponade physiologies, termed effusive-constrictive physiology (Fig. 22.27B). This phenomenon may occur in as many as 16% of cases in recent series and not necessarily require pericardiectomy as previously believed.²¹

PHYSIOLOGIC AND PHARMACOLOGIC MANEUVERS AND PV LOOPS

It is important to be aware of the fact that even clinically significant cardiac disease states can be diagnostically silent until revealed by physiological or provocation maneuvers such as exercise, strain or Valsalva, Mueller maneuvers, pharmacologic stimulation, or cardiac pacing. Every case should be thoroughly reviewed for the clinical question

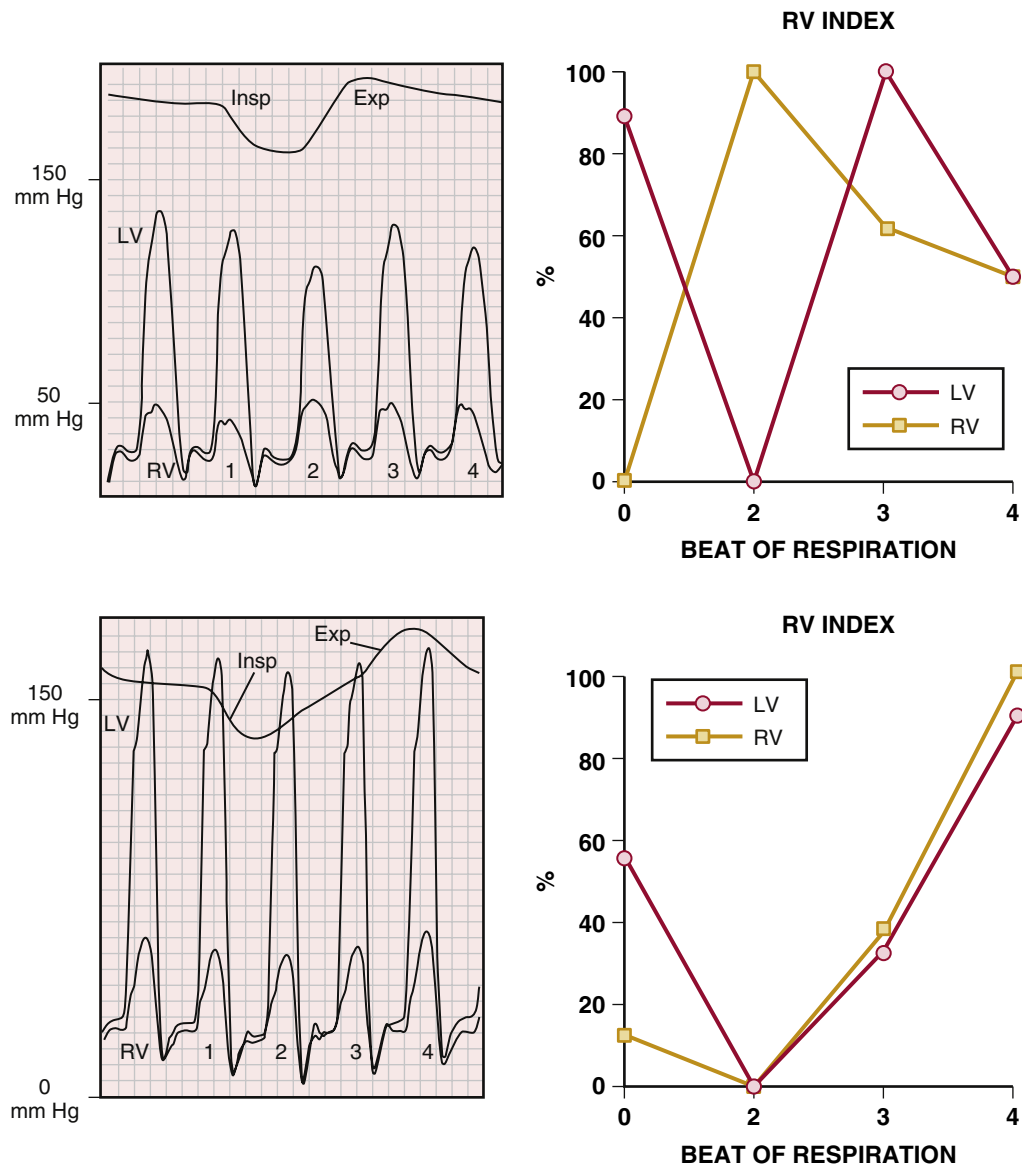


FIGURE 22.11 Dynamic respiratory variation of LV and RV systolic pressures differentiate constrictive from restrictive physiology. Top RV/LV discordance = constriction; bottom RV/LV concordance = restriction. (From Hurrell DG, et al. Hurrell DG, Nishimura RA, Higano ST, Appleton CP, Danielson GK, Holmes DR, Jamil TA. Value of Dynamic Respiratory Changes in Left and Right Ventricular Pressures for the Diagnosis of Constrictive Pericarditis. *Circulation* 1996;93:2007-2013.)

**TABLE 22.3 Comparison of Traditional and Dynamic Respiratory Criteria for Diagnosis of Constrictive Pericarditis**

	CRITERIA	SENSITIVITY (%)	SPECIFICITY (%)	PPV	NPV
Traditional	LVEDP versus RVEDP <5	60	38	4	57
	RVEDP versus RVSP >1/3	93	38	52	89
	PASP <55	93	24	47	25
	Right ventricular free wall >7 mm	93	57	61	92
	Respiratory: Change of right atrial pressure <3 mm Hg	93	48	58	92
Dynamic Respiratory Factors	Pulmonary capillary wedge versus LV >5 mm Hg	93	81	78	94
	LV/RV interdependence	100	95	94	100

LVEDP–RVEDP, Left and right ventricular end-diastolic pressure; RVSP, right ventricular systolic pressure; PASP, pulmonary artery systolic pressure; PPV, positive predictive value; NPV, negative predictive value; RFW, rapid filling wave; RAP, right atrial pressure; PCWP, pulmonary capillary wedge pressure; RV, right ventricular. From Hurrell DG, et al. Value of dynamic respiratory changes in left and right ventricular pressures for the diagnosis of constrictive pericarditis. *Circulation* 1996;93:2007-2013.

to be addressed and the cardiac catheterization protocol should be planned accordingly. Poor planning of critical measurements may lead to inconclusive results or, even worse, false conclusions.

Exercise Provocation

Exercise is a commonly used and valid provocation method, aiming to recapitulate what patients are experiencing in daily life. An adequate response to exercise entails a normal ventilatory response (i.e., oxygen consumption), a normal chronotropic response (i.e., HR increases in response to an increase in demand), a normal blood pressure response (i.e., systolic BP increases as a consequence of increased CO), normal ventricular volume responses (i.e., decrease in cardiac filling pressures due to higher CO and increase in diastolic relaxation), and adequate metabolic substrate use (i.e., appropriate use of glucose as an energy source without generating lactic acid). Right-heart (and left-heart as needed) catheterization pressures are measured before, during every phase or stage of exercise, and after exercise. Two forms of exercise are to be distinguished in this context: dynamic and static.

Dynamic Exercise

Dynamic exercise is still the most physiologic way of challenging the heart to unmask cardiac pathology. In the catheterization laboratory, this can be performed by arm exercise with weights or by leg exercise with supine bicycle ergometry. Using a pulmonary artery balloon flotation catheter (inserted from the arm or internal jugular vein), upright bicycle and treadmill exercise can also be performed with hemodynamic monitoring outside the catheterization laboratory.

Supine exercise differs from normal upright exercise in several ways: (1) Ventricular volumes are larger when the patient is supine rather than upright, (2) HR and diastolic arterial pressure are higher when the patient is upright rather than supine, (3) pulmonary and intracardiac filling pressures are lower when the patient is upright, (4) SV increases by 100% with maximal exercise when the patient is upright and only 20% to 50% when the patient is supine, and (5) both upright and supine exercise is normally associated with increases in LV end-diastolic volume (EDV) and decreases in end-systolic volume (ESV), with a concomitant increase in LV ejection fraction. In patients with coronary artery disease (CAD), these findings may either be absent or limited due to exercise limitation.

Under normal conditions, the increased oxygen demand induced by exercise is met by an increase in cardiac output and peripheral oxygen extraction. Cardiac dysfunction impairs the increase in cardiac output, and the demands of exercise can only be met by increased peripheral oxygen extraction, leading to often profound drops in mixed venous oxygen saturation and thus marked increases in arteriovenous oxygen difference. The fact that cardiac output and oxygen consumption are linearly correlated allows for a prediction of the cardiac index (CI) at a given level of oxygen consumption. This linear relationship forms the basis to calculate the exercise index (also known as the Dexter index), the ratio of the observed to the predicted CI. The predicted CI with exercise is equal to $2.99 \times 0.0059 \times \text{measured } O_2 \text{ consumption index}$ with exercise. The measured CI is the CO divided by body surface area (BSA). The normal Dexter index equals the measured CI with exercise

divided by the predicted CI. A value of ≥ 0.8 reflects a normal cardiac output response to exercise.

Another way of expressing the same relationship is the *exercise factor*, defined as the increase in cardiac output divided by the increase in oxygen consumption. An exercise factor of ≥ 6 is normal; that is, for every 100 mL/min increase in oxygen consumption, cardiac output should increase by at least 600 mL/min with exercise.

There are important nuances to supine exercise as performed in the cardiac catheterization lab. In the early phase of exertion, there is increased venous return, augmenting LVEDV and stroke volume. However, at progressively higher levels of exercise, LVESV and LVEDV decrease, minimizing stroke volume increase. The augmentation in cardiac output with this form of stress testing is primarily due to an increase in heart rate. Exercise-induced cardiac output may be limited in patients with chronotropic incompetence in the absence of other cardiac disease.

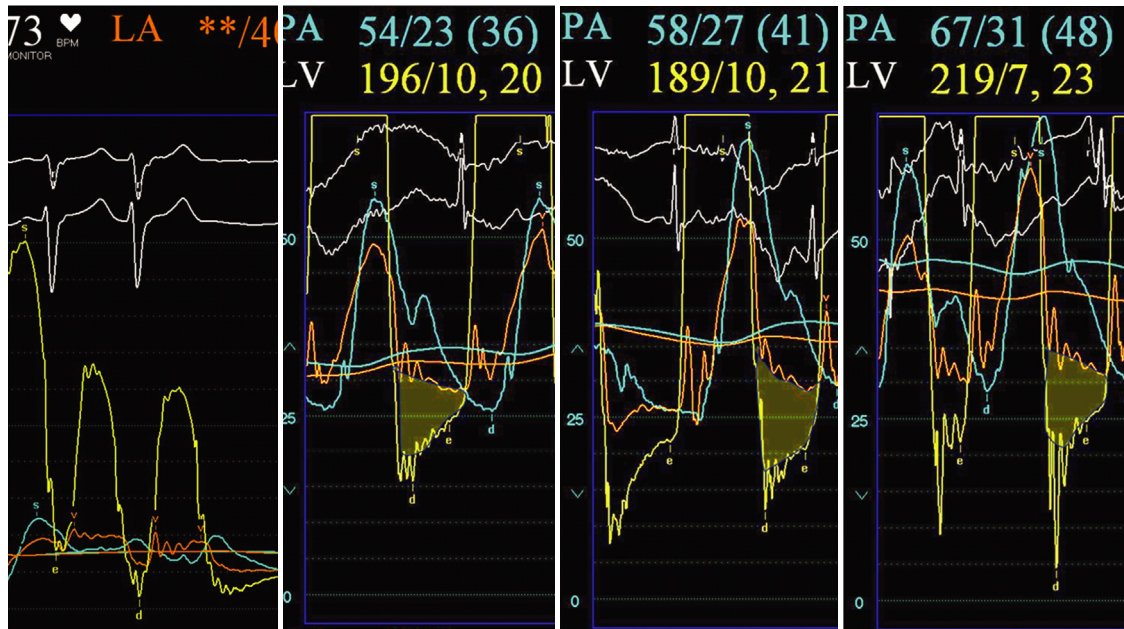
Despite these caveats, invasive hemodynamics during exercise are very useful for the diagnostic evaluation of patients with suspected heart failure with preserved ejection fraction (HFpEF) or valvular heart disease, particularly as many patients have only mild hemodynamic abnormalities at rest.²² Exercise increases LVEDP, PCWP, and PAP in patients with HFpEF. It increases transvalvular mitral gradient and PAP in mitral stenosis (eFig. 22.12, left). In patients with clinically relevant valvular regurgitation, exercise increases LVEDP, PCWP, PAP, and SVR in conjunction with a reduced exercise index (<0.8) and abnormal exercise factor (<6) (eFig. 22.12, right). Simultaneous echocardiographic evaluation of valvular regurgitation and invasive hemodynamic assessment is also useful in equivocal cases.

Static Exercise

Isometric exercise consists of skeletal muscle contraction without shortening. In the cardiac catheterization laboratory, isometric exercise commonly is performed using a handgrip with a graded hand dynamometer. Measurements of hemodynamics and ventricular function are obtained during sustained handgrip at a predetermined range (15% to 50% of the maximal handgrip contraction) for a period of 3 to 4 minutes. The size of the involved muscle group is unimportant, provided that maximal voluntary contraction is maintained to increase oxygen demand during the isometric exercise period. Isometric exercise is easy to perform (repeatedly) and requires only minimal (inexpensive) equipment. It does not involve body motion that may interfere with hemodynamic measurements. An involuntary Valsalva maneuver may occur during unsupervised isometric exercise. Careful monitoring, patient cooperation, and practice with the use of the handgrip dynamometer will minimize false hemodynamic information. In patients with CAD, isometric exercise rarely precipitates ischemia but may induce new LV wall motion abnormalities, a decrease in LV ejection fraction, and an increase in ESV with no change in diastolic volume. SV and CO may decline during isometric exercise. In patients with CHF, HR and systemic pressure may rise appropriately with a fall in SV and CO, resulting in an increase in LVEDV and PA pressure.

Pacing Tachycardia

Although rarely used, rapid atrial or RV pacing increases myocardial oxygen consumption and myocardial blood flow, LVEDV decreases



EFigure 22.12 LV, PA, LA pressures at the three phases of arm exercise. **Left**, Baseline before exercise (scale 0 to 200 mm Hg). **Right three panels**, For exercise hemodynamics the pressure scale is 0 to 50 mm Hg. During exercise pulmonary artery pressure rises from 54/23 to 67/31, left atrial pressure rises from 30 to 42 mm Hg, and left ventricular end-diastolic pressure rises from 8 to 30 mm Hg. The mitral valve gradient (*yellow shading*) remains only slightly increased to 6 or 7 mm Hg. Further exercise increases PA pressure without changing the mitral valve gradient. (From Kern MJ, et al. Evaluation of the severity of mitral stenosis in patient with pulmonary hypertension: role of exercise hemodynamics. *Catheter Cardiovasc Interv* 2019; 94:301-307.)

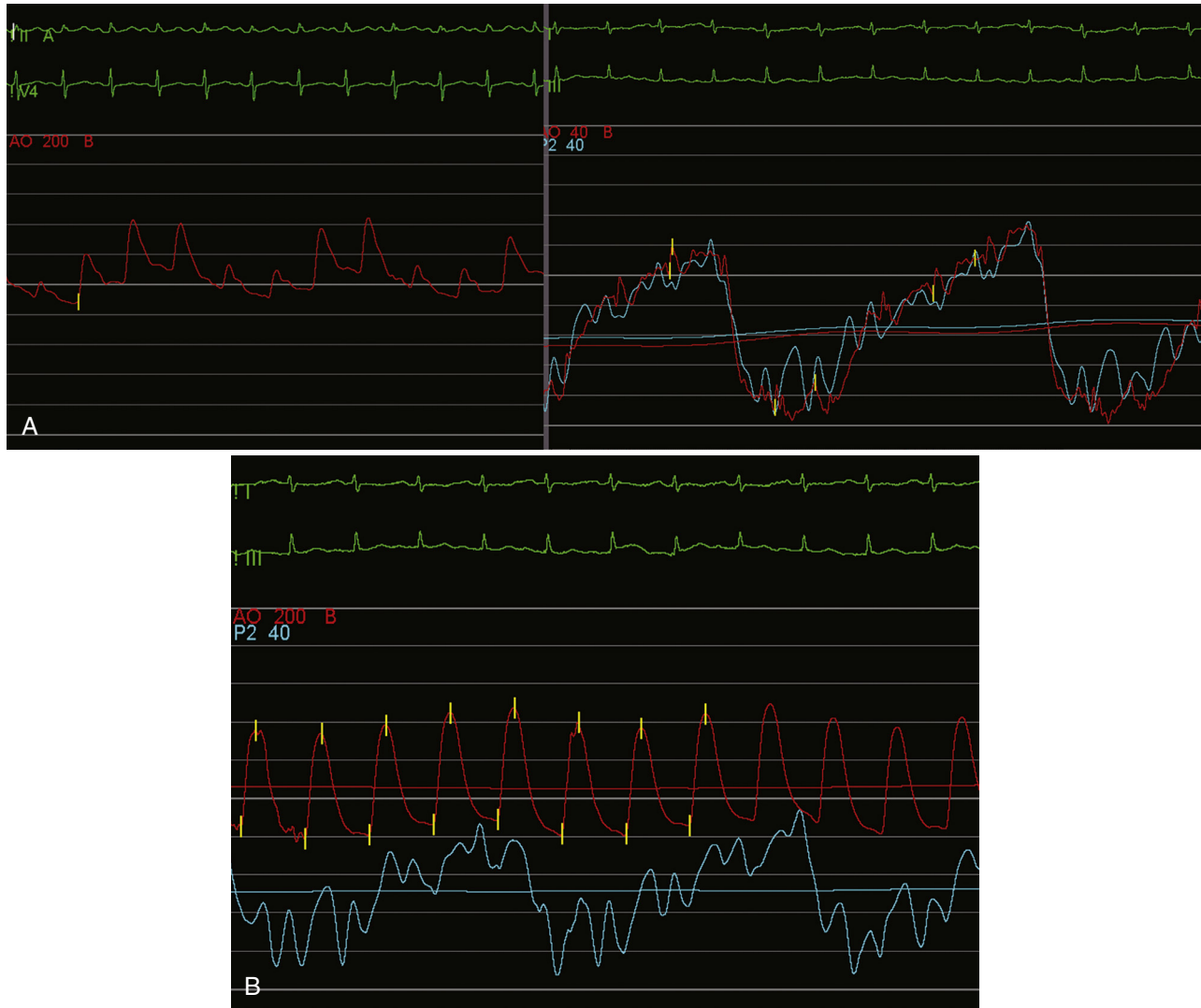


FIGURE 22.27 **A**, *Left*, Arterial pressure in patient with cardiac tamponade (scale 0 to 200 mm Hg). Note the large respiratory decrease in systolic pressure of pulsus paradoxus. *Right*, Left atrial (red) and pericardial pressure at the beginning of the pericardiocentesis. Atrial waveforms are blunted without distinct a or v waves. (scale 0 to 40 mm Hg). **B**, Arterial (red) and LA pressure (blue) after withdrawal of pericardial fluid. Note the return of normal arterial waveform and response to respiration.

with little change in cardiac output. It can be a useful method to define the severity of mitral valve stenosis and is safe with the ability to immediately terminate pacing if needed.

Physiologic Maneuvers and Volume Challenge

Various physiologic maneuvers can be used to alter the filling conditions of the heart. For example, the Valsalva maneuver in the strain phase decreases venous return and thus LV preload, which increases the systolic LV outflow tract pressure gradient in patients with HCM. In these patients, induction of a premature ventricular beat paradoxically decreases the pulse pressure (Brockenbrough-Braunwald-Morrow sign) and accentuates the spike-and-dome configuration on the aortic pressure waveform of the subsequent ventricular beat as the LV outflow gradient increases.

Another very useful physiologic challenge is rapid volume loading, which may distinguish pericardial constriction from myocardial restriction. Both conditions share hemodynamic patterns of early rapid filling dynamics and equalization of LV and RV pressure at end-expiration. Since pericardial restraint does not allow any overall volume expansion of the cardiac chambers, any volume expansion of the right ventricle will be at the cost of volume contraction of the left ventricle and vice versa, so-called exaggerated ventricular interdependence. Volume loading can cause equalized diastolic pressures between the two ventricles to differ in the setting of constriction.

Pharmacologic Challenges

Drugs that enhance contractility or vasodilate are useful for the hemodynamic diagnosis of various conditions and are readily available in the cardiac catheterization laboratory. Several of these have been previously discussed.

Dobutamine

Up to one-third of patients with LF/LG AS may be incorrectly defined as having severe AS by the Gorlin formula. To differentiate true from pseudo-severe AS, dobutamine can be infused at 5 $\mu\text{g}/\text{kg}/\text{min}$ and increased by 3 to 10 $\mu\text{g}/\text{kg}/\text{min}$ every 5 minutes. The test is ended once a maximum dose of 40 $\mu\text{g}/\text{kg}/\text{min}$ is reached, the heart rate is >140 beats/min and/or cardiac output is increased by 50%, or the mean gradient increased to >40 mm Hg. Patients with a final AVA <1.2 cm^2 and mean gradient >30 mm Hg are considered to have severe AS. Excluding ischemia during the dobutamine infusion is important and a coronary angiogram is advised before dobutamine infusion in those patients. For patients with systemic hypertension and severe AS, afterload reduction with sodium nitroprusside can be useful to define the degree of AS.

Isoproterenol

In patients with HCM, various physical and pharmacologic manipulations can be performed to confirm the dynamic nature of the LV



outflow tract gradient. The LVOT gradient is increased by isoproterenol due to increased inotropy and chronotropy and by nitroglycerin or amyl nitrate due to decreased preload and afterload. The dynamic LVOT outflow tract gradient can be reduced by administering phenylephrine thus increasing afterload (SVR).

Pulmonary Vasodilators

In patients with pulmonary hypertension, the response to pulmonary vasodilators can dictate future therapies. Vasodilator testing with epoprostenol, adenosine, nitroprusside, or nitric oxide is used to identify potential responders to therapy with calcium channel blockers and to establish prognosis.²³ In these cases, right-heart catheterization is required for the diagnosis of pulmonary arterial hypertension, which is defined by a mean PAP (mPAP) >25 mm Hg, a PCWP or LVEDP <15 , and a pressure-volume relationship (PVR) >3 Wood units.

Vasodilator hemodynamic testing is also an important part of the evaluation for patients with advanced systolic heart failure who are being considered for orthotopic heart transplantation (OHTx). Relative contraindications to OHTx include a PVR ≥ 5 , a pulmonary vascular resistance index (PVRI) ≥ 6 , and a transpulmonary gradient (TPG) ≥ 16 . A PA systolic pressure ≥ 60 mm Hg and any of the aforementioned elevations in pulmonary pressures are associated with increased mortality after OHTx. For these reasons, RHC is required in all OHTx candidates and should be repeated annually until transplantation or every 3 to 6 months if the patient has documented pulmonary hypertension.

Vasodilator testing is recommended in potential OHTx candidates with a pulmonary artery systolic pressure (PASP) ≥ 50 , TPG ≥ 15 , or PVR ≥ 3 . Ideally, patients should have a PCWP <25 before testing to limit contribution from ongoing pulmonary venous congestion. Agents (e.g., nitroglycerine, nitroprusside, inhaled nitric oxide, epoprostenol, or milrinone) are also used to assess pulmonary pressures in patients with advanced heart failure. If acute vasodilator testing fails, patients are often admitted for 48 to 72 hours of continuous infusion therapy with milrinone and diuretics to optimize pulmonary pressures.

Nitric Oxide

Nitric oxide is an endothelium-derived vasodilator administered by inhalation and rapidly inactivated, making it safe to use without causing sustained systemic hypotension. It produces a pulmonary vasodilator response, the magnitude of which is a fairly accurate predictor of the response to oral vasodilator medical therapy and of overall prognosis. The pulmonary and systemic hemodynamic effects can be observed during escalating doses (doubling) in 2- to 5-minute intervals from 10 to 80 ppm. Cardiac output, PAP, and PCWP are the key study parameters, allowing for the calculation of PVR. A positive vasodilator response (i.e., reversibility) is defined as a decrease in mean PAP of ≥ 10 mm Hg to an absolute mean PAP of ≤ 40 mm Hg without a decrease in cardiac output.

A cautionary note for patients with elevated PCWP at baseline: Inhaled nitric oxide can reduce PVR leading to pulmonary edema. The mechanism is increased forward flow through the pulmonary vasculature with increased filling of left-sided heart chambers that have already reached their maximum compliance, precipitating further increase in PCWP and pulmonary congestion.

Nitroprusside

In patients with an elevated PCWP, sodium nitroprusside is preferred to document if reduction in afterload and LV filling pressure also lowers PAP and improves cardiac output. This holds true in cases of MR, dilated cardiomyopathy, and HFpEFA typical protocol is to commence the infusion at 0.25 to 0.5 $\mu\text{g}/\text{kg}/\text{min}$ following acquisition of baseline hemodynamic data and to up-titrate at the same dose range in 2- to 5-minute intervals until PCWP is <18 mm Hg, systemic blood pressure <90 mm Hg, or development of symptoms (e.g., lightheadedness).^{24,25} On reaching those hemodynamic endpoints, a positive response is usually defined as a drop in PVR of at least 20%.

Pressure-Volume (PV) Relationships

The ejection fraction is the most commonly used parameter to reflect on cardiac function, but it remains sensitive to afterload as

well as preload and heart size. A widely used invasive parameter is the maximal rate of pressure rise during isovolumic contraction (dP/dt_{max}); however, this parameter is also influenced by preload and heart rate as well as cardiac dyssynchrony. Relating cardiac pressure to cardiac volume has come the closest to providing the ideal parameter of cardiac contractility, one that is independent of preload, afterload, heart rate, and remodeling. A series of pressure-volume (PV) loops can be obtained to describe contractile function, relaxation properties, stroke volume, cardiac work, and myocardial oxygen consumption. Hemodynamic alterations and interventions change the PV relationship in predictable ways, and comparisons of various hemodynamic interventions can be made more precisely by examining the PV loop (Fig. 22.28). For example, increasing peripheral resistance decreases stroke volume while raising blood pressure, whereas reducing afterload has the opposite effect. Positive and negative inotropes increase and decrease stroke volume and stroke work by increasing or decreasing the slope of the end-systolic elastance (Ees).

A PV loop plots the changes of these variables over a cardiac cycle.²⁶⁻²⁸ Each PV loop (see Fig. 22.28) represents one cardiac cycle. Beginning at end-diastole (point a), LV volume has received the atrial contribution and is maximal. Isovolumic contraction (a to b) increases LV pressure with no change in volume. At the end of isovolumic contraction, LV pressure exceeds aortic pressure, the aortic valve opens, and blood is ejected from the LV into the aorta (point b). Over the systolic ejection phase, LV volume decreases, and as ventricular repolarization occurs, LV ejection ceases and relaxation begins. When LV pressure falls below aortic pressure, the aortic valve closes, a point also known as the end-systolic pressure-volume point (ESPV) (point c). Isovolumic relaxation occurs until LV pressure decreases below the atrial pressure, opening the mitral valve (point d).

The stroke volume (SV) is represented by the width of the PV loop, the difference between end-systolic and end-diastolic volumes. The area within the loop represents stroke work. Load-independent LV contractility, also known as E_{max} , is defined as the maximal slope of the ESPV points under various loading conditions, the line of these points is the ESPV relationship (ESPVR). Effective arterial elastance (E_{a}), a measure of LV afterload, is defined as the ratio of end-systolic pressure to stroke volume. Maximal LV performance as measured as stroke work occurs when $E_{\text{a}} = E_{\text{max}}$. LV performance is more efficient when, for a given stroke work, myocardial oxygen consumption is lower, which occurs when $E_{\text{a}} = 0.5 E_{\text{max}}$.

Acute changes in cardiac function, for example, in the setting of an acute myocardial infarction (AMI), are also easily demonstrated (eFig. 22.13). In AMI, LV contractility (E_{max}) is reduced; LV pressure, SV, and LV stroke work may be unchanged or reduced; and LVEDP is increased. In more severe cases of myocardial infarction, which evolve into cardiogenic shock, LV contractile function (E_{max}) is more severely reduced with associated significant increases in end-diastolic volume (LVEDV) and pressure (LVEDP). The LV impairment results in a markedly reduced stroke volume, acute diastolic dysfunction, and increased myocardial oxygen demand.

Most reports using PV loops characterize only LV hemodynamics. For research into RV function or extra-cardiac problems, the standard PV loops become complex and affected by additional factors altering the PV loop configuration and interpretation.²⁹

Last but not least, it should be mentioned that careful assessment of the hemodynamics in the catheterization laboratory not only helps to diagnose and define the patient's cardiac disease status but also aids in its dynamic management. Examples include guidance for preload and afterload and optimization of cardiac filling pressures, initiation of inotropic therapy, and mechanical circulatory support. These elements integrate into the management of heart failure. Likewise, the invasive measurement of pulmonary arterial pressures and resistance and their modulation by pulmonary vasodilator therapy plays a central element in the management of patients with pulmonary arterial hypertension. This is further outlined in the corresponding disease chapters.

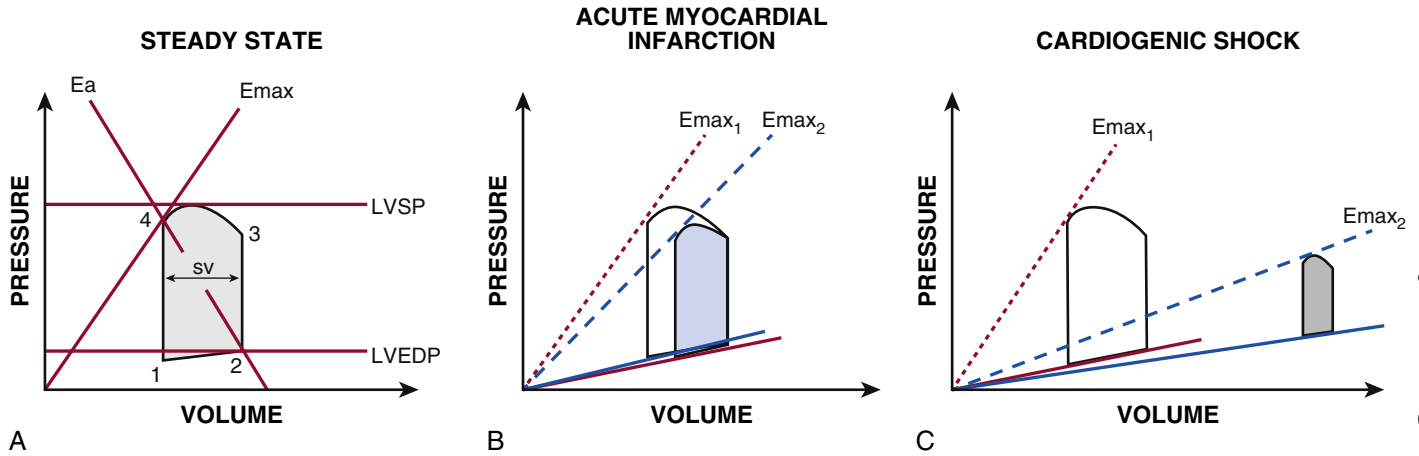


FIGURE 22.13 PV loop hemodynamics of acute myocardial infarction and cardiogenic shock. Load-independent LV contractility, also known as E_{max} , is defined as the maximal slope of the ESPV point under various loading conditions, known as the ESPV relationship (ESPVR). Effective arterial elastance (E_a) is a component of LV after-load and is defined as the ratio of end-systolic pressure and stroke volume. **Left**, Under steady state conditions, optimal LV pump efficiency occurs when the ratio of $E_a:E_{max}$ approaches 1. **Middle**, Representative PV loop in AMI (*blue loop*). LV contractility (E_{max}) is reduced; LV pressure, SV, and LV stroke work may be unchanged or reduced; and LVEDP is increased. **Right**, Representative PV loop in cardiogenic shock (*gray loop*). E_{max} is severely reduced; LVEDV and LVEDP are increased; and SV is reduced. (From Rihal C, et al. J Am Coll Cardiol. 2015;65(19):e7-e26.)

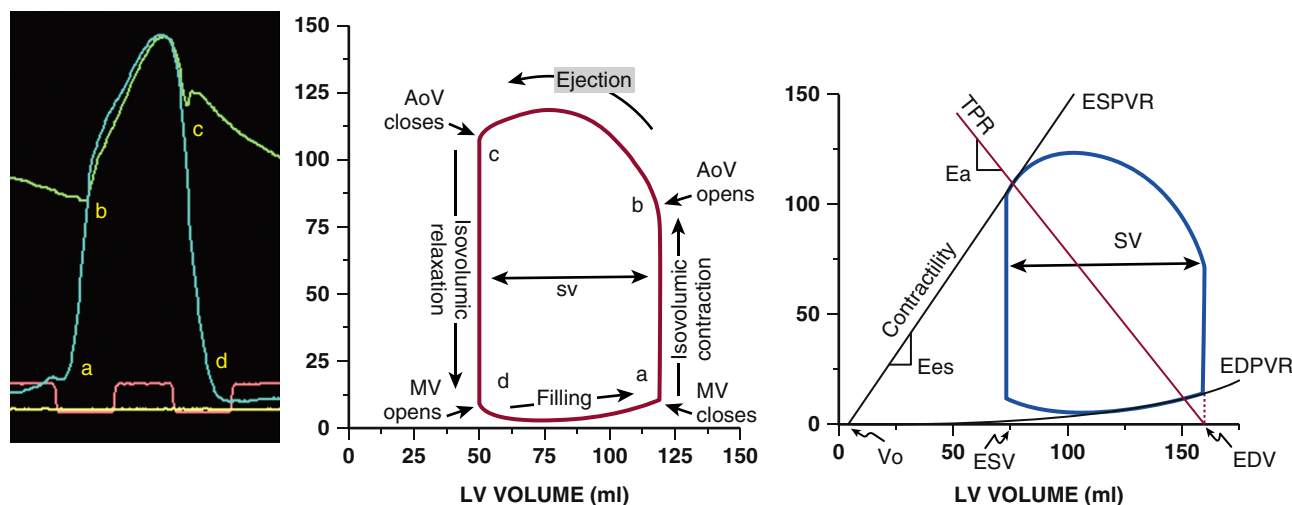


FIGURE 22.28 Origin of the pressure-volume loop relationship. **Left**, LV aortic pressure curves are used to generate the PV loop. Point *a* is LV end-diastolic pressure and the initiation of isovolumetric contraction. Point *b* is aortic valve opening as LV pressure exceeds aortic pressure. Systolic ejection continues until repolarization causes LV pressure to fall, crossing aortic pressure, point *c*, with the aortic pressure diastolic notch beginning isovolumetric relaxation. The width of the PV loop is the stroke volume (SV). The area within the loop is the ventricular stroke work. **Right**, Ventricular filling occurs along the end-diastolic pressure-volume relationship (EDPVR), or passive filling curve for the ventricle. The slope of the EDPVR is the reciprocal of ventricular compliance. Changes in ventricular compliance alter the slope of the passive filling curve. The maximal pressure that can be developed by the ventricle at any given left ventricular volume is defined by the end-systolic pressure-volume relationship (ESPVR), which represents the inotropic state of the ventricle.

ACKNOWLEDGMENT

This section extends the corresponding chapter of prior editions of *Braunwald's Heart Disease*, which was authored by Drs. Charles J. Davidson and Robert O. Bonow.

REFERENCES

- Bashore TM, Balter S, Barac A, et al. 2012 American College of Cardiology Foundation/Society for Cardiovascular Angiography and Interventions expert consensus document on cardiac catheterization laboratory standards update: a report of the American College of Cardiology Foundation task force on expert consensus documents developed in collaboration with the Society of Thoracic Surgeons and Society for Vascular Medicine. *J Am Coll Cardiol*. 2012;59:2221–2305.
- Mason PJ, Shah B, Tamis-Holland JE, et al. An update on radial artery access and best practices for transradial coronary angiography and intervention in acute coronary syndrome: a scientific statement from the American Heart Association. *Circulation: Cardiovasc Interv*. 2018;11(9):e000035.
- Seto AH, Roberts JS, Abu-Fadel MS, et al. Real-time ultrasound guidance facilitates transradial access: RAUIST (Radial Artery access with Ultrasound Trial). *JACC Cardiovasc Interv*. 2015;8:283–291.
- Skelding KA, Tremmel JA. Arterial and venous access. In: Kern M, Lim M, Sorajja P, eds. *The Cardiac Catheterization Handbook*. 6th ed. Philadelphia: Elsevier; 2016:55–98.
- Sobolev M, Slovut DP, Lee Chang A, et al. Ultrasound-guided catheterization of the femoral artery: a systematic review and meta-analysis of randomized controlled trials. *J Invasive Cardiol*. 2015;27:318–323.
- Brass P, Hellmich M, Kolodziej L, et al. Ultrasound guidance versus anatomical landmarks for internal jugular vein catheterization. *Cochrane Database Syst Rev*. 2015;1:CD006962.5.
- Alkhouli M, Rihal CS, Holmes Jr DR. Transseptal techniques for emerging structural heart interventions. *JACC Cardiovasc Interv*. 2016 Dec 26;9(24):2465–2480. <https://doi.org/10.1016/j.jcin.2016.10.035>.
- Sorajja P, Lim MJ, Kern MJ, eds. *Kern's Cardiac Catheterization Handbook*. 7th ed. Philadelphia: Elsevier; 2020.
- Nagueh SF, Smiseth OA, Appleton CP, et al. Recommendations for evaluation of left ventricular diastolic function by echocardiography: an update from the American society of Echocardiography and the European Association of Cardiovascular Imaging. *J Am Soc Echocardiogr*. 2016;29:277–314.
- Gorlin R, Gorlin SG. Hydraulic formula for calculation of stenotic mitral valve, other cardiac valves, and central circulatory shunts. *Am Heart J*. 1951;41:1–29.
- Hakki AH, Iskandrian AS, Bemis CE, et al. A simplified valve formula for the calculation of stenotic cardiac valve areas. *Circulation*. 1981;63:1050.
- Abbas AE, Pibarot P. Hemodynamic characterization of aortic stenosis states. *Catheter Cardiovasc Interv*. 2019;93:1002–1023.
- Lloyd JW, Nishimura RA, Borlaug BA, Eleid MF. Hemodynamic response to nitroprusside in patients with low-gradient severe aortic stenosis and preserved ejection fraction. *J Am Coll Cardiol*. 2017;70(11):1339–1348.
- Maron BJ. Clinical course and management of hypertrophic cardiomyopathy. *N Engl J Med*. 2018;379:655–668. <https://doi.org/10.1056/NEJMra1710575>.
- Geske JB, Ommen SR, Gersh BJ. Hypertrophic cardiomyopathy - clinical update. *JACC (J Am Coll Cardiol): Heart Fail*. 2018;6(5). <https://doi.org/10.1016/j.jchf.2018.02.010>.
- Spaziano M, Sawaya FJ, Lefevre T. Alcohol septal ablation for hypertrophic obstructive cardiomyopathy: indications, technical aspects, and clinical outcomes. *J Invasive Cardiol*. 2017;29(12):404–410.
- Cui W, Dai R, Zhang G. A new simplified method for calculating mean mitral pressure gradient. *Catheter Cardiovasc Interv*. 2007;70:754–757.
- Freihage JH, Joyal D, Arab D, et al. Invasive assessment of mitral regurgitation: comparison of hemodynamic parameters. *Catheter Cardiovasc Interv*. 2007;69:303–312.
- Hurrell DG, Nishimura RA, Higano ST, et al. Value of dynamic respiratory changes in left and right ventricular pressures for the diagnosis of constrictive pericarditis. *Circulation*. 1996;93:2007–2013.
- Talreja DR, Nishimura RA, Oh JK, Holmes DR. Constrictive pericarditis in the modern era: novel criteria for diagnosis in the cardiac catheterization laboratory. *J Am Coll Cardiol*. 2008;51:315–319 (constrict v restrict).
- Kim KH, Miranda WR, Sinak LJ, et al. Effusive-constrictive pericarditis after pericardiocentesis: incidence, associated findings, and natural history. *JACC Cardiovasc Imaging*. 2018;11(4):534–541. <https://doi.org/10.1016/j.jcmg.2017.06.017>.
- Borlaug BA, Nishimura RA, Sorajja P, et al. Exercise hemodynamics enhance diagnosis of early heart failure with preserved ejection fraction. *Circ Heart Fail*. 2010;3:588–595.
- Galiè N, Humbert M, Vachiery JL, et al. 2015 ESC/ERS guidelines for the diagnosis and treatment of pulmonary hypertension: the joint task force for the diagnosis and treatment of pulmonary hypertension of the European Society of Cardiology (ESC) and the European Respiratory Society (ERS). Endorsed by: Association for European Paediatric and Congenital Cardiology (AEPC), International Society for Heart and Lung Transplantation (ISHLT). *Eur Heart J*. 2016;37:67–119.
- Schwartzberg S, Redfield MM, From AM, et al. Effects of vasodilation in heart failure with preserved or reduced ejection fraction implications of distinct pathophysiologies on response to therapy. *J Am Coll Cardiol*. 2012;59:442–451.
- Yancy CW, Jessup M, Bozkurt B, et al. 2017 ACC/AHA/HFSA focused update of the 2013 ACCF/AHA guideline for the management of heart failure: a report of the American College of Cardiology/American Heart Association task force on clinical practice guidelines and the Heart Failure Society of America. *J Am Coll Cardiol*. 2017;70(6):776–803.
- Burkhardt D, Mirsky I, Suga H. Assessment of systolic and diastolic ventricular properties via pressure-volume analysis: a guide for clinical, translational, and basic researchers. *Am J Physiol Heart Circ Physiol*. 2005;289(2):H501–H512.
- Borlaug BA, Kass DA. Invasive hemodynamic assessment in heart failure. *Heart Fail Clin*. 2009;5(2):217–228.
- Seemann F, Arvidsson P, Nordlund D, et al. Noninvasive quantification of pressure-volume loops from brachial pressure and cardiovascular magnetic resonance. *Circ Cardiovasc Imaging*. 2019;12(1):e008493.
- Kapur NK, Esposito ML, Bader Y, et al. Mechanical circulatory support devices for acute right ventricular failure. *Circulation*. 2017;136:314–326.